POLITECNICO DI MILANO

Scuola di Ingegneria Industriale e dell'Informazione

Corso di Laurea Specialistica in Ingegneria Chimica

Dipartimento di Chimica, Materiali e Ingegneria Chimica "G. Natta"

KINETIC MODELING OF METHYL CHLORIDE PYROLYSIS AND COMBUSTION

Relatore:
Prof. Tiziano Faravelli

Co-relatore:
Ing. Matteo Pelucchi

Tesi di Laurea di:
Giorgio PORRO
Matr. 804466

Anno Accademico 2014/2015

Index

LIST OF FIGURES 5

LIST OF TABLES 9

ABSTRACT 10

SOMMARIO 11

1. INTRODUCTION 12

1.1 Effect of trace species on hydrocarbon chemistry 13
1.2 Health and environmental issues 14
1.2.1 Formation of chlorinated aromatics 14
1.2.2 Formation of NOx in CHC combustion 16

2. KINETIC AND THERMOCHEMISTRY PRINCIPLES 17

2.1 Basic principles 17

3. MODELING AND SIMULATIONS 21

3.1 Kinetic schemes 21
3.2 OpenSMOKE basic functioning 22
3.3 Sensitivity analysis 26
3.4 Rate of production analysis 27

4. CHLORINATED HYDROCARBONS 29

4.1 Chlorine electric structure and chemical nature 29
4.2 Chlorine termochemistry 31

5. KINETIC MECHANISM 34

5.1 Chemistry of HCL and CL2 systems 34
5.2 Chemistry of CH3CL systems 40
5.2.1 Kinetic scheme generation 40
5.2.2 Kinetic scheme analysis 47

6. MODELING RESULTS 60

6.1 Flow reactor systems 60
6.1.1 Pyrolysis and oxidation of CH3CL in Ar/H2O/O2 mixtures 60
6.1.2 Oxidative-pyrolysis of CH3CL in argon 64
6.1.3 Pyrolysis of CH3CL in excess hydrogen atmosphere 69
6.1.4 Inhibition of chloromethane in reacting CO/H2O/O2 mixtures 72

6.2 Shock tube ignition delays 78
6.2.1 Ignition delay time of CH3CL fuel 78
6.2.2 Effect of CH3CL addition on methane ignition behind reflect shock wave 81

6.3 Premixed laminar flames of CH3CL/CH4 85
6.3.1 Chemical structure of CH3CL/CH4 premixed flat flames 85

6.4 Laminar flame velocities 94
6.4.1 Laminar burning velocities of CH3CL/CH4/Air flames 94
6.4.2 Study of CH4/CH3CL/O2/N2 premixed flames under oxygen enrichment 97
6.4.3 Study on premixed flames of CH3CL/CH4/Air 101

7. CONCLUSION AND FUTURE OUTLOOKS 106

APPENDIX A 110

APPENDIX B 112

BIBLIOGRAPHY 114

LIST OF FIGURES

Figure 1.1: Typical dioxins and furan molecules.....15
Figure 1.2: 2,3,7,8 TCDD formation by chlorophenoles combination.....15
Figure 3.2: Generation of a kinetic model with OpenSMOKE [7].....22
Figure 3.3: Generation of a kinetic model with OpenSMOKE.....23
Figure 3.4: OpenSMOKE++ thermodynamic input files for some chlorinated species.....24
Figure 3.5: OpenSMOKE++ transport input files for some chlorinated species.....24
Figure 3.6: Example of a PFR input file in OpenSMOKE++.....25
Figure 3.7: schematic representation of a simulation with OpenSMOKE++ framework.....26
Figure 4.1: Equilibrium product distributions in methane and chloromethane combustion [13].....32
Figure 5.1.0: Arrhenius plot for the reaction CL+H_2. Experimental results (symbol) and rate constant recommended by Kumaran et al. (solid line).....37
Figure 5.1.1: Arrhenius plot for the reaction Cl + HO_2. Experimental results (symbols). The data from Gavriliv et al. is obtained for the reverse reaction and then converted through equilibrium constant. The solid line represent a best fit to experimental data [9].....38
Figure 5.1.2: Arrhenius plot for the reaction Cl + Cl + M. Experimental results (symbols). The data from Jacobs and Giedt and from Blauer et al. were obtained for the reverse reaction and converted through the equilibrium constant. The solid line represents the preferred rate constant in the work, while the dashed line represents the recommendation of Leylegian et al. [9].....40
Figure 5.2.0: Arrhenius plot for the reaction CH_3Cl=CH_3+Cl. Experimental and theoretical results (symbols). Solid line represent the adopted rate value.....49
Figure 5.2.1: Arrhenius plot for the reaction CH_3Cl+H=CH_3+HCl. Experimental and theoretical results (symbols). Solid line represent the adopted rate value.....51

Figure 5.2.2: Arrhenius plot for the reaction $CH_2Cl+H_2=CH_3Cl+H$. Experimental and theoretical results (symbols). Solid line represent the adopted rate value.....51
Figure 5.2.3: Arrhenius plot for the reaction $CH_3Cl+Cl=CH_2Cl+HCl$. Experimental and theoretical results (symbols). Solid line represent the adopted rate value.....52
Figure 5.2.4: Arrhenius plot for the reaction $CH_4+Cl=CH_3+HCl$. Experimental and theoretical results (symbols). Solid line represent the adopted rate value.....53
Figure 5.2.5: Arrhenius plot for the reaction $CH_2Cl+CH_2Cl=C_2H_4Cl+Cl$. Experimental and theoretical results (symbols). Solid line represent the adopted rate value.....55
Figure 5.2.6: Arrhenius plot for the reaction $CH_2Cl+CH_2Cl=C_2H_3Cl+HCl$. Experimental and theoretical results (symbols). Solid line represent the adopted rate value.....55
Figure 5.2.7: Arrhenius plot for the reaction $CH_2Cl+CH_3=C_2H_4+HCl$. Experimental and theoretical results (symbols). Solid line represent the adopted rate value.....56
Figure 5.2.8: Arrhenius plot for the reaction $Cl+ C_2H_4=C_2H_3+HCl$. Experimental and theoretical results (symbols). Solid line represent the adopted rate value.....58
Figure 6.1.0: Comparison between CH_3CL experimetal measures [50] and calculated profiles at different reaction temperatures.....61
Figure 6.1.1: Sensitivity coefficients of CH_3Cl to rate constants for $CH_3Cl/H_2/O_2/Ar$ mixture at different temperature, P=1 atm and ϕ=4.....62
Figure 6.1.2: Comparison of calculated and experimental [50] products distribution versus residence time a 1173 K.....63
Figure 6.1.3: Flux analysis for the C_2H_2 consumption. Different path from acetylene to carbon monoxide.....64
Figure 6.1.4: Comparison between CH_3Cl experimetal measures [72] and calculated profiles in oxidative and pyrolytic condictions.....65
Figure 6.1.5: Sensitivity coefficients of CH_3Cl to rate constants at oxidative (blue) and pyrolytic (red) condition, P= 0.68 atm and T=1123...66

Figure 6.1.6: Comparison of calculated and experimental [72] species distribution versus distance along reactor at 1223 K.....67
Figure 6.1.7: Comparison of calculated and experimental [72] species distribution versus residence time at 1223 K.....68
Figure 6.1.8: Comparison of calculated and experimental [73] species distribution versus residence time at 1123 K for CH_3Cl/H_2 system. (a) C1 species, (b) C2 species.....70
Figures 6.1.9: Comparison between experimental [58] data and model predictions for main species vs reaction time at T_0=1050 K (a) and T_0=1145 K (b) Simulated profile shifted to the 50% fuel combustion.....73
Figure 6.1.10: Sensitivity coefficients of CH_3Cl to rate constants for $CO/H_2O/O_2/CH_3Cl$ mixture at 1050 and 1145 K.....74
Figure 6.1.11: Rate costant of different reaction vs reaction time.....75
Figure 6.1.12: Comparison between experimental [58] data and model predictions for intermediate species vs reaction time at T_0=1050 K (a) and T_0=1145 K (b).....77
Figure 6.1.13: Sensitivity coefficients of CH_2O to rate constants for $CO/H_2O/O_2/CH_3Cl$ mixture at 1050 K.....78
Figure 6.2.0: Experimental [74] and simulated ignition delay time for different reacting mixture.....79
Figure 6.2.1: Sensitivity coefficients of CH radical to rate constants for mixture A at 1530 K and 1300 K.....80
Figure 6.2.2: Molar fraction profiles for CH_3Cl ignition in shock tube reactor.....81
Figure 6.2.3: Experimental [75] and simulated ignition delay time for different $CH_3Cl/CH_4/O_2$ mixtures.....82
Figure 6.2.4: Experimental [75] and simulated ignition delay time for different $CH_3Cl/CH_4/O_2$ mixtures. Comparison between different C1-C3 modules. "AramcoMech_1.3" (dashed), "C1C3HT1412" (solid).....83
Figure 6.2.5: Sensitivity coefficients of IDT to rate constants for mixture 3 at 1588 K and 1850 K.....84
Figure 6.3.0: Corrected experimental temperature profiles [77] for laminar flat flames.....86

Figure 6.3.1: Comparison of experimental [77] and predicted profiles for CH_3Cl/CH_4 flame.....88
Figures 6.3.2: Comparison of experimental [77] and predicted profiles for CH_4 flame.....89
Figures 6.3.3: Comparison of experimental [77] and predicted profiles for CH_3Cl/CH_4 flame. Comparison between different C1-C3 modules. "AramcoMech_1.3" (dashed), "C1C3HT1412" (solid).....90
Figures 6.3.4: Comparison of experimental [77] and predicted profiles for CH_3Cl/CH_4 flame. Comparison between different C1-C3 modules. "AramcoMech_1.3" (dashed), "C1C3HT1412" (solid).....91
Figures 6.3.5: Rate profiles for reactions having the highest net rates that involve CH_3Cl.....92
Figures 6.3.6: Rate profiles for reactions having the highest net rates that involve CH_4.....93
Figure 6.4.1: Experimental [78] and simulated laminar burning velocities of chlorinated and not chlorinated methane.....95
Figure 6.4.2: Experimental [78] and simulated laminar flame velocities of CH_3CL-CH_4-air mixtures at different *R* values.....96
Figure 6.4.3: Sensitivity coefficients of LFS to rate constants for mixture at different R values.....99
Figure 6.4.4: Experimental [79] and simulated laminar flame velocities for CH_4 and CH_4/CH_3Cl flames at different oxygen enrichments.....98
Figure 6.4.5: Comparison of the measured (points) [79] and calculated (curves) flame speeds different levels of oxygen enrichment and Φ= 0.8 (a), 1.0 (b), 1.2 (c).....99
Figure 6.4.6: Concentration of radicals O, H, and OH for different levels of oxygen enrichment and Φ = 0.8 (a), 1.2 (b).....100
Figure 6.4.7: Experimental [80] and simulated laminar flame velocities as function of equivalnce ratio for CH_3Cl and CH_4/CH_3Cl flames.....101
Figure 6.4.8: The variation of the burning velocity of stoichiometric mixtures of chloromethane, methane and air as a function of chloromethane mole-% in the fuel, from experiments (squares) [80] and simulation (line).....102

LIST OF TABLES

Table 1.1: Chlorine impurities (% weight) in selected liquid and solid fuels [2].....12

Table 4.1: Enthalpies of formation and bond dissociation energies of C_1 and C_2 chlorinated hydrocarbons and select chlorinated species (values given in kcal/mol). Boldfaces represent stable species [13].....30

Table 5.1: Detailed Mechanism for HCL/Cl_2 Reaction System.....34

Table 5.2: Detailed Mechanism for CH_3Cl Reaction System.....41

Table 6.1.1: Experimental initial conditions for CH_3Cl oxidation.....72

Table 6.2.1: Initial concentrations for the different experimental and simulation tests.....79

Table 6.2.2: Initial concentrations for the different experimental and simulation tests.....81

Table 6.3.1: Initial concentrations for the different experimental and simulation tests.....86

ABSTRACT

One of the most exploited techniques for wastes disposal, both domestic or industrial, generated by humans activities or derived by natural biomasses, is definitely incineration.
Waste materials incineration generates different types of pollutant as nitrogen oxides (NOx), sulphur oxides (SOx), sulphates, sulphides, unburned hydrocarbons, particulate matter (PM) and chlorinated hydrocarbons.
Despite their relative small amounts, chloride and generally halogen compounds largely impact combustion processes, mainly in terms of flame inhibitors. Moreover, the presence of chlorinated hydrocarbons gives rise to the formation of dioxins in the lower temperature post combustion zones.

A better fundamental knowledge of the chemical kinetics behind chlorinated species combustion, constitutes the first step towards an improved waste treatment processes efficiency and a remarkable decrease of pollutants formation.

Starting from a recent revision of the HCl and Cl_2 system, a kinetic mechanism for methyl chloride (CH_3Cl) has been developed and validated over all the experimental data available in the literature, constituting, at present, the first and only one in the literature. Based on analogy rules similar to those in use at Politecnico di Milano (CRECK Modeling Group) for hydrocarbon, biofuels and aromatic species combustion, this work will contribute to an easier extension the heavier molecular weight and more dangerous chlorinated molecules.

Kinetic analyses, such as sensitivity analyses and reactive fluxes analyses, allow a better understanding of the reaction channels dominating CH_3Cl pyrolysis and oxidation, highlighting where further attention should be devoted in the future.

SOMMARIO

Una delle tecniche preferite e di più pratico utilizzo per lo smaltimento dei rifiuti, siano essi industriali o domestici, derivanti da lavorazioni umane o da biomasse di origine naturale, è ad oggi senza dubbio l'incenerimento.
Come è noto l'incenerimento di prodotti di scarto porta alla produzione di una serie di inquinanti quali ossidi di azoto (NO_x), ossidi di zolfo (SO_x), solfuri, idrocarburi incombusti, materiale particolato (PM) e idrocarburi clorurati.Il cloruro e gli alogeni in generale, seppur presenti in piccole quantità,sono in grado di influire notevolmente sul processo di combustione, soprattutto come inibitori di fiamma. Inoltre la pesenza di idrocarburi clorurati può causare la formazione di molecole molto tossichecome le diossine, specialmente nelle zone di post combustione a bassa temperatura. Una conoscenza migliore dei meccanismi di combustione coinvolgenti il cloro può permettere senza dubbio una gestione più accurata dei processi e una diminuzione, se non la completa eliminazione, degli inquinanti.

A partire da una recente revisione del sistema HCl e Cl_2, un nuovo meccanismo cinetico è stato sviluppato e successivamente validato utilizzando i dati sperimentali disponibili in letteratura. Questo schema ad oggi si presenta come primo ed unico disponibile in letteratura. Basato su regole d'analogia simili a quelle in uso presso il Politecnico di Milano (CRECK Modeling Group) per la combustione degli idrocarburi, dei biofuel e delle specie aromatiche, questo lavoro contribuirà successivamente ai lavori estesi a specie clorurate più pesanti e potenzialmente più pericolose.Analisi cinetiche, come l'analisi di sensitività e dei flussi reattivi, permettono una migliore comprensione dei percorsi reattivi dominanti la pirolisi e la combustione del CH_3CL, mettendo in evidenza quali ulteriori studi debbano essere sviluppati in futuro.

1. INTRODUCTION

Combustion of chlorinated hydrocarbon is of practical interest because thermal treatment and incineration are practical ways to dispose of toxic, hazardous and organic wastes containig chlorine.
This work is justified mainly by two aspect which are linked each others.
The first aspect is rapresented by chlorine nature and its behaviour, typical of all halogens compunds, to influence combustion processes, acting as a suppressant and inhibitor.
Although chlorine is contained only in small quantities, it can considerably influence combustion and change the fuel consumption rate.
The second aspect includes an enviromental interest. Combustion of chlorinated compounds can cause production of potentially toxic and hazardous byproducts. It is important to notice that with "chlorinated compounds" we mean not only environmentally dangerous synthetic compounds, but also chlorine containing biomass, treated to recover thermal energy. Table 1.1 reports chlorine impurities in selected liquid and solid fuels [2].

Table 1.1
Chlorine impurities (% weight) in selected liquid and solid fuels [2]

FUEL	Cl
Fuel oil	<0.1
Straw	0.1-1.7
Other annual biomass	0.01-0.6
Wood	<0.10
Coal	0.01-0.10
Plastics	0.0; 50
Paper	0.03-0.40
Residential solid waste	0.1-0.9

Plastic such as PE contain no chlorine while PVC typically contains about 50%.

A proper control of combustion process needs a better knowledge of chlorine chemistry and its role in combustion kinetics. Starting from this it will be possible, not only to select the best conditions for disposal processes management, to more efficiently transform methane in more valuable products is possible [1].

1.1 EFFECT OF TRACE SPECIES ON HYDROCARBON CHEMISTRY

When compared to the reactions of analogous nonsubstituted hydrocarbons, the kinetics of chlorinated hydrocarbon (CHCs) reactions exhibit several peculiar features. As a consequence of the lower C-Cl bond dissociation energies (BDEs), CHCs decompose at temperatures that are significantly lower than hydrocarbons resulting in the generation of reactive Cl radicals. For example, the C-Cl BDE in CH_3Cl is 351 kJ/mol compared to 414 kJ/mol for a primary C-H BDE. This is relevant because C-Cl and C-H dissociation processes proceed via the same loose transition states meaning that the activation energy would be very close to the bond dissociation energy, which is lower for chlorinated compounds[13].
Moreover the chemistries of hydrocarbon stable species and radicals and chlorine containing species are highly correlated and their interactions chlorine largely affect the radical pool, both directly and indirectly [2].
Considering flames propagation we can undestand how chlorine can act to promote or inhibit the overall reaction rate. In order to propagate, a flame needs the formation of a radical pool, and this process is self-sustained mainly through the branching reaction $H + O_2 \rightarrow O + OH$.
A change in the relative importance of chain branching and chain termination reaction dramatically influence the reactivity of the system. As an exampletrace species like Cl may enhance oxidation by the simple sequence:

$$CL + XY \rightarrow CLX + Y \tag{1.0}$$

$$CLX + M \rightarrow CL + X + M \tag{1.1}$$

Where X and Y are radical species like O, H or OH. As reported, a new radical is formed,and Cl is regenerated in a chain branching sequence
Considering the reverse cycle:

$$CL + X + M \rightarrow CLX + M \tag{1.2}$$

$$CLX + Y \rightarrow CL + XY \tag{1.3}$$

two radical species are consumed via a chain termination cycle.
Depending on the operating conditions, one of the two cycle can prevail over the other.

Nowadays the ihnibiting nature of chlorine is quite weel known, therefore its tendency to lower the flame speed, to limit ignition and flame quenching.

1.2 HEALTH AND ENVIROMENTAL ISSUES

Suitable ways to dispose of organic wastes, referring in particular to the class of hazardous wastes including chlorinated hydrocarbon, are: (a) conversion to HCl and CO_2 by oxidation, (b) conversion to HCl and hydrocarbons by pyrolysis in methane or hydrogen enriched atmosphere [3].
These processes are used both for industrial wastes, like solvents and polymers, and biomasses, which can contain considerable quantities of chloride in some cases as shown in Table 1. Specially cereals like oat, barley and rape, or grass plant like corn and sugarcane can contain more than 1% in mass of chlorine.
These disposal processes present some issues related to both environmental and human health aspects. Thereforethe need of a careful analysis of the kinetic mechanism involved.

1.2.1 FORMATION OF CHLORINATED AROMATICS

Combustion of chlorinated compounds is associated with the formation of potentially toxic byproducts, while the final product awaited from incineration is HCl that is easily removable from flue-gas by a scrubbing process. These byproducts include chlorinated alkenes, such as C_2HCl_3, $C2Cl_4$ as well as chlorinated aromatics, such as C_6H_5Cl, chlorinated dioxins and furans. The most critical byproducts in CHC combustion continues to be highly controversial, because of uncertainties about the degree of toxicity of these molecules. It is important to recognize that all compounds can be in principle toxic at a proper dose, and the threshold varies significantly.
However, for dioxins the toxicity is well-known. We generally refer to dioxins for semplification, meaning polychlorinated dibenzo dioxins (PCDD).
PCDDs and polychlorinated dibenzo furans (PCDFs) are two important classes of toxic pollutants that can be formed in the combustion of chlorinated hydrocarbons. The molecular structures of these compounds are shown in Figure 1.1).

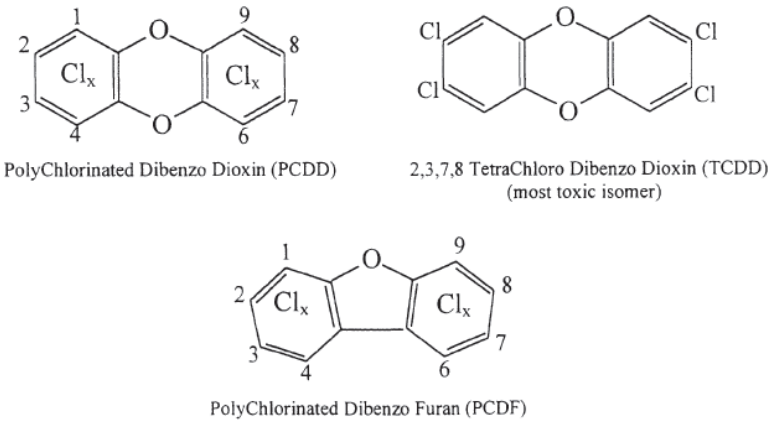

Figure 1.1: Typical dioxins and furan molecules [13]

Great attention has been devoted to TetraChloro Dibenzo Dioxin (TCDD) for its high toxicity. In fact, it has been shown that TCDD bio-accumulates in humans and animals due to their lipophilic properties. Moreover they are known teratogens, mutagens, and carcinogens. Despite chlorine is largely present in nature and PCDDs are largely produced through natural activitiessuch as volcanic eruptions and forest fires) the main source remain human activities.
Two mechanisms were identified as the possible paths through which these molecules are formed. An homogeneous route from aromatic precursors like chlorinated benzenes and phenoles, and a heterogeneous route from carbanaceous materials with particulate carbon and carbon species with different functional groups.
Conceptually, PCDD can be formed by simple recombination of two chlorinate phenols followed by HCl elimination as shown in Figure 1.2 for . 2,3,7,8-TCDD formation from 2,4,5 trichlorophenol.
It is clear that the formation process is not an elementary stepand a more complex mechanism is involved. However, despite the process complexity, dioxines formation is thermodynamically favored and kinetically feasible[13].
Some condition have to be satisfied in order to allow dioxines formation.

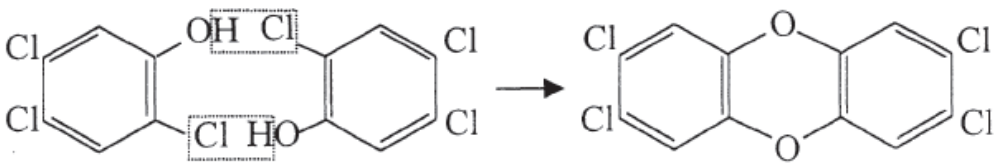

Figure 1.2: 2,3,7,8-TCDD formation by chlorophenoles combination [13]

In principles all kind of hydrocarbon species could produce PCDD in presence of chlorinated compounds or chlorine, both in solid or gas phase conditions. Organic molecules like CH_3Cl, C_6H_5Cl or phenols, or inorganic species like HCl, Cl_2, KCl, $CuCl_2$ can act as promoters or chlorine source.
Moreover, temperature plays an important role. In fact, dioxines formation is favored at low temperatures, tipically from 400 to 700 K.

1.2.2 FORMATION OF NOx IN CHC COMBUSTION

Chlorinated hydrocarbons can influence NOx formation through a complex network of competitive reactions.
Firstly, as already stated chlorinated hydrocarbons can easily consume large amounts of H, OH and O radicals, decreasing their concentrations in the earlier and cooler part of a premixed flame. These radicals are largely involved in NOx formation.
Moreover the lower BDE of C-Cl with respect to C-H allows the formation of CH, CCl, CH_2 and CHCl radicals, considered to be precursor for prompt NOx in flames [13] .
Thermal NOx formation is not promoted by chlorinated species, instead the decrease in flame temperature is expected to reduce their formation [4].

2. KINETIC AND THERMOCHEMISTRY PRINCIPLES

In order to fully undestand how chloride and specially chloromethane influnce the reagent systems where they are involved, it's necessary to be familiar with the basic principles of kinetic and thermodinamic which regulate these systems.

2.1 BASIC PRINCIPLES

A major requirement for the development of kinetic models attempting to emulate reaction systems in combustion and other related fields is accurate thermodynamic property data (estimated or experimental) for all molecular and radical species considered in the mechanism. In addition, accurate thermodynamic property data over a wide temperature range are needed for chemical reaction equilibria calculations and safety evaluations of chemical incompatibility and explosion hazards.
When a chemical reaction *j* proceeds in gas phase to a state of dynamic equilibrium, that state is completely described by the specification of *T*, *P* and chemical composition *x*. From *P* and *x* the equilibrium constant and the standard Gibbs free energy change can be calculated as follows:

$$aA + bB \leftrightarrow \mathrm{rR} + \mathrm{qQ}$$

$$K_{eq,j} = \frac{R^r Q^q}{A^a B^b} = \exp\left(-\frac{\Delta G_{Tj}^0}{RT} \right)$$

where $\Delta G_{Tj}^0 = \sum_{i=1}^{NS} v_{ij}\, \Delta G_{fi}^0(T)$ represents the standard Gibbs free energy of formation of 1 mole of the species *i* at temperature T and pressure of 1 atm from the elements in their standard states at T and 1 atm pressure.
The rate of reaction in homogeneous condition R_i^V [mol/cm^3/s] represents the moles of the species *i*, n_i, formed within a time unit and in a certain volume. The rate of reaction is obviously a function of T, P and the concentration of all the species in that volume (C_i).

$$R_i^V = R_i^V(T, P, C_i)$$

It is quite complicated to define R_i^V, especially because of the dependency from C_i is usually non-linear. This is caused by the fact that a common reaction occurs through a certain number of steps, called elementary reactions.
Hence, a single species can appear in the kinetic scheme either as a reactant or a product in all of the different elementary reactions. Defining ν_{ij} as the matrix of stoichiometric coefficients, R_i^V can be related to its own elementary reactions through the statement of r_{ij} indicating the number of moles of a certain species *i* produced in the reaction *j*.

$$R_i^V = \sum_{i=1}^{NR} r_{ij} = \sum_{i=1}^{NR} \nu_{ij} r_j$$

It is theoretically confirmed and experimentally proved that the rate r_j of each elementary act is proportional, through the rate constant k_j, to all of the reactants' concentrations raised to the ν_{ij}-th power.

$$r_j = k_j(T,P) \prod_{i=1}^{Nreactants} C_i^{\nu_{ij}}$$

The previous relation can be generalized defining a *power law*, where all the species are considered. The exponent θ_{ij}, defined as reaction order, is usually determined by an experimental data fitting.

$$r_j = k_j(T,P) \prod_{i=1}^{NS} C_i^{\theta_{ij}}$$

kj is defined through the Arrhenius equation:

$$k_j = A_j \exp\left(-\frac{Ea_j}{RT}\right)$$

where A_j is the pre-exponential factor, Ea_j is the activation energy, R is the universal gas constant and T is the temperature in K.
To obtain a better agreement with the experimental data available, the Arrhenius equation is commonly used in its modified form:

$$k_j = A_j \mathrm{T}^{\mathrm{n}} \exp\left(-\frac{Ea_j}{RT}\right)$$

In a gas phase reactive system we can identify two classes of processes: unimolecular processes and bimolecular. The first one, undergone by an energetically activated chemical species isolated from other species, may correspond to an internal rearrangement of atoms, a bond breaking, a rotation

or simply an internal redistribution of energy; the second one is a composite process consisting of the formation of a collision complex (bimolecular process), followed by a unimolecular kinetic process leading to products.

The unimolecular processes, also known as first order reaction, can either be:

$$A \rightarrow B \quad \text{or} \quad A \rightarrow B + C$$

The rate of reaction is expressed as:

$$r = k\, C_A \; [mol/cm^3/s]$$

with *k* turning out to be a frequency, measured as $[s^{-1}]$.
The rate of reaction is

$$r = k\, C_A\, C_B \; [mol/cm^3/s]$$

with *k* turning out to be expressed in $[cm^3/mol/s]$.
Two more concepts which need to be discussed are: the thermodynamic consistency of a chemical reaction and the microscopic reversibility principle.
A common reaction is usually indicated connecting reactants and products with a double arrow, which indicates that the reaction can occur in both the directions, through the direct (D) or reverse (R) reaction.

$$A + B \leftrightarrow C$$

$$D:\ A + B \rightarrow C \qquad R:\ C \rightarrow A + B$$

Supposing that $t \rightarrow \infty$, A, B and C will get to an equilibrium state where r_D will be equal to r_R :

$$r_D^{eq} = r_R^{eq}$$

$$k_D^{eq} C_A^{eq} C_B^{eq} = k_R^{eq} C_C^{eq}$$

Hence:

$$k_R^{eq} = k_D^{eq} \frac{C_A^{eq} C_B^{eq}}{C_A^{eq}}$$

For an ideal gas phase system the equilibrium constant Keq is equal to:

$$K_{eq}(T,P) = \prod_{i=1}^{N_c} \left(\frac{c_i}{c_{i,rif}}\right)^{v_i} = \exp\left(-\frac{\Delta G_r^0(T,P_{rif})}{RT}\right)$$

where for a gas species $C_{i,rif} = P_{rif} / RT$
Through some simple algebraic rearrangement, the reverse rate constant k_R^{eq} can be expressed as:

$$k_R^{eq} = k_D^{eq} C_{rif} \exp\left(\frac{\Delta G_{Tj}^0}{RT}\right)$$

This relation, known as thermodynamic consistency, allows to calculate from thermodynamic data the reverse rate constant from the direct rate constant, being the reaction either an elementary reaction or a global reaction.
The microscopic reversibility principle is closely related to the thermodynamic consistency of a reaction. It states that, strictly for an elementary reaction, the atoms during a reaction follow the same pathway in both the direct and the reverse direction on the Potential Energy Surface (PES) of the considered reaction, via the Minimum Energy Path (MEP).

3. MODELING AND SIMULATIONS

3.1 KINETIC SCHEME

The simulations have been performed using the OpenSMOKE code, developed by Cuoci et al. [5] from the CRECK Modeling group at Politecnico di Milano.
The OpenSMOKE framework consists of a collection of C++ libraries specifically conceived to manage large, detailed kinetic schemes (with hundreds of species and thousands of reactions) in numerical simulations of reacting flows.
The OpenSMOKE library is coupled to the BzzMath libraries [6] to solve typical systems of interest for the combustion community (ideal reactors, laminar opposed flames, laminar premixed flames, flamelets, etc.).

The kinetic schemes used and developed in this work are also provided by the CRECK Modeling group [7].
Two important features of those kinetic models are modularity and hierarchy.
The “Polimi kinetic schemes” used for simulations are in fact divided in subsystems, or modules, each containing a set of reactions related to a family of species. These modules can be added or removed depending on the system and on the operative conditions of interest.
The kinetic schemes provided by CRECK Modeling at Politecnico di Milano are also hierarchically organized. In fact, the modules for the smaller species are always present in the set of reactions for larger species, but an analysis of smaller hydrocarbons can avoid to include the modules of the higher ones. All the mechanisms are provided in Chemkin format.

To form the final mechanism, four differents modules are linked in order to simulate systems containing different species and molecules.
In particular the three modules are:

- "C1C3HT1412" [8] containig the reactions that involve hydrocarbons with a number of carbons varing from one to three. The reactions involved are typical of oxidation and pyrolysis processes.
- "H_2/CO mechanism" [8] containing the reactions involving syn-gas.
- "Kinetics_HCl_Cl_2" [9] containig the module which deal with the reactions of Cl and HCl.

- "vco9410" which contains all the reactions of pyrolysis and oxidation which can start from the molecule of methyl-chloride. This package inCludes not only methy-chloride, but also all the chlorinated species with more than one carbon atom containig chlorine.

This last module will be investigated and tuned in order to obtain a reliable kinetic model, through which understand better pyrolysis and oxydation when chlorine is present.

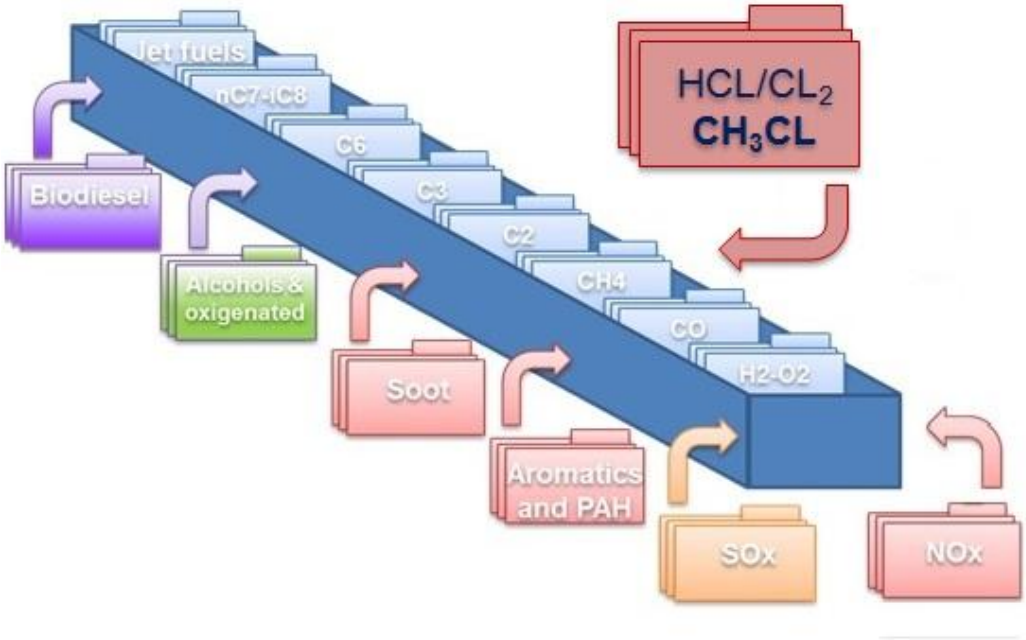

Figure 3.2: Generation of a kinetic model with OpenSMOKE [7]

3.2 OpenSMOKE BASIC FUNCTIONING

The kinetic scheme, together with thermodynamic and transport properties, are inputs to an interpreter, “Open_SMOKE_Chemkin_Interpreter”, which generates a kinetic model in binary format and additional output files, as reported in figure 3.3.

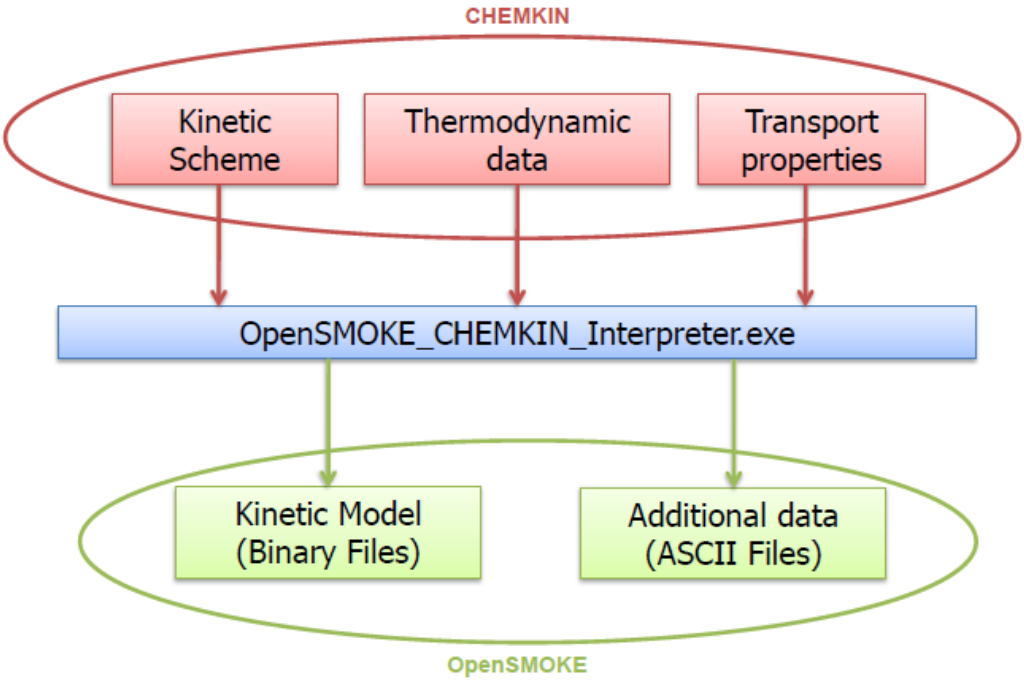

Figure 3.3: Generation of a kinetic model with OpenSMOKE

The thermodynamic database is based on the 7-coefficient NASA polynomials, through which thermochemical properties (specific heat C_P, enthalpy of formation ΔH_f, entropy of formation ΔS_f and Gibbs free energy ΔG_f) are calculated as a function of temperature.
The 7 term polynomials include 15 parameters. The first set of 7 constants belongs to the high temperature (T > 1000 K) polynomial, the second set of 7 constants belongs to the low T (T = 300-1000 K) polynomial, and the fifteenth constant is $H_{298}/R = \Delta H_{f298}/R$ [10].

The transport database includes six molecular parameters for each species [11]:

1) An index indicating whether the molecule has a monatomic, linear or nonlinear geometrical configuration. If the index is 0, the molecule is a single atom. If the index is 1 the molecule is linear, and if it is 2, the molecule is nonlinear.
2) The Lennard-Jones potential well depth ε/k_B [K].
3) The Lennard-Jones collision diameter σ [Å].

4) The dipole moment μ [D].
5) The polarizability α [Å3].
6) The rotational relaxation collision number Z_{rot} at 298 K.

An example of input thermodynamic and transport file is reported respectively in figure 3.4 and figure 3.5

```
CH2CL2                  C   1H   2CL  2     G    300.00   4000.00 1000.00      1
 .629318149E+01 .598773270E-02-.215635738E-05 .348717095E-09-.209014331E-13    2
-.139806830E+05-.590810756E+01 .309078884E+01 .835269259E-02 .125182071E-04    3
-.246845519E-07 .111752358E-10-.128332020E+05 .120563837E+02                   4
CH3CL                   C   1H   3CL  1     G    300.00   4000.00 1000.00      1
 .397883949E+01 .791729094E-02-.281713927E-05 .451715634E-09-.269086155E-13    2
-.116761879E+05 .258272676E+01 .396611858E+01-.505692958E-02 .402006413E-04    3
-.482781901E-07 .186721580E-10-.110729538E+05 .570446517E+01                   4
```

Figure 3.4: OpenSMOKE++ thermodynamic input files for some chlorinated species

```
CH2CL2              2   406.000     4.759     0.000     0.000     1.000
CH3CL               2   855.000     3.375     0.000     0.000     1.000
CH2CL               2   858.000     3.400     0.000     0.000     0.000
```

Figure 3.5: OpenSMOKE++ transport input files for some chlorinated species

The final inputs to simulate the system in OpenSMOKE are:

1) The kinetic model
2) A flame/reactor input file, describing composition, temperature, pressure of the inlet mixture and all the operating conditions, such as residence time, as well as simulation parameters, like tolerances of ODE solver

An example of an input files describing the reactor and the gas inlet stream is reported in figure 3.6

```
//-------------------------------------------------------------------//
//     ____                   _____ __  __  ____  _  ________        //
//    / __ \                 /  ___ |  \/  |/ __ \| |/ /  ____|      //
//   | |  | |_ __   ___ _ __ |  (___ | \  / | |  | | ' /| |__        //
//   | |  | | '_ \ / _ \ '_ \ \___  \| |\/| | |  | |  < |  __|       //
//   | |__| | |_) |  __/ | | |____)  | |  | | |__| | . \| |____      //
//    \____/| .__/ \___|_| |_|_____/|_|  |_|\____/|_|\_\_____|       //
//          | |                                                      //
//          |_|                                                      //
//                                                                   //
//                http://www.opensmoke.polimi.it/                    //
//             http://creckmodeling.chem.polimi.it/                  //
//-------------------------------------------------------------------//

Dictionary PlugFlowReactor
{
    @KineticsPreProcessor Chloromethane;

    @Type                 Isothermal;

    @InletStatus          inlet-mixture;

    @ResidenceTime        2.5 s;

    @ConstantPressure     true;

    @Diameter             1.05 cm;

    @MoleFlowRate         1 mol/s;

    @OdeParameters        ode-parameters;

    @SensitivityAnalysis  sensitivity-options;

    @Options options;
}
Dictionary Chloromethane
{
    @Kinetics         C:\Users\Porro\Desktop\Uni\Tesi\Cloro_metano\test_20_05-Dean\KineticOS\Chloromethane.CKI;
    @Thermodynamics   C:\Users\Porro\Desktop\Uni\Tesi\Cloro_metano\Simulazioni++\Kinetic\Chloromethane.CKT;
    @Output           kinetics;
}

Dictionary inlet-mixture
{
    @Temperature        1173.   K ;
    @Pressure           101325  Pa;
    @MoleFractions      CH3CL 0.02
                        H2    0.01
                        O2    0.01
                        AR    0.96 ;
}

Dictionary ode-parameters
{
    @OdeSolver OpenSMOKE;
}

Dictionary sensitivity-options
{
  @Type               kinetic-constants;
  @DenseSolver        Eigen;
  @DenseFullPivoting  false;
  @Species            CH3CL CH4 CO;
  @SubSteps           5;
}

Dictionary options
{
 @StepsVideo    10;
 @StepsFile     10;
 @OutputFolder  Output1173;
 @OutputSpecies CO CH4 CH3CL HCL CO2;
 }
```

Figure 3.6: Example of a PFR input file in OpenSMOKE++

A schematic representation of a simulation with OpenSMOKE++ framework is shown in Figure 3.7.

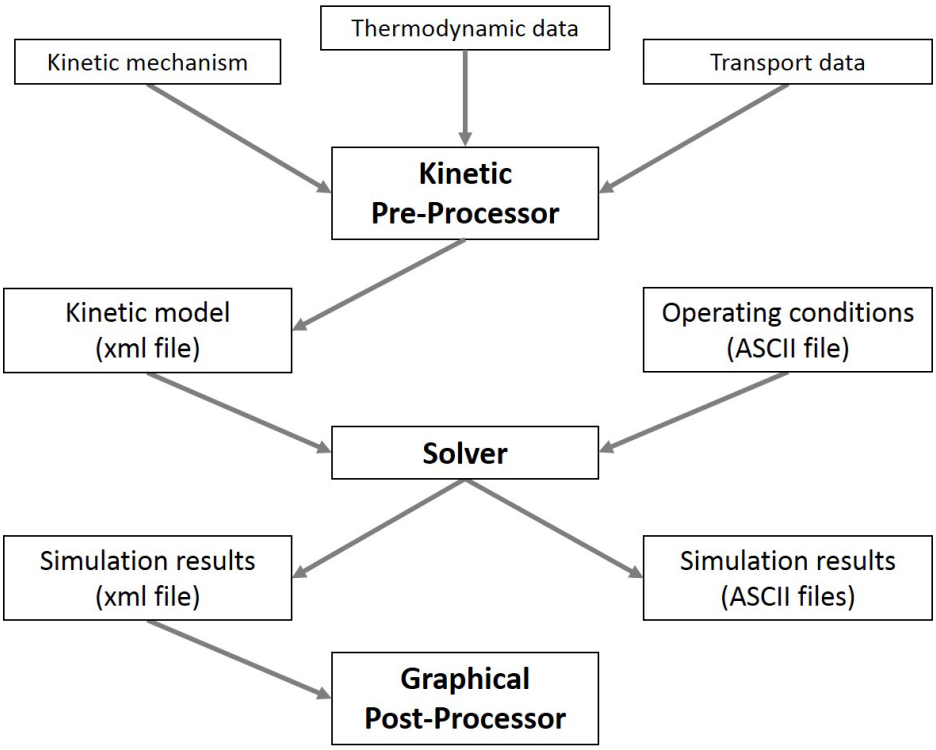

Figure 3.7: schematic representation of a simulation with OpenSMOKE++ framework

3.3 SENSITIVITY ANALYSIS

Sensitivity analysis is very important for kinetic studies, since it allows the quantitative understanding of how the numerical solution of the governing equations depends on the various parameters contained in the model itself.
Only the first-order sensitivity coefficients with respect to the reaction rate coefficients (pre-exponential factors, activation energy or kinetic constant) can be calculated [5].

The equations for the sensitivity coefficients can be easily obtained starting from the ODE system describing the system under investigation:

$$\frac{dy}{dt} = f(y, t, \alpha)$$

The functions f do not depend only on the unknowns y, but also on a number of parameters α, corresponding to the kinetic parameters of the chemical reactions.
The first-order sensitivity coefficients are then defined as:

$$s_{ij} = \frac{\partial y_i}{\partial \alpha_i}$$

where the index j refers to the variable and i to the parameter.
If the initial ODE system equations are differentiated with respect to the parameters s_{ij}, the following additional ODE system is obtained:

$$\begin{cases} \frac{ds_j}{dt} = Js_j + \frac{\partial f}{\partial \alpha_j} \\ s_j(t_0) = 0 \end{cases}$$

where s_j is the set of sensitivity coefficients of all the variables y_i with respect to the j-th parameter α_j and J is the Jacobian matrix of the main ODE system.
OpenSMOKE++ calculates the sensitivity coefficients using a modified version of the staggered direct method, normalizing them in the form of logarithmic derivatives, in order to make them more useful for analyses and comparisons [5].

3.4 RATE OF PRODUCTION ANALYSIS

The rate of production analysis (ROPA) is another useful tool to better understand kinetic aspects in the simulation of reactive flows. Basically, the rate of production analysis determines the contribution of each reaction to the production or consumption rates of a species.
For each species i it is often convenient to separate the chemical production rates into creation ($\dot{c}_i$) and destruction rates ($\dot{d}_i$):

$$\dot{c}_i = \sum_{j=1}^{NR} v_{ij}^f r_j^R + \sum_{j=1}^{NR} v_{ij}^b r_j^D$$

$$\dot{d}_i = \sum_{j=1}^{NR} v_{ij}^f r_j^D + \sum_{j=1}^{NR} v_{ij}^b r_j^R$$

where ν_{ij}^f and ν_{ij}^b are the stoichiometric coefficients of, respectively, the i-th reactant (forward) and i-th product (backward) species in the j-th reaction ($\nu_{ij} = \nu_{ij}^f - \nu_{ij}^b$), while r_j^D and r_j^R represent the direct and the reverse reaction rates.
For each species *i* and each reaction *j* it is then possible to define a normalized production contribution C_{ij}^p and a normalized destruction contribution C_{ij}^d:

$$c_{ij}^p = \frac{max\left(v_{ij}^f - v_{ij}^b, 0\right) r_j}{\sum_{k=1}^{NR} max\left(v_{ij}^f - v_{ij}^b, 0\right) r_k}$$

$$c_{ij}^d = \frac{max\left(v_{ij}^f - v_{ij}^b, 0\right) r_j}{\sum_{k=1}^{NR} max\left(v_{ij}^f - v_{ij}^b, 0\right) r_k}$$

The normalized contributions to production and consumption sum to 1.

$$\sum_{j=1}^{NR} c_{ij}^p = 1$$

$$\sum_{j=1}^{NR} c_{ij}^d = 1$$

They compare the relative importance of each reaction to the production or consumption rates of a species [5].

4. CHLORINATED HYDROCARBONS

4.1 CHLORINE ELECTRIC STRUCTURE AND CHEMICAL NATURE

Chlorine belongs to the VIIA group of the periodic table and it has 17 electrons organized in the eletronic structure $1s^2 2s^2 2p^6 3s^2 3p^5$. This means that it reacts in order to couple the 3p unpaired electrons. When the outer shell is closed, electric structure of argon is obtained. This behaviour forces chlorine to have high electron affinity and electronegativity. The electronegativity of Cl is 3.16 on the Pauling scale, while C, O and H have 2.55, 3.44 and 2.2 respectively l.
Reacting with hydrocarbons and oxigenated hydrocarbons, Cl "replaces" H to form the relative chlorinated compounds; for example from CH_4, C_2H_2, CH_2CHCH_3 and C_6H_6 it can form CH_3Cl, C_2HCl, CH_2CHCH_2Cl and C_6H_5Cl. The same happens with oxigenated hydrocarbons, for example: CH_2O yields CHClO and CCl_2O (phosgene), CH_3CHO forms CH_3CClO, $CH_2ClCCLO$, $CHCl_2CCLO$ and CCl_3CClO. As clear from these examples, Cl maintains a single bond structure in chlorinated hydrocarbons, due to its higher electronegativity compared to C. When combine with the more electronegative oxygen, Cl exhibits multiple bonds, as a consequence of the participation of its electrons in 3s and 3p orbitals. Therefore, CL can form as many as 7 bonds, which corresponds to the full pairing of its electrons in the M shell. Examples can be species like: ClO, Cl_2O, Cl_2O_3, ClO_2, Cl_2O_4, Cl_2O_3, ClO_4 and Cl_2O_7.
However, these species all have largely positive enthalpies of formation [12], therefore they hardly form.

Table 4.1 reports a series of chlorinated species, C_1 and C_2 hydrocarbons and other compounds, with their enthalpies of formation (ΔH^o_f). Moreover, also C-H and C-Cl bond dissociation energies are listed. Some important features can be observed. i) Increasing chlorination tends to stabilize the hydrocarbon molecule or radical species. For example, the enthalpies of formation of increasingly chlorinated methanes decrease from -75 for CH_4 to -84, -95, -97, and -84 kJ/mol for CH_3Cl, CH_2Cl_2, $CHCl_3$, and CCl_4, respectively. A similar behaviour can be observed in chlorinated C_2 alkanes, alkenes and alkynes. Also for C_1 radicals the enthalpies of formation decrease from 146 kJ/mol for CH_3 to 69 kJ/mol for CCl_3. ii) Increasing chlorination decreases the C-H bond dissociation energies (BDE) of hydrogens in alkanes ([13]. For example, for the case of chlorinated methanes, the C-H BDEs decrease from 435 kJ/mol in CH_4 to 415 kJ/mol in CH_3Cl, to 397 kl/mol in CH_2Cl_2 and to 384 kJ/mol in $CHCl_3$) in chlorinated ethanes, the chlorine substitution increases the C-H BDE at the β

positions. For example, although the BDE of α-H in C_2H_5Cl decreases to about 406 kJ/mol, from 418 kJ/mol in C_2H_6, the BDE of β-Hs increase to about 426 kJ/mol. Additional chlorination of a carbon atom ultimately leads to the strengthening of the β C-H bond to 435 kJ/mol, a value that is virtually identical to that of CH_4. These results have important implications for the rates and channels of elementary reaction involving CHCs. For example, the attack of electronegative radicals, such as Cl, O, and OH on chlorinated alkanes (C_2 and higher) results in the preferential abstraction of hydrogens sited in α, and this, in turns, leads to the production of chlorinated alkenes by subsequent reactions of the product via β-scission or by hydrogen atom abstraction by O_2 ($R+O_2$=Olefin+HO_2).

Table 4.1

Species	**Δh^o_f**	**αC-H**	**βC-H**	**αC-Cl**	**βC-Cl**	**C-C**
H	52.1					
Cl	28.9					
HCl	-22.1					
ClO	29.2(24.4)					
ClOO	33.6(23.1)					
$ClOO_2$	-16.7					
ClO_3	-52					
Cl_2O	-19.5					
Cl_2O_2	-31					
Cl_2O_3	-34					
HOCl	-18					
$COCl_2$	-52.6			77.5		
COCl	-6.48					
CH_4	-17.9	104				
CH_3	34.8					
CH_3Cl	-20.1	99		84		
CH_2Cl	27.1					
CH_2Cl_2	-22.8	95		79		
$CHCl_2$	19.5					
$CHCl_2O_2$	-1.33					
$CHCl_3$	-23.3	92		72		
CCl_3	16.6					
$CCHO_2$	-0.71					
CHCl	80.					

CCl_2	53.					
CCl_4	-20.2	68				
C_2H_5Cl	-27.2	97	102	84	89	
CH_3CHCl	18.2					
CH2ClCH$_2$	22.9					
CH3CHCl$_2$	-32.1	94	104	79		87
CH_3CCl_2	10.3					
$CHCl_2CH_2$	20.2					
CH_3CCl_3	-33.6	104		72		85
CH_3CCl_2	10.2					
CCl_3CH_2	18.8					
CH_2ClCH_2Cl	-32.4	97		84		86
$CH_2ClCHCl$	13.1					
$CH_2ClCHCl_2$	-35.2	93	97	77	84	83
$CH_2ClCCl2$	6.05					
$CHCl_2CHCl$	10.3					
CH_2ClCCl_3	-35.4	98		69	82	78
CCl_3CHCl	11.1					
$CHCl_2CHCl_2$	-36.1	95		75		77
$CHCl_2CCl_2$	8.45					
C_2HCl_5	-35.2	94		72	75	72
C_2Cl_5	7.34					

Table 4.1: Enthalpies of formation and bond dissociation energies of C_1 and C_2 chlorinated hydrocarbons and select chlorinated species' (values given in kcal/mol). Boldfaces represent stable species [13].

4.2 CHLORINE THERMOCHEMISTRY

Normally pollutant emissions are controlled by kinetics or rate limitations in system of practical interest. However can be fundamental understand what happens at system equilibrium and what are the products that can form as a consequence of CHC combustion.

In figure 4.1 we can see equilibrium product distributions associated with the oxidation and pyrolysis of CH_4 and CH_3Cl, respectively as a function of temperature for oxygen rich (equivalence ratio Φ=0.5), near stoichiometric (Φ =1.1) and fuel rich (Φ =2.0) conditions. For clarity only the most significant species are prensented in the figures, i.e. those with a mole fraction of the order greater or equal than 10^{-8}.

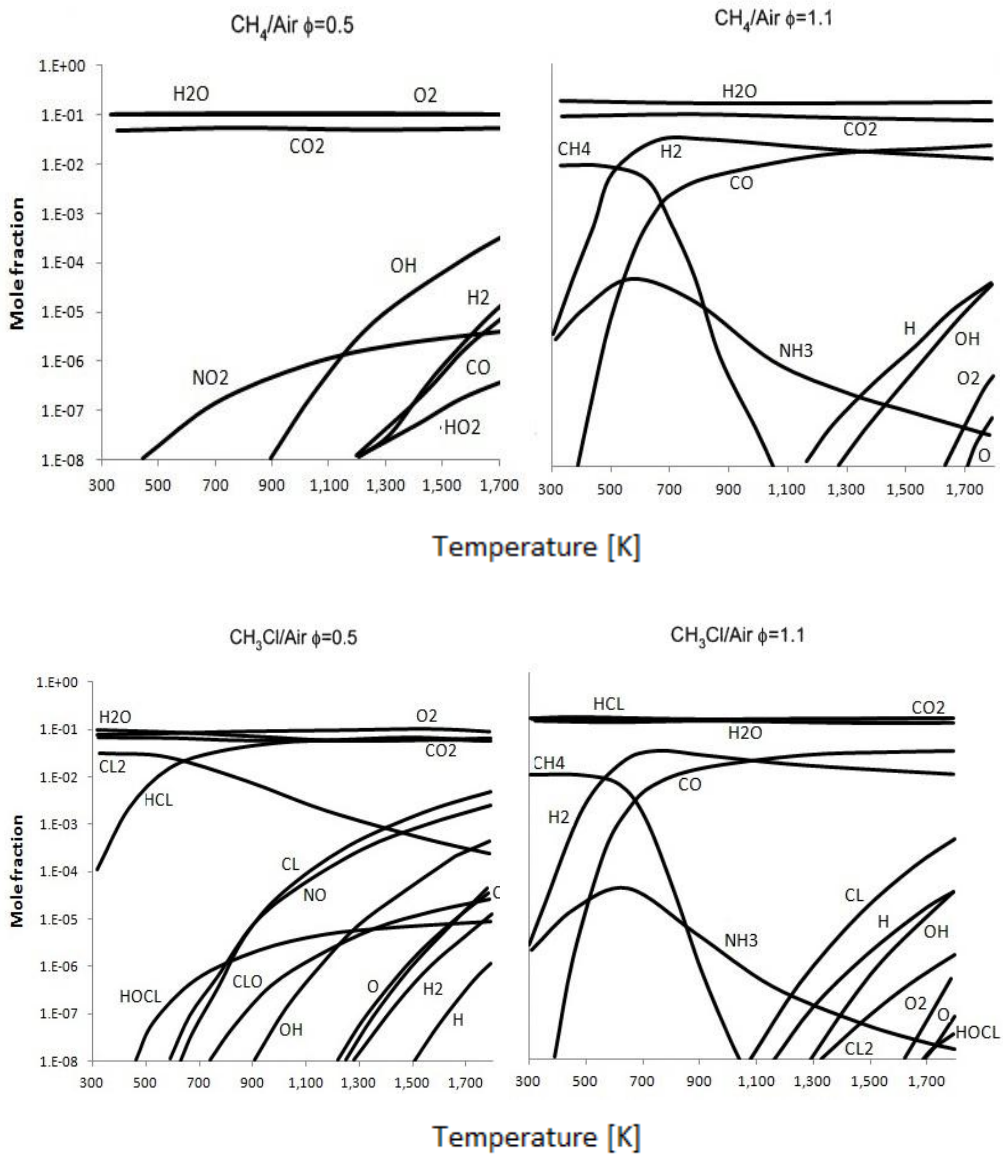

Figure 4.1: Equilibrium product distributions in methane and chloromethane combustion [13].

From figure 4.1 is also clear as Cl/H ratio affect greatly the variety of products and their distribution at the equilibrium. As it shown in the figures, the number of combustion species present at the equilibrium is significantly increased . If we look at figure 4.1 we can note that HCl is the main product, for chlorine-containing system, especially when overall H/Cl ratio is greater than 1. When there is excess of oxygen, the formation of Cl_2 is promoted, but increasing

temperature can favor its dissociation in atomic chlorine. So at the equilibrium Cl_2 mole fraction decrease. Increasing Cl/H ratio also increases the level of HCl relative to H_20 and render HCl as the major combustion product. Looking at figure 4.1, it's easy to note that formation of chlorinated aromatics, polyaromatics, such as dioxins and furans is not predicted from equilibrium considerations. Consequently, their production must be dominated by processes that are limited by reaction kinetics.

5. KINETIC MECHANISM

Three different modules are implemented in the mechanism discussed in the following: 1) the syngas mechanism H2/CO [14,15], 2) the HCl/Cl2 mechanism [9], 3) the CH3Cl mechanism developed in this study and the C_1-C_3 mechanism [8]. Only the HCl/Cl2 and CH3Cl mechanism will be discussed in the following.Each module is composed of a set of reactions together with their rate constants in the usual Arrhenius form ($k=\boldsymbol{A}\ T^{n}\ exp(-\boldsymbol{E_a}/RT)$) as discussed in Section 2.

5.1 CHEMISTRY OF HCL AND CL_2 SYSTEMS

The first module here discussed is the HCl/Cl_2 set of reactions.
A system of 25 species and 102 reactions was obtained by adding the HCl/Cl2 sub-mechanism to the syngas mechanism, and validated through selected experimental data.
Thermodynamic parameters for the chlorine-containing species are obtained from the work of Pelucchi et al. [9] based on the Active Thermochemical Tables (ATcT) approach. ATcT outputs, in form of tables of enthalpies of formation, heat capacities, entropies, and enthalpy increments, covering the range 298–6000 K, were fitted to 7-term polynomials (see chapter 3.2) using the NASA program of McBride and Gordon [16]**.**

Table 5.1.
Detailed Mechanism for HCL/CL_2 Reaction System

ID	Reaction	A	N	Ea
1.	H+CL+M=HCL+M	2.00E+23	-2.45	0.0
	H_2/ 2.00/CL_2/ 2.00/N_2/ 2.00/			
2.	CL+H_2=HCL+H	9.50E+07	1.72	3060.0
3.	HCL+O=CL+OH	5.90E+05	2.11	4024.0
4.	HCL+OH=CL+H_2O	4.10E+05	2.12	-1284.0
5.	CL+H_2O_2=HCL+HO_2	6.60E+12	0.00	1950.0
6.	CL+HO_2=HCL+O_2	7.50E+14	-0.63	0.0
7.	CL+HO_2=CLO+OH	3.80E+13	0.00	1200.0
8.	CL+O_3=CLO+O_2	1.50E+13	0.00	417.0
9.	CL+CL+M=CL_2+M	2.30E+19	-1.50	0.0
	H_2/ 2.00/CL_2/ 6.90/N_2/ 2.00/			
10.	CL_2+H=HCL+CL	8.60E+13	0.00	1172.0
11.	CL_2+O=CL+CLO	4.50E+12	0.00	3279.0
12.	CL_2+OH=HOCL+CL	2.20E+08	1.35	1480.0

13.	CL+OH+M=HOCL+M	1.20E+19	-1.43	0.0
14.	HOCL=CLO+H	8.10E+14	-2.09	93690.0
15.	HOCL+H=CLO+H_2	4.40E-04	4.89	425.0
16.	HOCL+H=HCL+OH	6.10E+07	1.96	421.0
17.	HOCL+O=CLO+OH	3.30E+03	2.90	1592.0
18.	HOCL+OH=CLO+H_2O	1.30E+00	3.61	-2684.0
19.	HOCL+HO_2=CLO+H_2O_2	8.80E-07	5.35	6978.0
20.	HOCL+CL=HCL+CLO	3.60E-01	4.07	-337.0
21.	CLO+H=CL+OH	3.80E+13	0.00	0.0
22.	CLO+H=HCL+O	8.40E+12	0.00	0.0
23.	CLO+O=CL+O_2	1.50E+13	0.00	-219.0
24.	CLO+OH=HCL+O_2	3.50E+05	1.67	-3827.0
25.	CLO+HO_2=HOCL+O_2	7.80E+03	2.40	5110.0
26.	CLO+HO_2=HCL+O_3	4.60E+03	2.05	1699.0
27.	CLO+HO_2=CLOO+OH	4.60E+05	1.80	2116.0
28.	CLO+HO_2=OCLO+OH	1.30E+03	2.32	5099.0
29.	CLO+CLO=CL_2+O_2	6.60E+10	0.66	3760.0
30.	CLO+CLO=CL+CLOO	8.20E+10	0.77	4308.0
31.	CLO+CLO=CL+OCLO	3.80E+13	0.01	5754.0
32.	CLO+O(+M)=OCLO(+M)	2.60E+13	-0.03	-85.0
	LOW/ .3100E+28 -4.100 835.0/			
33.	OCLO(+M)=CL+O_2(+M)	1.10E+16	-0.28	58756.0
	LOW/ .9900E-23 11.000 33100.0/			
34.	OCLO+H=CLO+OH	4.70E+13	0.00	0.0
35.	OCLO+O=CLO+O_2	5.20E+07	1.45	876.0
36.	OCLO+OH=HOCL+O_2	3.30E+04	2.07	-4102.0
37.	OCLO+CLO=CLOO+CLO	6.00E+01	2.80	155.0
38.	CL+O_2(+M)=CLOO(+M)	1.00E+14	0.00	0.0
	LOW/ .6000E+29 -5.340 1341.0/			
39.	CLOO+H=CLO+OH	3.40E+13	0.00	0.0
40.	CLOO+O=CLO+O_2	1.50E+12	0.00	1910.0
41.	CLOO+OH=HOCL+O_2	2.00E+12	0.00	0.0
42.	CLOO+CL=CL_2+O_2	1.30E+14	0.00	0.0
43.	CH_2O+CL=HCO+HCL	4.90E+13	0.00	68.0
44.	CH_2O+CLO=HCO+HOCL	7.20E+10	0.79	5961.0
45.	HCO+CL=CO+HCL	1.00E+14	0.00	0.0
46.	HCO+CL_2=CLCHO+CL	3.80E+12	0.00	70.0
47.	HCO+CLO=HOCL+CO	3.20E+13	0.00	0.0
48.	CO+CLO=CO_2+CL	2.40E+05	2.02	10500.0
49.	CLCHO+H=CLCO+H_2	9.90E+05	2.25	3861.0
50.	CLCHO+H=HCO+HCL	1.10E+06	2.12	6902.0
51.	CLCHO+OH=CLCO+H_2O	2.20E+13	0.00	2822.0
52.	CLCHO+O=CLCO+OH	4.20E+11	0.57	2760.0
53.	CLCHO+CL=CLCO+HCL	7.20E+12	0.00	1620.0

54.	CL+CO+M=CLCO+M	1.20E+24	-3.80	0.0
55.	CLCO+H=CO+HCL	1.00E+14	0.00	0.0
56.	CLCO+O=CO+CLO	1.00E+14	0.00	0.0
57.	CLCO+O=CO_2+CL	1.00E+13	0.00	0.0
58.	CLCO+OH=CO+HOCL	3.30E+12	0.00	0.0
59.	CLCO+O_2=CO_2+CLO	7.90E+10	0.00	3300.0
60.	CLCO+CL=CO+CL_2	6.60E+13	0.00	1400.0

Reaction rate constant k = $A \cdot T^n \cdot e^{-Ea/RT}$; units in cm^3/mol/ s.

As stated before an high chlorine content can ihnibit ignition, lower laminar flame speed and enhance flame quenching, also in presence of syngas. Features of such mechanism have been deeply discussed by Pelucchi et al. [9], highlighting nowadays open questions and the need of a wider set of experimental data.
The inhibition takes place through simple cycles [9], initiated by chain propagating steps such as

$$HCL + H = H_2 + CL \tag{R2b}$$

$$HCL + OH = H_2O + CL \tag{R4}$$

ended by termination reaction like

$$CL + H + M = HCL + M \tag{R1}$$

$$CL + HO_2 = HCL + O_2 \tag{R6}$$

The reactions which generate Cl can be driven in reverse way or be equilibrated in the post-flame zone, when Cl atom concentration increase.
Under these conditions ihnibition is significantly reduced.
This ihnibition cycle compete with the propagation one

$$CL + HO_2 = CLO + OH \tag{R7}$$

$$CLO + CO = CL + CO_2 \tag{R48}$$

The competition between propagation and termination cycles determines if the chloride has an ihnibiting or promoting effect. The inhibition process is

sensitive to the branching ratio of the Cl + HO_2 reaction, which is well established only at low temperatures [17].
HCl thermal dissociation (R1 backward-R1b) has been measured in many shock tube studies [19-23] at high temperatures. In the present work, we chose the determination of Schading and Roth [18] in shock tube, who extended the temperature range down to 2500 K. Their measured value of k1b agrees within 50% with the previous studies, while the rate constant from Baulch et al. and Schading and Roth, does not work well at low temperature. Here recombination of H and Cl may become relevant and more reliable values for the reaction is needed.
The reaction between HCl and H (R2b) has been measured over a broad temperature range in both directions [24-31]. It has been chosen the rate constant by Kumaran et al. [32] that provides a good representation of the available measurements.

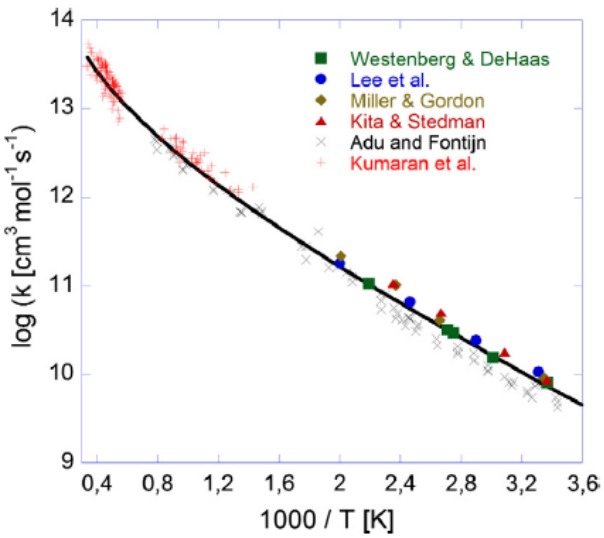

Figure 5.1.0: Arrhenius plot for the reaction CL+H_2. Experimental results (symbol) and rate constant recommended by Kumaran et al. (solid line) [9].

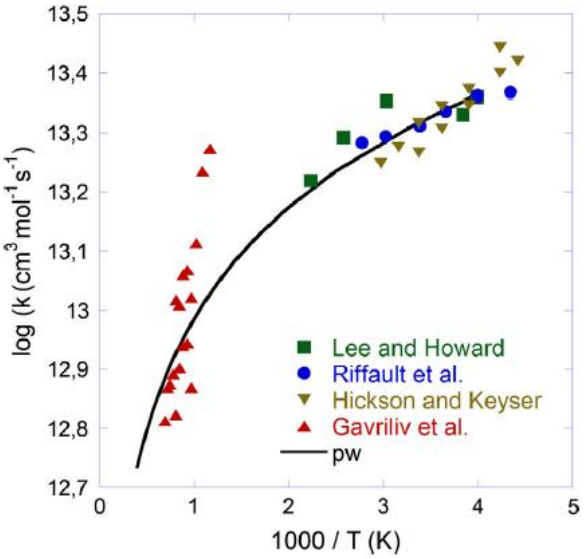

Figure 5.1.1: Arrhenius plot for the reaction CL + HO_2. Experimental results (symbols). The data from Gavriliv et al. is obtained for the reverse reaction and then converted through equilibrium constant. The solid line represent a best fit to the experimental data [9].

The reaction of HCl with OH which has been studied by Husain et al. [33],Ravishankara et al. [34] and Bryukov et al. [35], obtaining data above 500 K, present some scatter at higher temperatures, but the results of Bryukov et al. are in agreement with most data within the uncertainties.
Cl and HO_2 can react in two different way. The first path is a chain terminating step (R6), the second a thermo-neutral chain propagating step (R7). The two channels can compete each other affecting significantly the ihnibition effect of chlorine species on fuel oxidation. The rate chosen from Atkinson et al. [36] for k4 and k5 is based on the studies of Lee and Howard, Riffault et al. and Hickson and Keyser for the low temperature (230–420 K). The extrapolation to higher temperatures is uncertain. Gavriliv et al. [37] reported a rate constant for the HCl + O_2 reaction (R6b) of 5x10^12exp(-26000/T) cm^3 mol^{-1} s^{-1} for the temperature range 853–1423 K. Extrapolation of the low temperature values of k6 were obtained by convertion of measured values of k6b, through the use of equilibrium constant.
Oxidation of CO to CO_2 may be facilitated by reactions with chlorine species as in R48.

Louis et al. [38] calculated the rate constant for R6 from ab initio theory. Their value is well below the upper limit at 587 K reported by Clyne and Watson [39], but an experimental verification is desirable.
The reactions mentioned so far are fundamental to describe completely the reagent system, especially when hydrocarbons are not present, but they loss importance when hydrocarbons, in particular chlorinated hydrocarbons, are the main fuel and the principal source of chlorine in the system. More specifically these reactions don't control anymore the inibition cycles and the fuel consumption. For example the recombination reaction

$$CL + CL + M = CL_2 + M \qquad \text{(R9)}$$

show also in methyl-chloride systems some sensitivities, especially in the flame systems.
The recombination of atomic Cl to form Cl_2 has been measured at low temperature in the forward direction and at high temperature in shock tubes in the reverse direction. The results were evaluated by Lloyd [40] and Baulch et al. [41]. The data from Jacobs and Giedt are in good agreement and these data form the basis for the recommendation of Lloyd. The group of data reported by Blauer et al. [42], indicate a rate constant for Cl + Cl + Ar that is about a factor of five below the bulk data.
Baulch et al. chose to disregard most of the high temperature results for Cl_2 dissociation, claiming that high levels of Cl_2 made it difficult to separate the effects of Ar and Cl_2 as collision partners, and based their evaluation on the results of Blauer et al. As said before predicted flame speeds and ignition delays for Cl_2/H_2, but also CH_3Cl, mixtures are sensitive to the choice of reaction costant. The results [9] indicate a dissociation rate for Cl_2 that is higher than that proposed by Baulch et al. [41] and perhaps even faster than the recommendation of Lloyd. Our proposed rate constant is in reasonable agreement with the high-temperature recommendation of Lloyd (converted to values for the Cl + Cl recombination through the equilibrium constant) and with the data for low temperature.

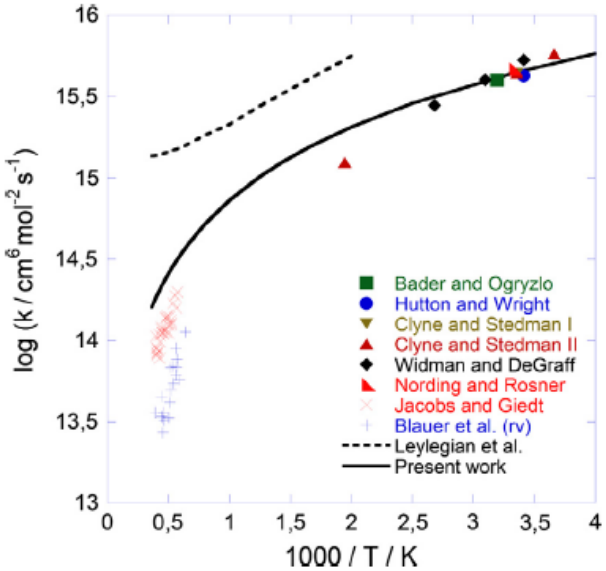

Figure 5.1.2: Arrhenius plot for the reaction Cl + Cl + M. Experimental results (symbols). The data from Jacobs and Giedt and from Blauer et al. were obtained for the reverse reaction and converted through the equilibrium constant. The solid line represents the preferred rate constant in the work, while the dashed line represents the recommendation of Leylegian et al. [9].

5.2 CHEMISTRY OF CH_3CL SYSTEMS

5.2.1 KINETIC SCHEME GENERATION

As for the HCL/Cl_2 subsystem, a kinetic model is created also for the CH_3Cl system.

The reaction mechanism was developed by considering systematically all plausible elementary pyrolysis and oxidation reactions of CH_3CL and their parent species consistent with experimental observations and the principles of chemical kinetics.

Linking this mechanism to the previous one (table 5.1) a new system of 75 species in 686 reactions was obteined. This kinetic scheme of methyl-chloride system is presented in table 5.2, together with a set of rate parameters for the forward reactions. The values of reverse reation are automatically determined and fitted during the kinetic mechanism generation by the OpenSMOKE++ framework through the the equilibrium constant.

Table 5.2
Detailed Mechanism for CH_3CL Reaction System

ID	Reaction	A	n	Ea
62.	$CL+CH_4=HCL+CH_3$	5.13E+06	2.10	1580.0
63.	$CH_3CL=CH_2+HCL$	1.06E+14	0.00	102700.0
64.	$CH_3CL+H=CH_3+HCL$	7.40E+13	0.00	9300.0
65.	$CH_3CL+CLO=CH_2CL+HOCL$	3.03E+11	0.00	10700.0
66.	$CH_3CL+CH_2=C_2H_5CL$	7.85E+31	-6.15	5830.0
67.	$CH_3CL+CH_2=C_2H_4+HCL$	1.60E+18	-1.47	2710.0
68.	$CH_3CL+CH_2=C_2H_5+CL$	3.09E+07	1.70	520.0
69.	$CH_2CL_2=CHCL+HCL$	1.81E+37	-7.43	85730.0
70.	$CH_2CL_2+H=CH_2CL+HCL$	7.00E+13	0.00	7270.0
71.	$CH_2CL_2+CH_3=CH_3CL+CH_2CL$	1.40E+11	0.00	4900.0
72.	$CH_2CL+H=CH_3+CL$	1.02E+15	-0.22	310.0
73.	$CH_2CL+H=CH_2+HCL$	9.48E+04	1.91	2600.0
74.	$CH_2CL+O_2=CH_2O+CLO$	3.61E+14	-1.27	4810.0
75.	$CH_2CL+O_2=CLCHO+OH$	4.00E+13	0.00	34000.0
76.	$CH_2CL+O=CH_2CLO$	1.29E+15	-1.98	1100.0
77.	$CH_2CL+O=CH_2O+CL$	5.59E+13	-0.13	710.0
78.	$CH_2CL+OH=CH_2O+HCL$	1.24E+22	-2.72	3860.0
79.	$CH_2CL+OH=CH_3O+CL$	2.00E+12	0.29	3270.0
80.	$CH_2CL+HO_2=CH_2CLO+OH$	1.00E+13	0.00	0.0
81.	$CH_2CL+CLO=CLCHO+HCL$	4.13E+19	-2.22	2360.0
82.	$CH_2CL+CLO=CH_2CLO+CL$	4.15E+12	0.07	11100.0
83.	$CH_2CL+CH_2CL=CH_2CLCH_2+CL$	9.34E+29	-4.95	14070.0
84.	$CH_2CL+CH_2CL=C_2H_3CL+HCL$	3.75E+35	-6.73	13160.0
85.	$CH_2CL+CH_3=C_2H_4+HCL$	3.50E+28	-4.49	9180.0
86.	$CH_2CL+CH_3=C_2H_5+CL$	9.27E+19	-2.07	10130.0
87.	$CH_2CL+CHCL_2=CH_2CCL_2+HCL$	3.75E+36	-7.22	13620.0
88.	$CH_2CL+CHCL_2=CLCHCHCL+HCL$	1.22E+37	-7.20	13640.0
89.	$CHCL_2+H=CH_2CL+CL$	1.25E+14	-0.03	570.0
90.	$CHCL_2+CH_3=CH_3CHCL+CL$	2.74E+25	-3.45	12810.0
91.	$CHCL_2+CH_3=C_2H_3CL+HCL$	1.35E+30	-4.96	11550.0
92.	$CHCL_2+CHCL_2=C_2H_2CL_3+CL$	1.36E+30	-5.23	14180.0
93.	$CHCL_2+CHCL_2=C_2HCL_3+HCL$	6.72E+35	-7.11	13210.0
94.	$CHCL_3=CCL_2+HCL$	5.20E+12	0.00	51500.0
95.	$CHCL_3+H=CHCL_2+HCL$	3.60E+12	0.00	6200.0
96.	$CHCL+O=CLCHO$	1.00E+13	0.00	0.0
97.	$CHCL+O_2=CLCHO+O$	1.50E+13	0.00	2860.0
98.	$CHCL+O_2=CO+HOCL$	1.20E+11	0.00	0.0
99.	$CCL_4+H=CCL_3+HCL$	2.00E+13	0.00	4500.0
100.	$CCL_4+OH=CCL_3+HOCL$	6.00E+11	0.00	4610.0

101.	$CCL_4+O=CCL_3+CLO$	3.00E+11	0.00	4400.0
102.	CLCHO=HCO+CL	1.99E+15	0.00	77600.0
103.	CLCHO=CO+HCL	1.10E+30	-5.19	92960.0
104.	$CLCHO+H=CH_2O+CL$	6.99E+14	-0.58	6360.0
105.	$CLCHO+CH_3=CLCO+CH_4$	2.50E+13	0.00	6000.0
106.	$CLCHO+CH_3=HCO+CH_3CL$	1.50E+13	0.00	8800.0
107.	$CLCHO+O_2=CLCO+HO_2$	1.00E+13	0.00	500.0
108.	$C_2H_3CL+H=C_2H_4+CL$	1.55E+13	-0.02	5840.0
109.	$C_2H_3CL+H=C_2H_3+HCL$	1.20E+12	0.00	15000.0
110.	$C_2H_3CL+O=CH_3+CLCO$	1.92E+07	1.80	220.0
111.	$C_2HCL_3+H=CH_2CLCCL_2$	1.51E+23	-4.18	7520.0
112.	$C_2HCL_3+H=C_2H_2CL_3$	2.87E+22	-4.09	10890.0
113.	$C_2HCL_3+H=CH_2CCL_2+CL$	1.45E+13	-0.01	5830.0
114.	$C_2HCL_3+H=CLCHCHCL+CL$	7.37E+12	-0.01	9220.0
115.	$CH_2CCL_2=C_2HCL+HCL$	1.45E+14	0.00	69220.0
116.	$CLCHCHCL=C_2HCL+HCL$	7.26E+13	0.00	69100.0
117.	$CH_2CCL_2+H=C_2H_3CL+CL$	7.21E+12	0.00	7510.0
118.	$CLCHCHCL+H=C_2H_3CL+CL$	3.44E+13	0.03	5890.0
119.	$CH_2CLCH_2CL+H=CH_2CLCH_2+HCL$	1.00E+14	0.00	7900.0
120.	$CH_2CLCH_2+H=C_2H_4+HCL$	1.00E+14	0.00	0.0
121.	$CH_3CHCL+CL=C_2H_3CL+HCL$	2.00E+13	0.00	0.0
122.	$CLCH_2CHCL+H=C_2H_3CL+HCL$	1.00E+14	0.00	0.0
123.	$C_2H_5CL+H=C_2H_5+HCL$	1.00E+14	0.00	7900.0
124.	$CH_2CLCH_2CL=CH_2CLCH_2+CL$	8.00E+15	0.00	83000.0
125.	$CH_2CL+CH_2CL=CH_2CLCH_2CL$	7.84E+45	-10.21	13150.0
126.	$CH_2CL+H=CH_3CL$	3.04E+25	-4.47	3490.0
127.	$CH_3CL=CH_3+CL$	1.90E+37	-6.91	90540.00
128.	$CH_2CL_2=CH_2CL+CL$	6.67E+14	0.00	79500.0
129.	$CHCL_3=CHCL_2+CL$	1.90E+16	0.00	77000.0
130.	$CCL_4=CCL_3+CL$	4.50E+15	0.00	70000.0
131.	$CH_3CHCL_2=CH_3CHCL+CL$	1.50E+16	0.00	81000.0
132.	$C_2H_5CL=C_2H_5+CL$	1.67E+15	0.00	83000.0
133.	$CH_2CL+CH_3=C_2H_5CL$	3.27E+40	-8.49	10590.0
134.	$C_2H_3Cl3=CL_2CHCH_2+CL$	8.00E+15	0.00	76000.0
135.	$CLCHCCL_3=>CL+CL+CLCHCHCL$	8.00E+15	0.00	76500.0
136.	$CL_2CHCHCL_2=C_2H_2CL_3+CL$	1.00E+16	0.00	81000.0
137.	$C_2HCL_5=>CL+0.5CL_2CCHCL_2+0.5CL_3CCHCL$	2.00E+16	0.00	76500.0
138.	$C_2H_3CL+M=C_2H_3+CL+M$	2.50E+18	0.00	78000.0
139.	$CL+CH_2CLCH_2CL=HCL+CLCH_2CHCL$	4.80E+13	0.00	3100.0
140.	$CL+CH_3CCL_3=>HCL+CLCHCHCL+CL$	2.00E+13	0.00	3100.0
141.	$CL+CL_2CHCHCL_2=>HCL+CL_2CCHCL_2$	1.50E+13	0.00	3100.0
142.	$CL+CLCHCCL_3=>HCL+CL_3CCHCL$	1.00E+13	0.00	3500.0
143.	$CL+C_2HCL_5=>HCL+C_2CL_5$	6.00E+12	0.00	3500.0
144.	$CL+C_2H_5CL=HCL+CH_2CLCH_2$	1.00E+13	0.00	3000.0

145.	$CL+C_2H_5CL=HCL+CH_3CHCL$	5.00E+12	0.00	3000.0
146.	$CL+CH_3CL=HCL+CH_2CL$	3.00E+13	0.00	3400.0
147.	$CL+C_2H_4=HCL+C_2H_3$	5.00E+13	0.00	7000.0
148.	$CL+C_2H_3CL=HCL+CHCLCH$	5.00E+13	0.00	7000.0
149.	$CL+CHCL_3=HCL+CCL_3$	7.00E+12	0.00	3400.0
150.	$CL+CH_2CL_2=HCL+CHCL_2$	1.81E+12	0.00	2186.0
151.	$CL+CH_3CHCL_2=HCL+CH_3CCL_2$	1.00E+13	0.00	3400.0
152.	$CL+CH_3CHCL_2=HCL+CL_2CHCH_2$	9.00E+12	0.00	1900.0
153.	$CL+C_2H_3Cl_3=HCL+C_2H_2CL_3$	2.50E+12	0.00	3600.0
154.	$CH_3+CL_2=CH_3CL+CL$	1.00E+13	0.00	2300.0
155.	$CH_2CL+CL_2=CH_2CL_2+CL$	4.00E+12	0.00	3000.0
156.	$CHCL_2+CL_2=CHCL_3+CL$	9.00E+11	0.00	5000.0
157.	$CCL_3+CL_2=CCL_4+CL$	5.00E+11	0.00	6000.0
158.	$CL+C_2H_5CL=>CL_2+C_2H_5$	1.00E+14	0.00	21500.0
159.	$CL+CH_2CLCH_2CL=>CL_2+CH_2CLCH_2$	2.00E+14	0.00	21300.0
160.	$CL+CL_2CHCHCL_2=>CL_2+CLCHCHCL+CL$	1.00E+14	0.00	20000.0
161.	$CL+CLCHCCL_3=>CL_2+CLCHCHCL+CL$	1.00E+14	0.00	20000.0
162.	$CL_2+CL_2CHCH_2=CL+C_2H_3Cl_3$	6.30E+11	0.00	41000.0
163.	$CL+C_2HCL_5=>CL_2+C_2HCL_3+CL$	3.00E+14	0.00	20000.0
164.	$H+C_2H_3CL=>CH_2CLCH_2$	1.00E+13	0.00	0.0
165.	$CL+C_2H_3CL=CL_2CHCH_2$	1.00E+13	0.00	1000.0
166.	$CH_3+C_2H_3CL=>C_3H_6+CL$	2.00E+11	0.00	7600.0
167.	$CH_2CL+C_2H_3CL=CLCH_2CLCHCH_2$	1.00E+10	0.00	6000.0
168.	$C_2H_3+C_2H_3CL=>C_4H_6+CL$	5.00E+11	0.00	5000.0
169.	$CHCLCH+C_2H_4=>C_4H_6+CL$	1.00E+11	0.00	9000.0
170.	$CHCLCH+C_2H_2=>C_4H_4+CL$	1.00E+11	0.00	5000.0
171.	$CHCLCH+C_4H_4=>C_6H_6+CL$	1.50E+11	0.00	5000.0
172.	$CHCLCH+C_2H_3CL=>CLCHCHCL+C_2H_3$	1.00E+11	0.00	11000.0
173.	$CH_2CLCH_2+C_2H_3CL=>C_4H_7CL+CL$	3.00E+11	0.00	7600.0
174.	$CH_3CHCL+C_2H_3CL=>C_4H_7CL+CL$	3.00E+11	0.00	7600.0
175.	$CH_2CLCH_2=C_2H_4+CL$	1.00E+14	0.00	19000.0
176.	$CH_3CHCL=C_2H_3CL+H$	1.00E+14	0.00	39000.0
177.	$CLCH_2CHCL=C_2H_3CL+CL$	1.50E+13	0.00	19000.0
178.	$CH_3CCL_2=>C_2H_3CL+CL$	2.00E+12	0.00	18000.0
179.	$C_2H_2CL_3=CLCHCHCL+CL$	2.00E+12	0.00	18300.0
180.	$CL_3CCHCL=>C_2HCL_3+CL$	1.00E+13	0.00	18000.0
181.	$CL_2CCHCL_2=>C_2HCL_3+CL$	1.00E+13	0.00	18000.0
182.	$C_2CL_5=>VCL_4+CL$	1.00E+13	0.00	18000.0
183.	$CHCLCH=C_2H_2+CL$	5.00E+12	0.00	23000.0
184.	$CLCH_2CLCHCH_2=CH_2CHCH_2CL+CL$	1.00E+13	0.00	19000.0
185.	$CLCH_2CH_2CHCL=>C_3H_4CL_2+H$	1.00E+14	0.00	37000.0
186.	$CLCH_2CH_2CHCL=CH_2CL+C_2H_3CL$	1.00E+14	0.00	32000.0
187.	$C_2H_5CL=C_2H_4+HCL$	2.50E+13	0.00	58000.0
188.	$CH_2CLCH_2CL=C_2H_3CL+HCL$	3.60E+13	0.00	58000.0

189.	$CH_3CHCL_2=C_2H_3CL+HCL$	4.00E+13	0.00	54300.0
190.	$C_2H_3Cl_3=CLCHCHCL+HCL$	5.80E+13	0.00	54000.0
191.	$CH_3CCL_3=CLCHCHCL+HCL$	2.00E+13	0.00	58000.0
192.	$CL_2CHCHCL_2=HCL+C_2HCL_3$	1.30E+13	0.00	58000.0
193.	$CLCHCCL_3=HCL+C_2HCL_3$	1.30E+13	0.00	58000.0
194.	$C_2HCL_5=HCL+VCL_4$	1.00E+13	0.00	58000.0
195.	$C_4CL=>HCL+C_4H_4$	1.00E+13	0.00	62000.0
196.	$C_4H_7CL=>HCL+C_4H_6$	1.30E+13	0.00	58000.0
197.	$C_2H_3CL=C_2H_2+HCL$	4.00E+13	0.00	67000.0
198.	$CHCL_2+CHCL_2=>CL_2CHCHCL_2$	1.50E+13	0.00	0.0
199.	$CCL_3+CCL_3=C_2CL_6$	8.00E+12	0.00	0.0
200.	$CH_2CLCH_2+CH_2CLCH_2=>CLCHCHCHCHCL+H_2+H_2$	1.00E+13	0.00	0.0
201.	$CH_3CHCL+CH_3CHCL=>CLCHCHCHCHCL+H_2+H_2$	5.00E+12	0.00	0.0
202.	$CH_3CHCL+CH_3CHCL=>C_2H_3CL+C_2H_5CL$	1.00E+12	0.00	0.0
203.	$CLCH_2CHCL+CLCH_2CHCL=>C_4H_6CL_4$	5.00E+12	0.00	0.0
204.	$CL_2CHCH_2+CL_2CHCH_2=>C_4H_6CL_4$	5.00E+12	0.00	0.0
205.	$CH_3CCL_2+CH_3CCL_2=>C_4H_6CL_4$	5.00E+12	0.00	0.0
206.	CHCLCH+CHCLCH=>CLCHCHCHCHCL	1.00E+13	0.00	0.0
207.	$CL+CLCH_2CHCL=>CH_3CCL_3$	4.00E+13	0.00	0.0
208.	$CL+CH_3CCL_2=>CH_3CCL_3$	4.00E+13	0.00	0.0
209.	$CL+CL_3CCHCL=>C_2HCL_5$	4.00E+13	0.00	0.0
210.	$CL+CL_2CCHCL_2=>C_2HCL_5$	4.00E+13	0.00	0.0
211.	$CL+C_2CL_5=>C_2CL_6$	4.00E+13	0.00	0.0
212.	CL+CHCLCH=>CLCHCHCL	6.00E+13	0.00	0.0
213.	$CH_3+CHCL_2=>CH_3CHCL_2$	1.00E+13	0.00	0.0
214.	$CH_3+CCL_3=>C_2H_3Cl_3$	1.00E+13	0.00	0.0
215.	$CH_3+CLCH_2CHCL=>C_3H_6CL_2$	1.00E+13	0.00	0.0
216.	$CH_3+CL_2CHCH_2=>C_3H_6CL_2$	1.00E+13	0.00	0.0
217.	$CH_3+CH_3CCL_2=>C_3H_6CL_2$	1.00E+13	0.00	0.0
218.	$CH_3+CHCLCH=>CH_2CHCH_2L$	3.00E+13	0.00	0.0
219.	$CH_2CL+CHCL_2=>CH_3CCL$	3.00E+13	0.00	0.0
220.	$CH_2CL+CCL_3=>CL_2CHCCL_2$	2.40E+13	0.00	0.0
221.	$CH_2CL+CH_2CLCH_2=>CH_6CL_2$	1.70E+13	0.00	0.0
222.	$CH_2CL+CH_3CHCL=>CH_6CL_2$	1.70E+13	0.00	0.0
223.	$CH_2CL+C_2H_3=>CH_2CHCH_2CL$	2.40E+13	0.00	0.0
224.	$CH_2CL+CHCLCH=>C_3H_4CL_2$	2.40E+13	0.00	0.0
225.	$CHCL_2+H=>CH_2C_2$	1.00E+14	0.00	0.0
226.	$CHCL_2+CCL_3=>C_2HCL_5$	2.40E+13	0.00	0.0
227.	$CHCL_2+C_2H_5=>C_3H_6CL_2$	2.00E+13	0.00	0.0
228.	$CHCL_2+C_2H_3=>C_3H_4CL_2$	2.40E+13	0.00	0.0
229.	$CHCL_2+CLCH_2CLCHCH_2=>C_4H_6CL_4$	5.00E+12	0.00	0.0
230.	$CHCL_2+CLCH_2CH_2CHCL=>C_4H_6CL_4$	5.00E+12	0.00	0.0
231.	$CCL_3+H=>CHCL_3$	5.00E+13	0.00	0.0
232.	$CLCH_2CHCL+CL_2CHCH_2=>C_4H_6CL_4$	1.00E+13	0.00	0.0

233.	$CLCH_2CHCL+CH_3CCL_2=>C_4H_6CL_4$	1.00E+13	0.00	0.0
234.	$CL_2CHCH_2+CH_3CCL_2=>C_4H_6CL_4$	1.00E+13	0.00	0.0
235.	$O_2+CH_3CL=HO_2+CH_2CL$	1.00E+14	0.00	49000.0
236.	$O_2+C_2H_5CL=HO_2+CH_3CHCL$	1.00E+14	0.00	46000.0
237.	$O_2+C_2H_5CL=HO_2+CH_2CLCH_2$	1.00E+14	0.00	48000.0
238.	$O_2+CHCLCH=>CO+CO+HCL+H$	2.00E+12	0.00	0.0
239.	$O_2+CH_3CHCL=>C_2H_3CL+HO_2$	1.50E+12	0.00	6000.0
240.	$O_2+C_2H_3CL=>CO+CO+HCL+H+H$	1.00E+13	0.00	36000.0
241.	$CH_2CL+H_2=>CH_3CL+H$	7.16E+11	0.00	13060.00
242.	$CHCL_2+H_2=CH_2CL_2+H$	2.45E+05	2.00	9025.6
243.	$CCL_3+H_2=CHCL_3+H$	4.07E+05	2.00	10025.6
244.	$CH_2CL+CH_4=CH_3CL+CH_3$	2.34E+05	2.00	10668.2
245.	$CHCL_2+CH_4=CH_2CL_2+CH_3$	2.94E+05	2.00	12876.8
246.	$CCL_3+CH_4=CHCL_3+CH_3$	4.88E+05	2.00	13973.1
247.	$H+CH_3CL=H_2+CH_2CL$	3.22E+07	2.00	6525.6
248.	$O+CH_3CL=>OH+CH_2CL$	4.06E+06	2.00	5025.6
249.	$OH+CH_3CL=>H_2O+CH_2CL$	3.50E+06	2.00	-921.1
250.	$HO_2+CH_3CL=>H_2O_2+CH_2CL$	1.62E+05	2.00	14530.4
251.	$HCO+CH_3CL=>CH_2O+CH_2CL$	3.79E+05	2.00	15525.6
252.	$CHCL_2+CH_3CL=>CH_2CL_2+CH_2CL$	1.23E+05	2.00	9025.6
253.	$CCL_3+CH_3CL=CHCL_3+CH_2CL$	2.04E+05	2.00	10025.6
254.	$CH_3O+CH_3CL=>CH_3OH+CH_2CL$	1.28E+05	2.00	3991.6
255.	$CH_3OO+CH_3CL=>CH_3OOH+CH_2CL$	2.28E+05	2.00	15591.6
256.	$O_2+CH_2CL_2=>HO_2+CHCL_2$	3.41E+06	2.00	45025.6
257.	$O+CH_2CL_2=>OH+CHCL_2$	2.71E+06	2.00	5025.6
258.	$OH+CH_2CL_2=>H_2O+CHCL_2$	7.99E+05	2.00	-396.9
259.	$HO_2+CH_2CL_2=>H_2O_2+CHCL_2$	1.08E+05	2.00	14121.2
260.	$HCO+CH_2CL_2=>CH_2O+CHCL_2$	2.53E+05	2.00	15525.6
261.	$CCL_3+CH_2CL_2=>CHCL_3+CHCL_2$	1.36E+05	2.00	10025.6
262.	$CH_3O+CH_2CL_2=>CH_3OH+CHCL_2$	8.56E+04	2.00	3938.1
263.	$CH_3OO+CH_2CL_2=>CH_3OOH+CHCL_2$	1.52E+05	2.00	15538.1
264.	$O_2+CHCL_3=>HO_2+CCL_3$	1.70E+06	2.00	45025.6
265.	$O+CHCL_3=>OH+CCL_3$	1.35E+06	2.00	5025.6
266.	$OH+CHCL_3=>H_2O+CCL_3$	3.99E+05	2.00	-154.9
267.	$HO_2+CHCL_3=>H_2O_2+CCL_3$	5.39E+04	2.00	13932.3
268.	$HCO+CHCL_3=>CH_2O+CCL_3$	1.26E+05	2.00	15525.6
269.	$CHCL_2+CHCL_3=>CH_2CL_2+CCL_3$	4.09E+04	2.00	9025.6
270.	$CH_3O+CHCL_3=>CH_3OH+CCL_3$	4.28E+04	2.00	3913.4
271.	$CH_3OO+CHCL_3=>CH_3OOH+CCL_3$	7.61E+04	2.00	15513.4
272.	$CH_2CL+C_2H_6=>CH_3CL+C_2H_5$	1.62E+05	2.00	7025.6
273.	$CHCL_2+C_2H_6=>CH_2CL_2+C_2H_5$	2.04E+05	2.00	9025.6
274.	$CCL_3+C_2H_6=>CHCL_3+C_2H_5$	3.39E+05	2.00	10025.6
275.	$O_2+C_2H_5CL=>HO_2+.25CH_2CLCH_2+.75CH_3CHCL$	8.52E+06	2.00	45025.6
276.	$H+C_2H_5CL=>H_2+.25CH_2CLCH_2+.75CH_3CHCL$	1.07E+07	2.00	6525.6

277.	$O+C_2H_5CL=>OH+.25CH_2CLCH_2+.75CH_3CHCL$	6.77E+06	2.00	5025.6
278.	$OH+C_2H_5CL=>H_2O+.25CH_2CLCH_2+.75CH_3CHCL$	2.00E+06	2.00	-274.4
279.	$HO_2+C_2H_5CL=>H_2O_2+.25CH_2CLCH_2+.75CH_3CHCL$	2.69E+05	2.00	14025.6
280.	$HCO+C_2H_5CL=>CH_2O+.25CH_2CLCH_2+.75CH_3CHCL$	6.32E+05	2.00	15525.6
281.	$CH_2CL+C_2H_5CL=>CH_3CL+.25CH_2CLCH_2+.75CH_3CH$	1.62E+05	2.00	7025.6
282.	$CH_3+C_2H_5CL=>CH_4+.25CH_2CLCH_2+.75CH_3CHCL$	2.46E+05	2.00	8425.6
283.	$CCL_3+C_2H_5CL=>CHCL_3+.25CH_2CLCH_2+.75CH_3CHCL$	3.39E+05	2.00	10025.6
284.	$O_2+CH_2CLCH_2CL=>HO_2+CLCH_2CHCL$	6.82E+06	2.00	45025.6
285.	$H+CH_2CLCH_2CL=>H_2+CLCH_2CHCL$	8.58E+06	2.00	6525.6
286.	$O+CH_2CLCH_2CL=>OH+CLCH_2CHCL$	5.41E+06	2.00	5025.6
287.	$OH+CH_2CLCH_2CL=>H_2O+CLCH_2CHCL$	1.60E+06	2.00	-38.2
288.	$HO_2+CH_2CLCH_2CL=>H_2O_2+CLCH_2CHCL$	2.16E+05	2.00	13841.2
289.	$HCO+CH_2CLCH_2CL=>CH_2O+CLCH_2CHCL$	5.05E+05	2.00	15525.6
290.	$CH_2CL+CH_2CLCH_2CL=>CH_3CL+CLCH_2CHCL$	1.30E+05	2.00	7025.6
291.	$CH_3+CH_2CLCH_2CL=>CH_4+CLCH_2CHCL$	1.97E+05	2.00	8519.6
292.	$CHCL_2+CH_2CLCH_2CL=>CH_2CL_2+CLCH_2CHCL$	1.64E+05	2.00	9025.6
293.	$CCL_3+CH_2CLCH_2CL=>CHCL_3+CLCH_2CHCL$	2.71E+05	2.00	10025.6
294.	$CH_3O+CH_2CLCH_2CL=>CH_3OH+CLCH_2CHCL$	1.71E+05	2.00	3901.5
295.	$CH_3OO+CH_2CLCH_2CL=>CH_3OOH+CLCH_2CHCL$	3.04E+05	2.00	15501.5
296.	$O_2+CH_3CHCL_2=>HO_2+CL_2CHCH_2$	1.70E+06	2.00	45025.6
297.	$H+CH_3CHCL_2=>H_2+CL_2CHCH_2$	2.15E+06	2.00	6525.6
298.	$O+CH_3CHCL_2=>OH+CL_2CHCH_2$	1.35E+06	2.00	5025.6
299.	$OH+CH_3CHCL_2=>H_2O+CL_2CHCH_2$	3.99E+05	2.00	466.6
300.	$HO_2+CH_3CHCL_2=>H_2O_2+CL_2CHCH_2$	5.39E+04	2.00	13447.1
301.	$CH_2CL+C_2H_4=>CH_3CL+C_2H_3$	4.09E+05	2.00	10668.2
302.	$HCO+CH_3CHCL_2=>CH_2O+CL_2CHCH_2$	1.26E+05	2.00	15525.6
303.	$CH_2CL+CH_3CHCL_2=>CH_3CL+CL_2CHCH_2$	3.25E+04	2.00	7025.6
304.	$CH_3+CH_3CHCL_2=>CH_4+CL_2CHCH_2$	4.91E+04	2.00	8720.5
305.	$CHCL_2+CH_3CHCL_2=>CH_2CL_2+CL_2CHCH_2$	4.09E+04	2.00	9025.6
306.	$CCL_3+CH_3CHCL_2=>CHCL_3+CL_2CHCH_2$	6.78E+04	2.00	10025.6
307.	$CH_3O+CH_3CHCL_2=>CH_3OH+CL_2CHCH_2$	4.28E+04	2.00	3850.0
308.	$CH_3OO+CH_3CHCL_2=>CH_3OOH+CL_2CHCH_2$	7.61E+04	2.00	15450.0
309.	$O_2+CH_3CHCL_2=>HO_2+CH_3CCL_2$	5.11E+06	2.00	45025.6
310.	$H+CH_3CHCL_2=>H_2+CH_3CCL_2$	6.44E+06	2.00	6525.6
311.	$O+CH_3CHCL_2=>OH+CH_3CCL_2$	4.06E+06	2.00	5025.6
312.	$OH+CH_3CHCL_2=>H_2O+CH_3CCL_2$	1.20E+06	2.00	-154.9
313.	$HO_2+CH_3CHCL_2=>H_2O_2+CH_3CCL_2$	1.62E+05	2.00	13932.3
314.	$HCO+CH_3CHCL_2=>CH_2O+CH_3CCL_2$	3.79E+05	2.00	15525.6
315.	$CH_2CL+CH_3CHCL_2=>CH_3CL+CH_3CCL_2$	9.74E+04	2.00	7025.6
316.	$CH_3+CH_3CHCL_2=>CH_4+CH_3CCL_2$	1.47E+05	2.00	8473.1
317.	$CHCL_2+CH_3CHCL_2=>CH_2CL_2+CH_3CCL_2$	1.23E+05	2.00	9025.6
318.	$CCL_3+CH_3CHCL_2=>CHCL_3+CH_3CCL_2$	2.04E+05	2.00	10025.6
319.	$CH_3O+CH_3CHCL_2=>CH_3OH+CH_3CCL_2$	1.28E+05	2.00	3913.4
320.	$CH_3OO+CH_3CHCL_2=>CH_3OOH+CH_3CCL_2$	2.28E+05	2.00	15513.4

321.	O_2+CH_3CCL_3=>HO_2+CLCHCHCL+CL	5.11E+06	2.00	45025.6
322.	H+CH3CCL_3=>H_2+CLCHCHCL+CL	6.44E+06	2.00	6525.6
323.	O+CH_3CCL_3=>OH+CLCHCHCL+CL	4.06E+06	2.00	5025.6
324.	OH+CH_3CCL_3=>H_2O+CLCHCHCL+CL	1.20E+06	2.00	-274.4
325.	HO_2+CH_3CCL_3=>H_2O_2+CLCHCHCL+CL	1.62E+05	2.00	14025.6
326.	HCO+CH_3CCL_3=>CH_2O+CLCHCHCL+CL	3.79E+05	2.00	15525.6
327.	CH_3+CH_3CCL_3=>CH_4+CLCHCHCL+CL	1.47E+05	2.00	8425.6
328.	CCL_3+CH_3CCL_3=>$CHCL_3$+CLCHCHCL+CL	2.04E+05	2.00	10025.6
329.	CH_3O+CH_3CCL_3=>CH_3OH+CLCHCHCL+CL	1.28E+05	2.00	3925.6
330.	CH_3OO+CH_3CCL_3=>CH_3OOH+CLCHCHCL+CL	2.28E+05	2.00	15525.6

Reaction rate constant $k = A \cdot T^n \cdot e^{-Ea/RT}$; units in cm^3/mol/ s

Thermodynamic parameters required to complete the mathematical model are taken from Burcat et al. database [43]**.** These parameters of the chlorine-containing species are given in ATcT form (Active Termochemical Tables). As for the HCl/Cl_2 module, also these ATcT outputs are fitted to 7-terms polynomials by NASA program. The respective NASA polynomials are given in the appendix A.

For an effective modeling of flame type systems we need also transport parameters for each chemical species.
These parameters (see cap 3.2), for the chlorinated species, are generated using a Reaction Mechanism Generator (RMG) developed at Massachusetts Institute of Technology [44].
This feature allows transport properties estimation using group additivity. The Lennard-Jones sigma and epsilon parameters are estimated using empirical correlations (based on a species' critical properties and acentric factor). The critical properties are estimated using a group-additivity approach and the acentric factor is also estimated using empirical correlations. While a standalone application for estimating these parameters is provided, and the output is stored in a CHEMKIN-readable format. Also the transport parameters for the chlorinated species are listed in appendix B.

5.2.2 KINETIC SCHEME ANALYSIS
The initiation step in this reaction system involves mostly the unimolecolar reaction of methyl chloride

$$CH_3CL = CH_3 + CL \qquad \text{(R127)}$$

$$CH_3CL = CH_2 + HCL \qquad \text{(R63)}$$

As a consequence of the weak C-Cl bond, CHCs decompose at temperatures that are significantly lower than the hydrocarbons and result in the generation of reactive Cl radicals. The same happens to CH3Cl compared to methane.
The unimolecolar decomposition to methyl radical and Cl is dominant, while R63 has a limited importance. Just looking at the reaction scheme of Table 5.2, we can observe that R63 has Ea of 102.7 Kcal/mol, compared to 90.5 Kcal/mol of R127, but in all the temperature range the R127 is much higher than R63. This reaction (R127) is a very key step in the reaction system, and many attention must be given to it.
Not so many informations are avaible about this relevant reaction channel, particularly very few experimental measurements are available.
Karra et al. [45] used for their kinetic scheme the value suggested by Kondo et al. [46]. They studied the reaction in shock-tube at high temperature (1680-2430 K).
However Karra et al. rate parameters take into account fall-off behavior at 1 atm, and were determined using the QRRK method (Robinson and Holbrook 1972) expressed in Troe's formalism (Gardiner and Troe 1984). Therefore the value from Karra results much higher than that from, in the temperature range investigated. Other experimental studies were made by Lim et al. [47] which estimate a value for k_{127} that overlap with Karra and Kondo misuration respectively at low and high values of temperature range. Also Abadzhev et al. [48] and Shilov et al [49] studied the reaction at temperaure lower than 1400 K and the proposed values are in good agreement with Karra et al. theory value. New theoretical values were determined by Ho and Bozzelli [50] through QRRK unimolecular dissociation calculation. Their value is in very good agreement with the other experimental measurements, and it also agrees with Karra theoretical value for temperature of interests(T>1000 K). So the k_{127} is assumed equal to the one suggested by Ho and Bozzelli.
Other reactions which could consume reactant and start the radical mechanism are the bimolecular reactions with O2

$$CH_3CL + O_2 = CH_2CL + HO_2 \qquad \text{(R235)}$$

however this reaction is driven in the reverse direction, and so it has a limited importance has an initiation step.
The fuel decomposition is also initiated by reactions with the radical pool.

$$CH_3CL + H = HCL + CH_3 \qquad \text{(R64)}$$

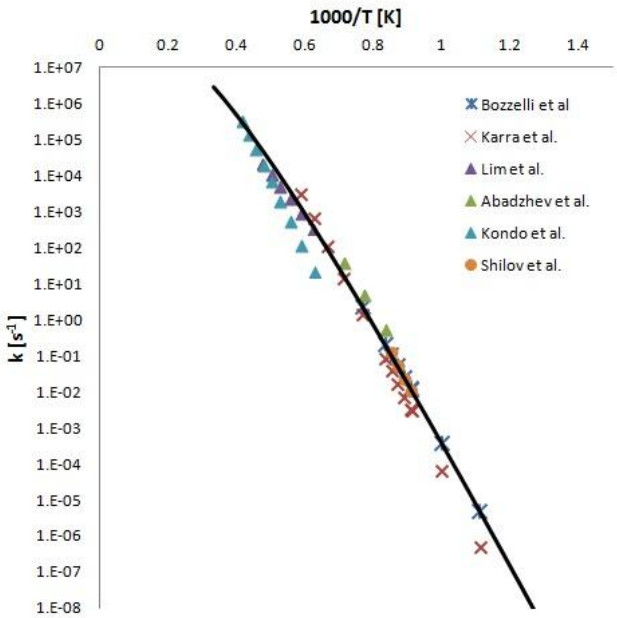

Figure 5.2.0: Arrhenius plot for the reaction $CH_3CL=CH_3+CL$. Experimental and theoretical results (symbols). Solid line represent the adopted rate value.

$$CH_3CL + H = H_2 + CH_2CL \tag{R247}$$

$$CH_3CL + OH = H_2O + CH_2CL \tag{R249}$$

$$CH_3CL + CL = HCL + CH_2CL \tag{R146}$$

Reactions R64, R247 and R249 have a great ihnibitory effect.
The first and second reactions consume H radicals and so they compete with the branching reaction

$$H + O_2 = O + OH \tag{5.1}$$

The third R249 competes to the consumption of OH radicals and inhibits reactivity by reducing the production of H-atoms from reaction

$$CO + OH = H + CO_2 \tag{5.2}$$

As shown later in this work (see Section 6), these are the main source of ihnibition due to the high sensitivity of the system to the rate costant of reactions aforementioned.

Reaction R64 has been studied recently by Bryukov et al. [51] and Louis et al. [52]. The first derived rate parameters from fits of a transition state theory model, while Louis through ab initio calculations. Their suggested values are in good agreement with some experimental data. In 1975 Westenberg et al. [53] measured the rate value over a wide temperature range using a discharge flow reactor, with pseudo first-order decays of CH_3Cl measured through mass spectrometry and excess H concentrations measured by electron spin resonance (ESR) . These values were confirmed by the recent study of Louis and Bryukov and were also used by other authors for their works (see [45]).
Other authors also focused on this reaction. Aders et al. [54] determined a rate value for lower temperatures, which is ten times higher than Westemberg's value.
For temperature range between 900-1300 K, Ho and Bozzelli has adopted a different value which is much higher than the others [55]. As shown in Figure 5.2.1, the adopted value for the reaction R64 lies between the two main groups of data observed, and in particular it is two times higher than the most reliable value by Westenberg.

No measurements are available for R247 nor R247b.
Karra et al. [45] estimated it using Benson's theoretical method. Another theoretical value is provided by Bryukov et al. [51] .
The two values are in good agreement only at low temperature, while there is a great gap at temperature higher than 1000 K, those typical of incineration processes.
In order to verify Bryukov's suggestions, also R247b was investigated. Bryukov et al. [51] determined the rate parameters again through theoretical calculation. Ho et al. suggested the value from Kerr and Moss [55] which is in reasonable agreement with Bryukov for temperature higher than 1000 K. A further check is carried out by calculating the rate parameters of R247b for Karra et al. values, from the equilibrium constant. The values obtained follow the general trend and overlap Bryukov at 900 K.
Figure 5.2.2 show the literature values and those adopted.

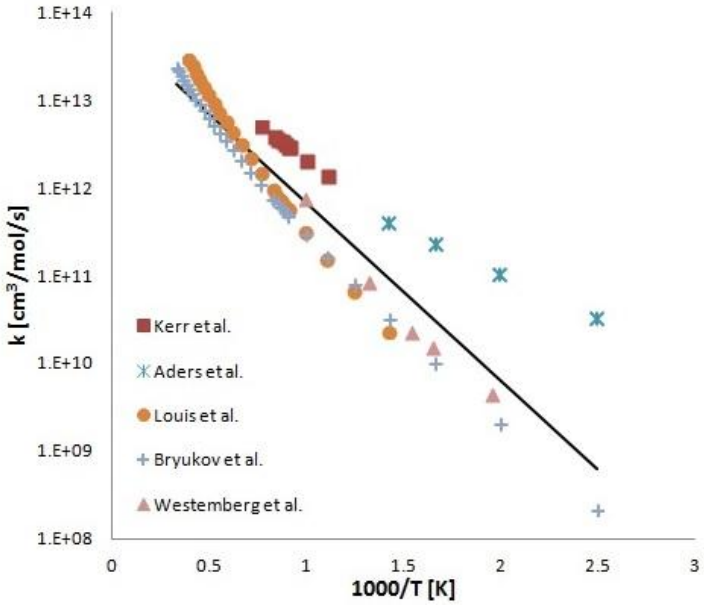

Figure 5.2.1: Arrhenius plot for the reaction $CH_3CL+H=CH_3+HCL$. Experimental and theoretical results (symbols). Solid line represent the adopted rate value.

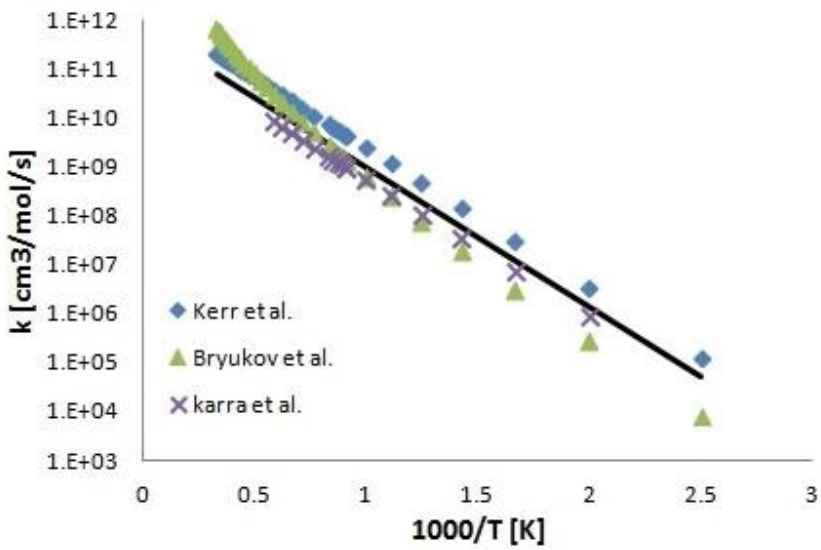

Figure 5.2.2: Arrhenius plot for the reaction $CH_2CL+H_2=CH_3CL+H$. Experimental and theoretical results (symbols). Solid line represent the adopted rate value.

Reaction between metyl-chloride and Cl atom can also affect negatively the reactivity of the system. Reaction R146 formed HCl, which rapidly undergoes the followig reaction
Reaction between metyl-chloride and Cl atom can also negatively affect the reactivity of the system. Reaction R146 forms HCl, which rapidly undergoes the followig reaction

$$HCL + CH_3 = CH_4 + CL \qquad \text{(R1b)}$$

regenerating Cl and forming CH_4 as an inevitable byproduct of pyrolysis of CH_3Cl. Reaction R1b also rapidly consumes CH_3, therefore making CH_2Cl the most abundant C1 radical in the system.
R146 has been widely studied by several authors, but only at low temperature. Therefore there is value scattering at high temperature. Sarzynski et al. [56], Bryukov et al. [51] and Clyne et al. [57] studied experimentally the reaction for temperaure range 300-800 K. Bryukov and Sarzynski got similar values at low temperature but extrapolating the corresponding value at high temperature, large differences are highlighted.
Karra et al. [45], Roesler et al. [58] suggest respectively Kerr et al. [55] and Senkan [59] theoretical values that are in good agreement at low temperature, but they diverge at high temperature (T>1000K). Therefore large uncertainties are associated with our choice.

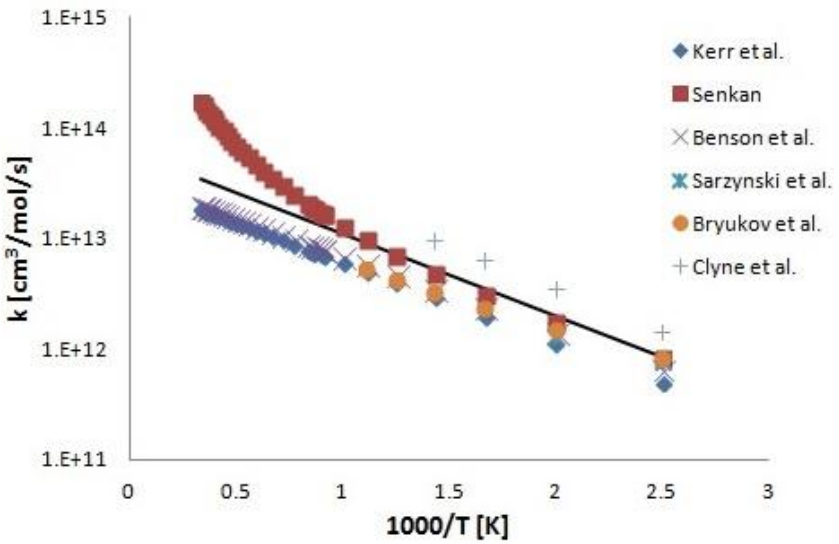

Figure 5.2.3: Arrhenius plot for the reaction $CH_3Cl+Cl=CH_2Cl+HCL$. Experimental and theoretical results (symbols). Solid line represent the adopted rate value.

In literature there are many proposed rate values for this reaction but only for low temperature.
The reverse reaction R1b has been studied extensively, also at high temperature, both experimentally and theoretically. For this reaction there is a good agreement between the values recently proposed by different authors. The less recent suggestion of Espinosa et al. [60]is ten times higher than bulk data.
Heneghan et al. studied the reaction by very-low-pressure reactor techniques. Obtained values are in very good agreement with those from Kerr et al. [55], Takahashi et al. [61] and Bryukov et al. [51] which measured it also experimentally. As in the other Figure previously discussed, the solid line represent the rate constant adopted in the mechanism.

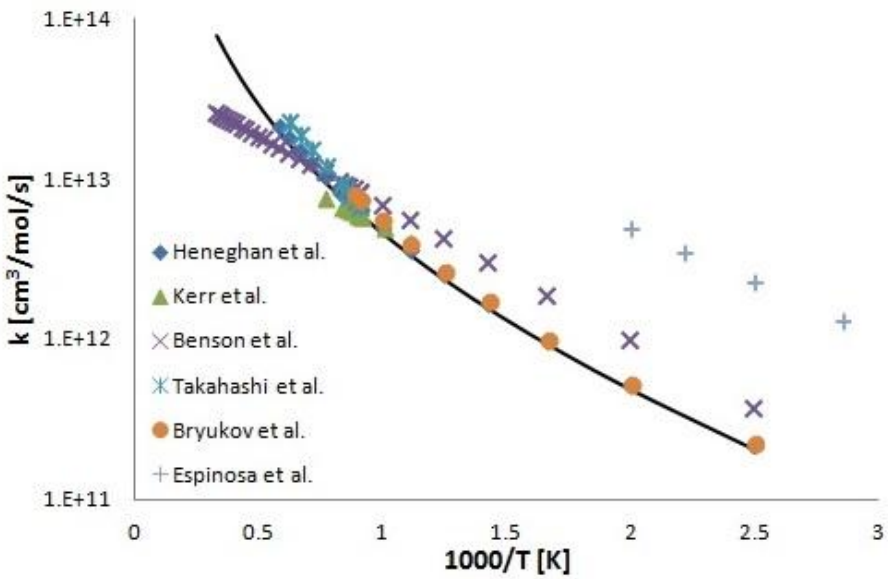

Figure 5.2.4: Arrhenius plot for the reaction CH_4+CL=CH_3+HCL. Experimental and theoretical results (symbols). Solid line represent the adopted rate value.

The radical pool composed of CH_2CL and CH_3 can recombine to form energized complexesin which are further decomposed tochlorinated C2 species.
The methyl and chloro-methyl radical combination pathways are significantly more important in the formation of C2 hydrocarbons (CH) and chloro-hydrocarbons (CHC) in reaction systems with CL presence, than in hydrocarbon oxidation. This is a result of atomic Cl being formed at early stages of reaction. Cl reacts very rapidly with the fuel, which is highly concentrated at the

beginning of the reaction. Therefore Cl enhance the formation of the radical pool promoting the rapid formation of CH and CHC. C1 radicals reactions with molecular oxygen are not as rapid as with C2 and larger radicals [50], therefore conversion of the C1 radicals into C2s via recombination becomes very important. Generally it was observed that,the pathways to the formation of C2 hydrocarbons aremore important in presence of Cl or HCl compared to hydrocarbons.

As previously mentioned CH_3 radical is in smaller quantities, so recombination of CH_2Cl radical is more probable

$$CH_2CL + CH_2CL = [C_2H_4CL_2]* \quad \text{(R125)}$$

$$CH_3 + CH_2CL = [C_2H_5CL]* \quad \text{(R133)}$$

these complexes can quickly decompose to more stable configuration

$$[C_2H_4CL_2]^* = C_2H_4CL + CL \quad \text{(R124)}$$

$$[C_2H_4CL_2]^* = C_2H_3CL + HCL \quad \text{(R188)}$$

$$[C_2H_5CL]^* = C_2H_4 + HCL \quad \text{(R187)}$$

$$[C_2H_5CL]^* = C_2H_5 + CL \quad \text{(R132)}$$

Clearly the energized adducts, highlighted as *, can also undergo stabilization and they do not further react.
As clear for these reactions, gas density, has a significant impact on the product distributions. For example, at higher pressures and lower temperatures where density is high, collisional stabilization of the chemically activated intermediates is enhanced; thus, the formation of recombination products would be favored. Conversely, at low pressures and/or higher temperatures where density is low, HCl and Cl elimination channels would gain greater significance. At the temperature and pressure typical of incineration processes, decomposition reaction are more important than stabilization ones. Between the two decomposition channels of $C_2H_4Cl_2$ the one leading to HCl and ethylene is rather favoured over Cl elimination.

Besides the aforementioned reactions, the kinetic mechanism includes also the direct bimolecular recombination of radicals to CHC hydrocarbons and Cl or HCl.

$$CH_2CL + CH_2CL = C_2H_4CL + CL \quad \text{(R83)}$$

$$CH_2CL + CH_2CL = C_2H_3CL + HCL \quad \text{(R84)}$$

$$CH_3 + CH_2CL = C_2H_4 + HCL \quad \text{(R85)}$$

$$CH_3 + CH_2CL = C_2H_5 + CL \quad \text{(R86)}$$

Reaction R83 is not well characterized in the literature.
Ho et al. [50] and Karra et al. [62] estimated the reaction theoretically through Quantum Rice-Ramsperger-Kassel (QRRK) thoery at temperatures in the range 500-1700 K and at pressures in the range 0.5-10 atm. Under these conditions, the unimolecular decomposition reactions are in the fall-off regime, and multiple reaction channels become available for the chemically activated adducts.
The two estimation overlap from low temperature (~500 K) to 1000 K, they start to deviate.
A similar consideration can be made for R84. Also this reaction has been evaluated in the aforementioned studies, showing similar behavior up to 1000 K. For T>1000 K to the two rate constants decrease but tend to diverge (Figure 5.2.6).

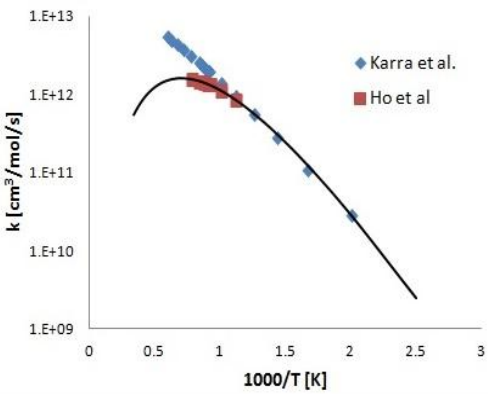

Figure 5.2.5: Arrhenius plot for the reaction CH_2Cl+ CH_2Cl =C_2H_4Cl+Cl. Experimental and theoretical results (symbols). Solid line represent the adopted rate value.

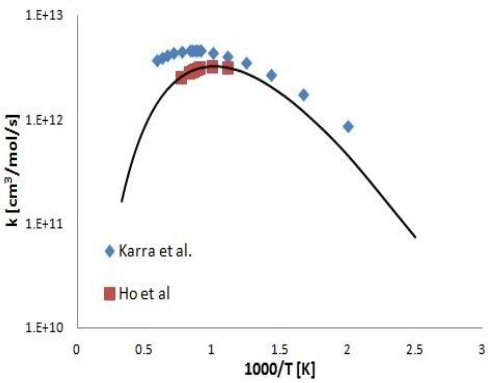

Figure 5.2.6: Arrhenius plot for the reaction CH_2Cl+ CH_2Cl =C_2H_3Cl+HCl. Experimental and theoretical results (symbols). Solid line represent the adopted rate value.

Bimolecular recombination of methyl and chloromethyl can proceed via different routes.
The first path, which produces ethylene and hydrogen chloride (R85), has not been extensively investigated. The few theoretical estimation available do not agree very well as reported in Figure 5.2.7.
The more recent data by Wang et al. [63] are largely higher than the others. In fact Wang's rate costant is a factor of ~2 higher than that of Karra et al. [62], ~5 times higherthan Ho et al. , and ~10times higher than Chiang e al.
Despite the large differences, the rate constants present a similar trend throughout the temperature range. In fact all the predictions show a decrease of costant rate at high and low temperature, with a maximum in the center. Ho et al. suggestion were adopted in this study, due to better agreement with experimental measurements.
The alternative path is defined by R86. The same disagreement is observed.

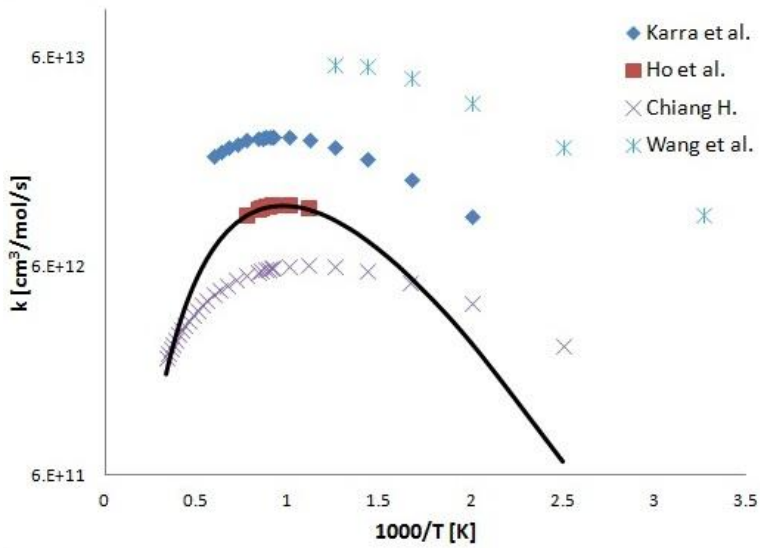

Figure 5.2.7: Arrhenius plot for the reaction CH_2Cl+ CH_3=C_2H_4+HCl. Experimental and theoretical results (symbols). Solid line represent the adopted rate value.

Products of recombination reactions, like C_2H_3Cl, C_2H_4Cl, C_2H_5 can undergoe pressure-dependent, unimolecular reactions leading to the formation of C_2H_2 and C_2H_4.

$$C_2H_3CL = C_2H_2 + HCL \qquad \text{(R197)}$$

$$C_2H_4CL = C_2H_4 + CL \quad \text{(R175)}$$

$$C_2H_5 = C_2H_4 + H \quad (5.3)$$

R197 is the major channel for the formation of C_2H_2 and for the consumption of C_2H_3Cl, while C_2H_4 comes primarily from R85 and only marginally by other decomposition reactions like R175.
R197 has been experimetally studied by Zabel [64] behind shock waves over the temperature range of 1350-1900 K. The other authors, Dean et al. [65] and Chiang et al [66], evaluated the rate costants for the reaction through theory. Despite the different techniques used by authors, the suggested values for k_{197} are overlapped and the associated uncertainties are very low.

An important step is that involving the subsequent reaction of C_2H_4.
Since Cl is present in the reacting system, ethylene can react with it through reaction R147.

$$CL + C_2H_4 = HCL + C_2H_3 \quad \text{(R147)}$$

Otherwise it can follow the path

$$CH_2CL + C_2H_4 = CH_3CL + C_2H_3 \quad \text{(R301)}$$

Radical C_2H_3 can then undergoes the sequent reactions

$$C_2H_3 = C_2H_2 + H \quad (5.4)$$

$$C_2H_3 + CH_2CL = C_3H_5CL \quad \text{(R223)}$$

$$C_2H_3 + C_2H_2 = CH_2CHCHCH \quad (5.5)$$

$$C_2H_3 + C_2H_4 = CH_2CHCH_2CH_2 \quad (5.6)$$

Hydrogen elimination path is much favoured over the recombination way, however R223 and the others represent the way to polymerization, which result in the formation of high molecular weight carbonaceous matter.
For reaction R147, the rate costant has been measured experimentally by Pilgrim et al. [67], Dobis et al. [68] and Kaiser et al. [69].
All the three authors determined a different rate value at T=298 K.

However the different trends seem to converge at same value when temperatures becomes of interest for this study (T>1000 K).
Benson et al. studied the reaction theoretically at high temperature (1260-1301 K) The rate constant reported in Figure 5.2.8 was estimated for the present mechanism.

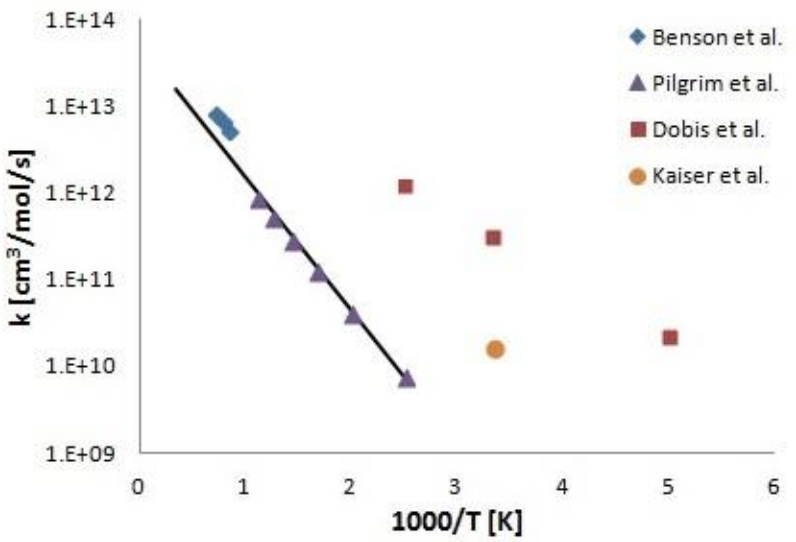

Figure 5.2.8: Arrhenius plot for the reaction CL+ C_2H_4=C_2H_3+HCL. Experimental and theoretical results (symbols). Solid line represent the adopted rate value.

Polymerization is not possible when CH_3Cl reacts in a oxidative system, like incineration processes.
So in these cases C_2H_3 react with O_2 to form oxigenated radicals that afterwards will react to form CO through different paths.
The oxidation reactions which mostly consume C_2H_3 are

$$O_2 + C_2H_3 = CH_2CO + OH \tag{5.7}$$

$$O_2 + C_2H_3 = O + CH_2CHO \tag{5.8}$$

Generally the O_2 doesn't react directly with C1 radicals, and reaction paths with C2 hydrocarbons are preferential.
However great importance is assumed by reaction

$$CH_2CL + O_2 = CH_2O + CLO \quad \text{(R74)}$$

Which present some intermediate steps [50]

$$CH_2CL + O_2 = [CH_2CLOO]^* = [CH_2OOCL]^* = CH_2O + CLO \quad (5.9)$$

Where []* denotes an energized complex which has excess energy corresponding to that of the newly formed CH_2Cl-OO bond (25.6 Kcal/mole). The energized complex can be stabilized, decomposed back to initial reactants, or further isomerize by Cl shift to [CH_2OOCl] *. This second complex, if formed, immediately dissociates to lower energy products such as CH_2O and ClO.

Sensitivity analysis showed that the reaction has great influence on the fuel consumption, most probably through the cycle [58]

$$CH_3CL + CL = CH_2CL + HCL \quad \text{(R146)}$$

$$CH_2CL + O_2 = CH_2O + CLO \quad \text{(R74)}$$

$$CO + CLO = CO_2 + CL \quad \text{(R48)}$$

Reaction R146 has not been studied at high temperature. The only data avaible is given by Ho et al. [50] which studied the high-temperature reaction of chloromethyl radical with O_2 using QRRK theory. At 800 K their estimation give k_{146} = 3.5E+19 cm^3 mol^{-1} s^{-1}.
Experimental data are provided by Shestov et al. [70] at 800 K. The value obtained in the study was five times lower than Ho prediction. Because loss of informations and recomendations Ho et al. rate value was selected and slightly modified based on its uncertainty.
Consequently, the reaction products ClO and CH_2O undergoes more reacting step which lead respectively to OH and CO.

6. MODELING RESULTS

After the kinetic model development led in the previous chapters, we are going to extimante its reliability.
Firstly the kinetic mechanism has been updated looking for avaible and reliable reaction rate parameters, and then modified making use of sensitivity analysis and comparing the simulations performed with experimental data.
In this section the kinetic model will be analyzed and validated through comparison with different experimental results in different experimental conditions.

All simulations, were performed with the OpenSMOKE code [5] using the kinetic scheme described above (chapter 5). Computed sensitivity coefficient, S_y, was normalized (s_y) as follows:

$$s_y = \frac{\delta lny}{\delta lnA} = \frac{A\delta y}{y\delta A} = \frac{A}{y} S_y$$

where y is the model variable (species concentration, temperature) and A the generic frequency factor of the rate constant expressed in the usual Arrhenius form, $k = A\ T^n \exp(-E_A/(RT))$.

6.1 FLOW REACTOR SYSTEMS

Different flow reactor speciation measurements have been compared to model simulations.The experimental data discussed in the following include both pyrolysis and oxidation of CH_3Cl in different reacting mixtures. Karra et al. [45] and Won Y. [71] tested CH_3Cl reactivity in pyrolytic environment, while Ho et al. [50] and Roesler et al. [58] studied the behaviour of chlorinated hydrocarbon in presence of oxygen.

6.1.1 PYROLYSIS AND OXIDATION OF CH_3CL IN $Ar/H_2/O_2$ MIXTURES

Ho et al. studied the thermal decomposition of methyl chloride in hydrogen/oxygen mixtures and argon as bath gas. Experimental measurements were carried out at p=1 atm in a tubular flow reactors with 1.6 cm internal diameter.
CH_3Cl intermediate, and final products were analyzed over the temperature range 1098 to 1273 K, at average residence times τ = 0.2-2.0 s.

The high temperature quartz, tubular flow reactor was heated in a three zone electric tube furnace in order to mantain isothermal conditions within ± 5 K.
All the experiments have been performed with a costant reactant ratio of $Ar:CH_3CL:H_2:O_2$ = 96:2:1:1.
Figure 6.1.0 compares experimental and calculated CH_3CL profiles as function of τ at different reaction temperatures.

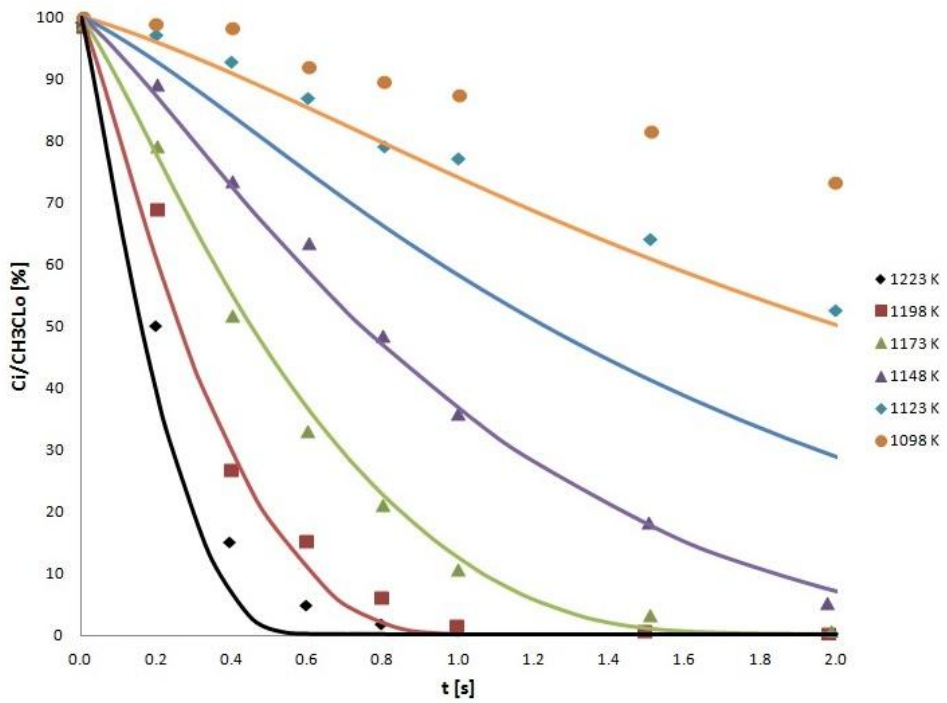

Figure 6.1.0: Comparison between CH_3CL experimetal measures [50] and calculated profiles at different reaction temperatures .

As shown in Figure 6.1.0 the model is able to estimate well the consumption of the fuel at the high temperatures. Larger deviation are observed for lower temperatures (1098K, 1123 K).

Sensitivity analysis has been carried out at different temperatures. Results are reported in Figure 6.1.1. No reactions sensitive only at low temperatures are highlighted, preventing any possibility of improving model performances.

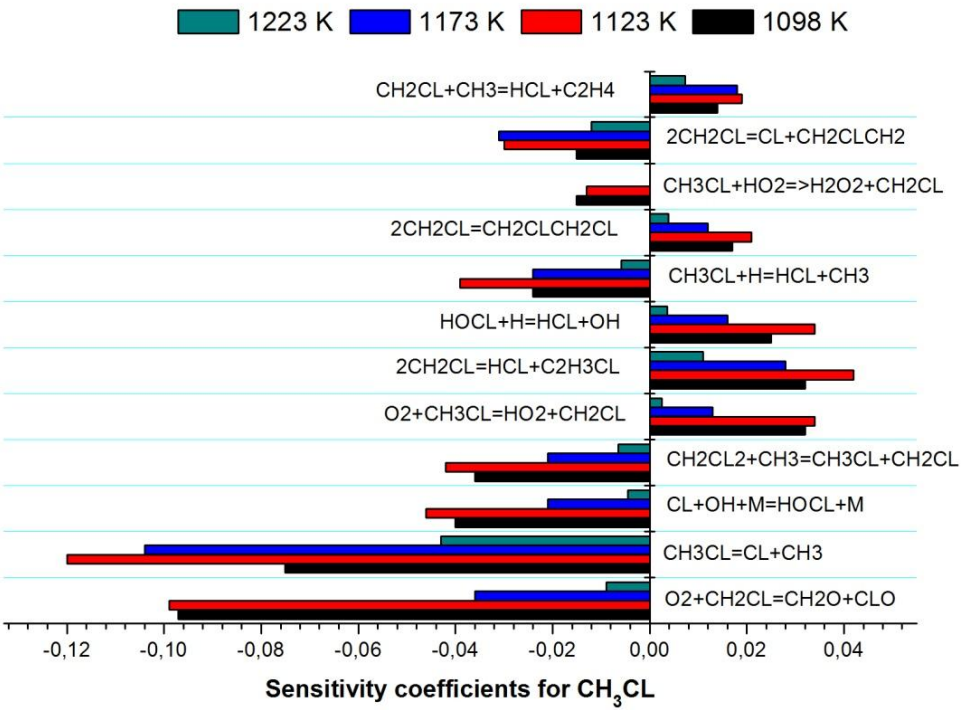

Figure 6.1.1: Sensitivity coefficients of CH_3CL to rate constants for $CH_3CL/H_2/O_2/Ar$ mixture at different temperature, P=1 atm and ϕ=4.

The most sensitive reactions at low temperature are sensitive for all the temperaure range analyzed. Only at 1223 K the sensitivities are sensibly lower for the selected reactions.
Figure 6.1.2 shows the intermediate and the final products trend at 1173 K.

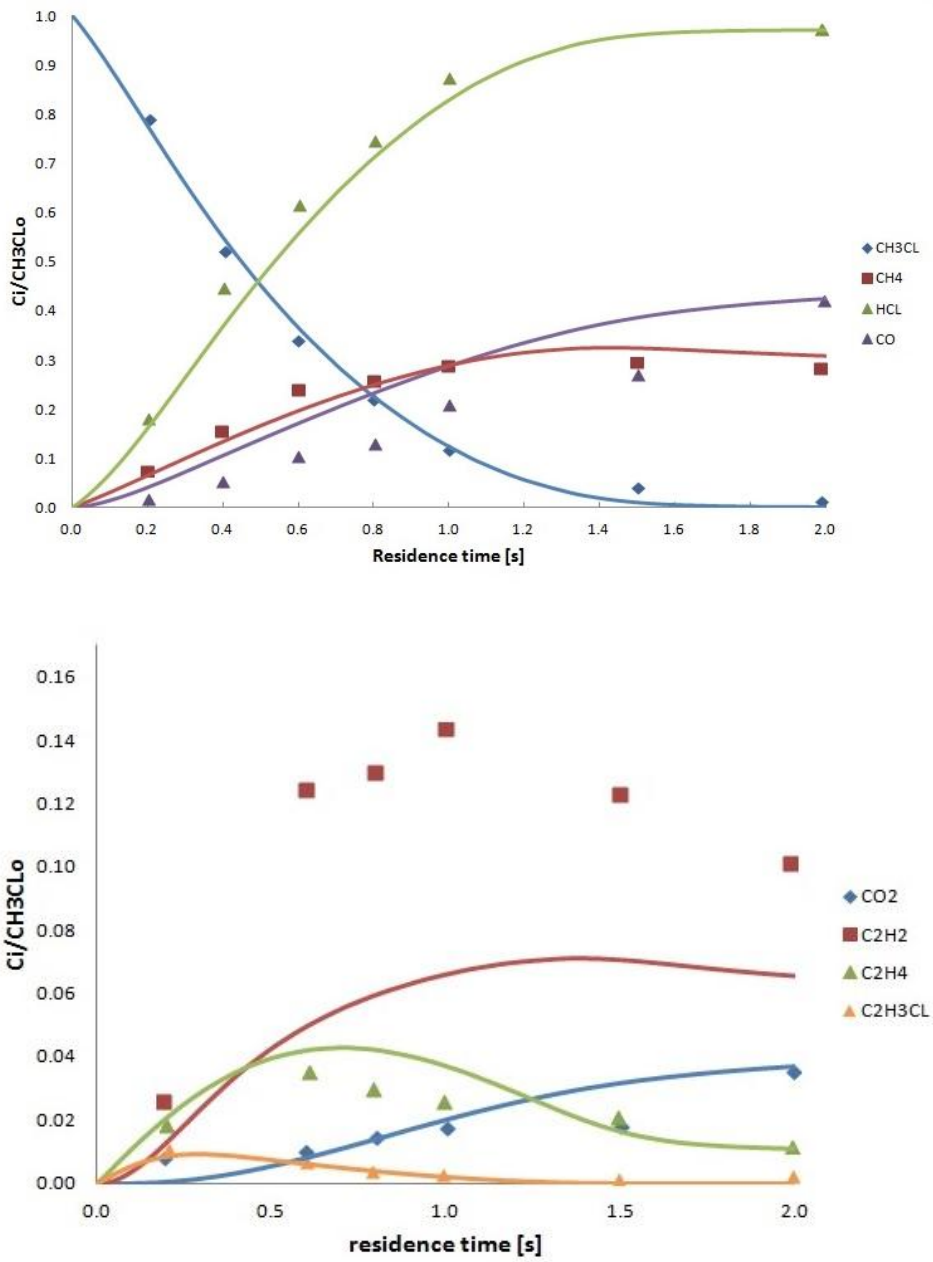

Figure 6.1.2: Comparison of calculated and experimental [50] products distribution versus residence time a 1173 K.

Model predictions and experimental mesurements are in good agreement, except for acetylene and carbon monoxide.
The first is greatly underestimated (~50%), while CO predictions are greater than experimental values for residence time between 0.3 and 2 seconds.

Acetylene can directly react to produce carbon monoxide through reaction

$$O_2 + C_2H_2 \rightarrow CO + CH_2O \tag{6.1}$$

and this path presents a great sensitivity to C_2H_2 consumption.

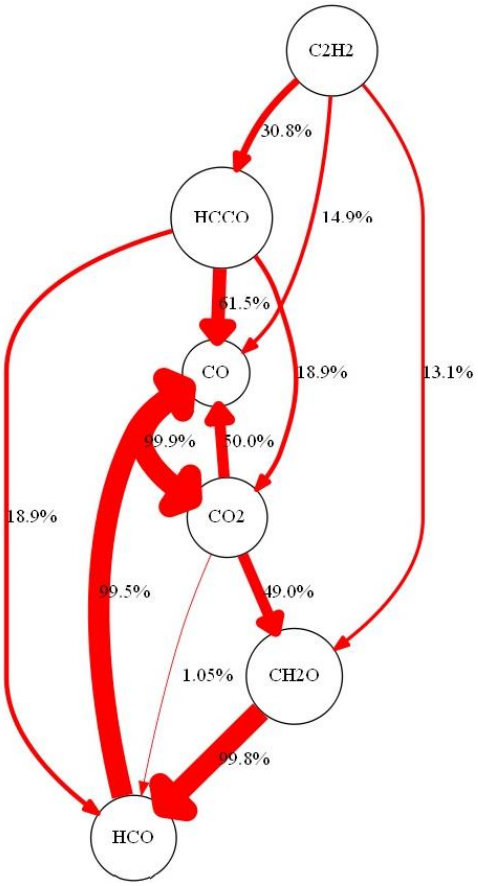

Figure 6.1.3: Flux analysis for the C_2H_2 consumption. Different path from acetylene to carbon monoxide.

Figure 6.1.3 shows the different paths leading to CO from acetylene All the available channels which convert C_2H_2 to CO belong to C1-C3 module, whose analysis is beyond the aim of this work.

6.1.2 OXIDATIVE-PYROLYSIS OF CH_3CL IN ARGON

Granada et al. [72] studied oxidative-pyrolysis of methyl chloride, which is the second stage in the chlorine-catalyzed oxidative pyrolysis (CCOP) of CH_4. Their study was aimed at developing a process through which improve CH_4 yields in

pyrolysis processes. The experimental facility used was a tubular quartz reactor with a 2.1 cm internal diameter and long 100 cm. Similarly to the previous example, the reactor was kept at isothermal conditions. Experimental measurements were carried out at pressure 0.68 atm, temperature of 1253 K in laminar flow conditions. Two different sets of measurement have been carried out under pyrolytic and oxidative conditions, but, according to the authors, only the oxidation case was considered to be reliable in terms of chlorinated C2 species. Experimental data are compared with model predictions in Figure 6.1.4 and 6.1.5.

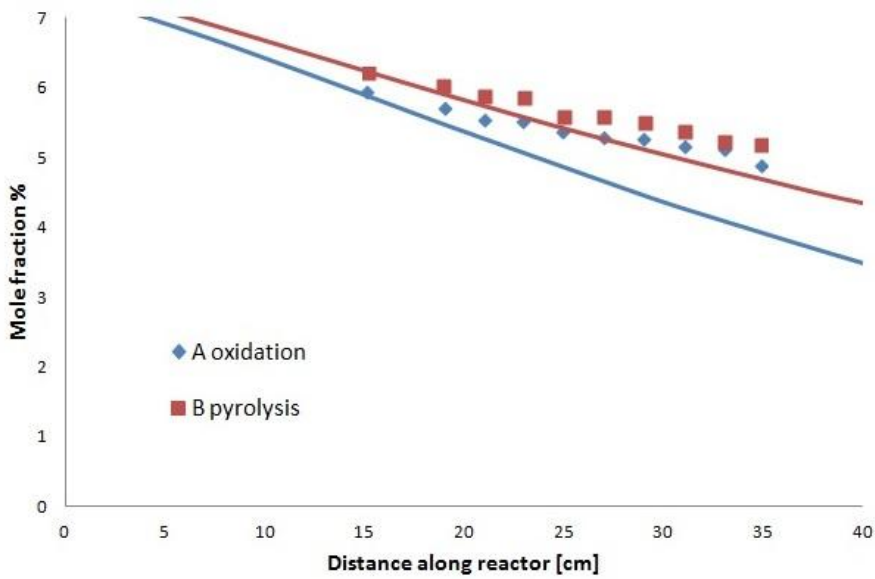

Figure 6.1.4: Comparison between CH_3CL experimetal measures [72] and calculated profiles in oxidative and pyrolytic condictions.

As reported in Figure 6.1.4 the kinetic model exhibits higher reactivity compared to the data, both under pyrolysis and oxidation conditions. This discrepancy is greater for oxidation, and also the differences between oxidation and pyrolysis are amplified by the kinetic model here presented. In fact, looking at experimental data, pyrolysis and oxidation do not seem to largely differ. For a better understanding a sensitivity analysis was performed.

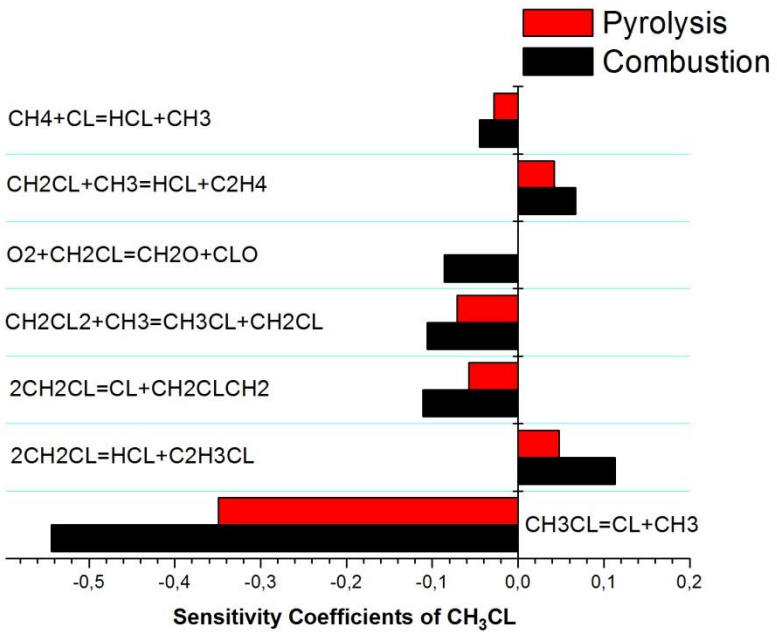

Figure 6.1.5 Sensitivity coefficients of CH_3CL to rate constants at oxidative (blue) and pyrolytic (red) condition, P= 0.68 atm and T=1123.

Sensitivity analysis shows that the most sensitive and important reaction in CH_3Cl consumption is R127 which unimolecularly consumes the fuel, generating CH_3 and Cl, which in turn can react again with the fuel.
the sensitivity analysis does not show great differences between the two cases and this can explaining the similar trend in fuel depletion. The oxidation, which is more reactive and present also higher sensitivities, is also sensitive to R74. This reaction is the only sensitive to fuel consumption in presence of oxygen.

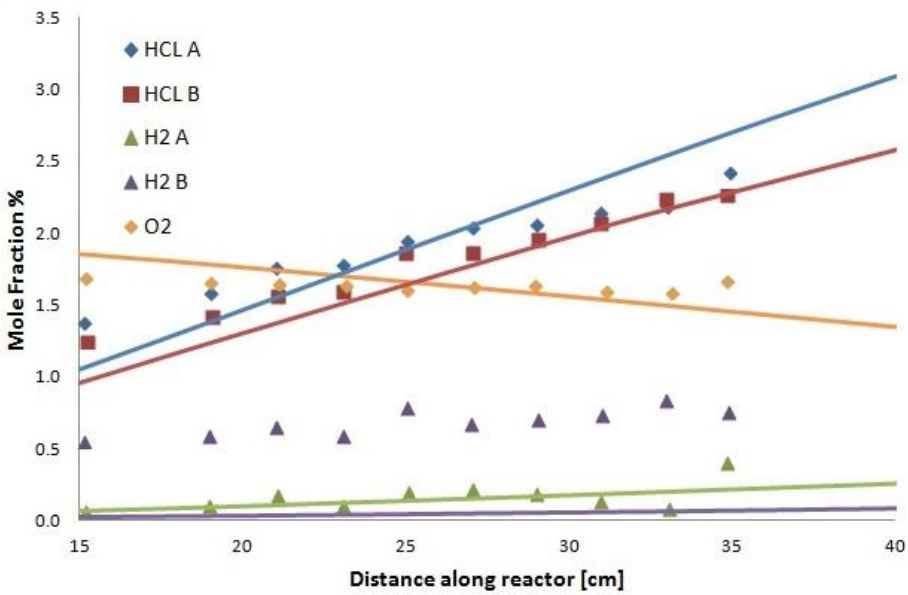

Figure 6.1.6: Comparison of calculated and experimental [72] species distribution versus distance along reactor at 1223 K.

The simulated products distributions shown in Figure 6.1.6 are in good agreement with the experimental data. As for the fuel, we can note a slightly higher reactivity of kinetic model with respect to the experimental data.
For the oxidation there is good agreement between solid lines and experimental points. However there is a great discrepancy for pyrolysis case. This is the main discrepancy between model and experiment.
Contrary to expectation kinetic model predicts a lower H_2 production in pyrolysis than oxydation, while experiments detect the opposite. The experimental behaviour should be the right one since pyrolysis is expected to produce hydrogen in grater quantities than oxidation.
This conflicting behaviour can be partially justified by the authors statement. Mole percents for H_2 were determined from hydrogen atom balances because of difficulties associated with the quantification of H_2 through mass spectrometry. Consequently, H_2 data have large uncertainties because of the cumulative errors associated with the measurement of all the species accounted for in the hydrogen atom balances [45]. Sensitivity analysis performed on both cases show us that the most sensitive reaction for hydrogen production is R127 again. The only reaction influencing directly the H_2 formation is R247. It would be possible to increase the molecular hydrogen amount by increasing the rate costant of this reaction. Nevertheless, this

reaction presents a great sensitivity in oxidation while its sensitivity value is halved for pyrolysis. This means that no real improvement could be obtained.
In order to understand which of the two behaviour is the most reliable more experimental data would be needed.
For the oxidation case, also the C2 species and other products and intermediates are detected and compared with simulated values.

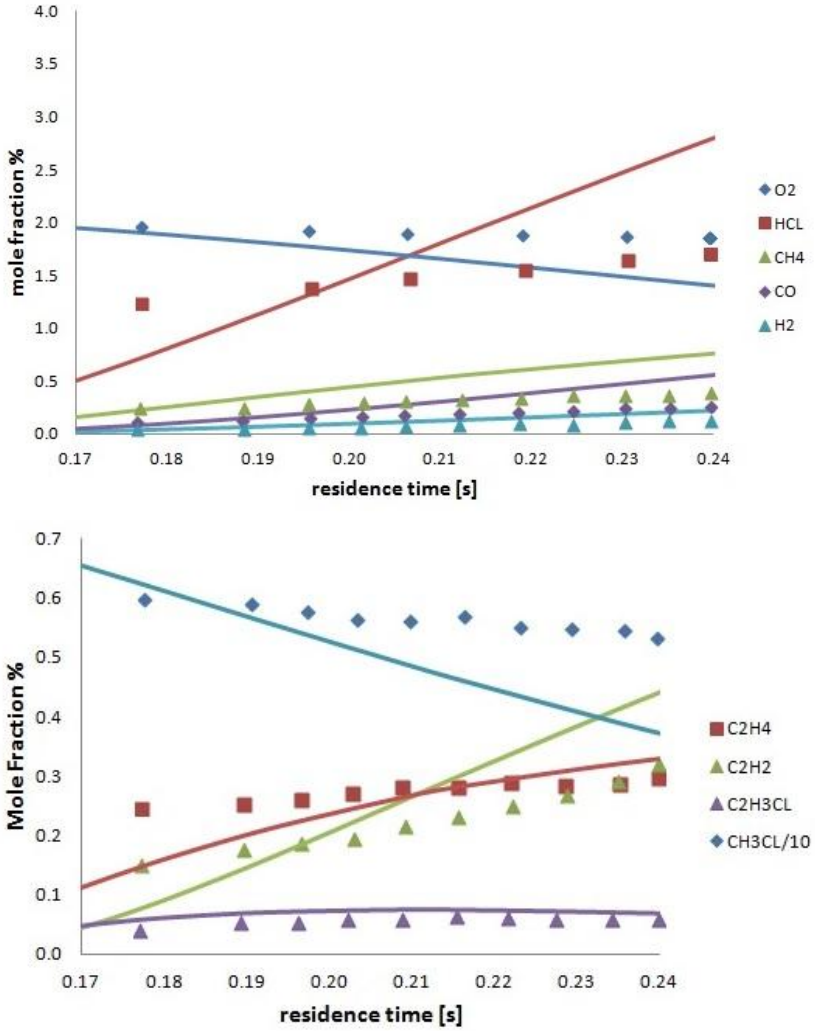

Figure 6.1.7: Comparison of calculated and experimental [72] species distribution versus residence time at 1223 K.

Figure 6.1.7 shows the products and intermediates trends predicted by kinetic model together with experimental measurements.
Apart from the higher reactivity, the model is able to satisfactorily represent the reacting system evolution.
As clearly highlight in Figure 6.1.7 acetylene production occur subsequently to ethylene, and this is consistent with the stepwise mechanism for acetylene formation involving the recombination of CH_2Cl radicals and the formation of C_2H_3Cl, followed by the decomposition of vinyl chloride via $C_2H_3Cl = C_2H_2 + HCL$. This is the main route together with the unimolecolar decomposition of C_2H_3 to C_2H_2. Chloroethyl trend is perfectly lined up with experimental data.

6.1.3 PYROLYSIS OF CHLOROMETHANE IN EXCESS HYDROGEN ATMOSPHERE

Won et al. [73] analyzed chlorinated methanes in excess hydrogen atmosphere,under pyrolysis conditions, using an isothermal tubular reactor of 8 mm internal diameter and 81 cm lenght.
Experimental measurements were performed at varying residence time τ from 0.3 to 2 seconds, and varying temperatures from 1013 to 1173 K. The reactor was kept at atmospheric pressure. For our purpose only the case at 1123 K has been analyzed in order to evaluate the reliability of the kinetic model. Results are reported in Figure 6.1.8a and 6.1.8b.

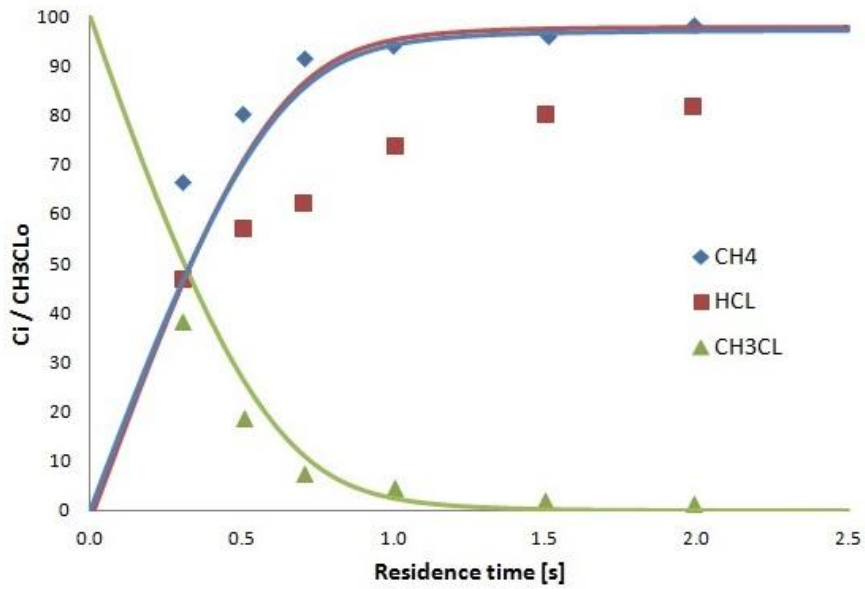

(a)

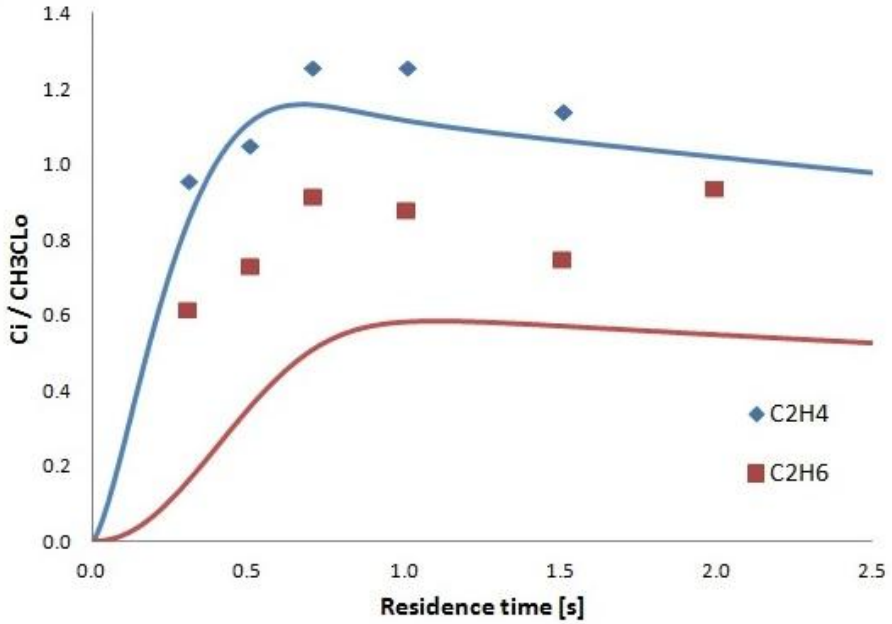

Figure 6.1.8: Comparison of calculated and experimental [73] species distribution versus residence time at 1123 K for CH_3CL/H_2 system. (a) C1 species, (b) C2 species.

Referring to Figure 6.1.8a reasonable agreement is observed between simulated profile and experimental data for the fuel and the main product except for HCL which apparently seems to be overestimated.
Sensitivity analysis on fuel consumption demostrates that mechanism is again started by unimolecular decomposition of methyl-chloride (R127). However the reaction which mostly consumes fuel is the radical attack of hydrogen to CH_3Cl (R64), that generates CH_3 and HCl.
Molecular hydrogen, which is predominant in the reaction system, is converted to radical hydrogen by reactions

$$CH_3 + H_2 = H + CH_4 \tag{6.2}$$

$$CL + H_2 = H + HCL \tag{R2}$$

So apparently the H cycle doesn't consume H_2 present in the atmosphere and plays a catalytic role in the acceleration of CH_3Cl decomposition.
Methane formation is proportional to fuel depletion and occurs mainly through the bimolecular reaction between methyl and molecular hydrogen just mentioned before (Sections 6.2), and less through reaction

$$HCL + CH_3 = CH_4 + CL \qquad \text{(R62b)}$$

Pyrolytic condition causes methane to be the main product togheter with HCl and prevents great formation of other species like C2 hydrocarbons.
Graphic 6.1.8a shows a considerable overstimation of HCL.
However reaction conditions, with a very huge quantity of H_2, suggest a similar product distribution. In fact Won et al. in their work [73] obtained a similar distribution using a similar kinetic model. Moreover the mass balances performed on the species distribution confirm the truthfulness of the profiles determined through numerical simulations. It is in fact to reasonable to expect such a trend where methane and HCl overlap.
Although C2 hydrocarbons are produced in small quantities, some data about these species have been measured. Simulations sligthly underestimate ethylene formation, and largely underestimate strongly ethane formation. However the shapes of the mole fraction profiles for these species qualitatively replicate the experimental observations. Looking at the experimental data we can observe that ethylene and ethane form at the same time, while model predict ethane formation to happen slightly after ethylene. Ethane production occur mainly through the reaction

$$C_2H_5 + H_2 = C_2H_6 + H \qquad (6.3)$$

while the cosumption is caused by reaction

$$CH_3 + CH_3 + M = C_2H_6 + M \qquad (6.4)$$

that, reversly to what expected, proceed in the opposite direction at reactor temperatures.
Ethylene is produced through reaction R85 which involved recombination between ethyl and chloroethyl radicals. The small quantities of C2 detected suggest that radical species more likely react with molecular hydrogen, which is highlt concentrated in the system, limiting the polymerization process.

6.1.4 INHIBITION OF CHLOROMETHANE IN REACTING $CO/H_2O/O_2$ MIXTURES

The inhibitory nature of CH_3Cl has been studied also in an oxidative environment. Methyl-chloride is added to moist CO in small quantities to evaluate its effects on reactivity. Experiments have been performed by Roesler et al. [58] in a high temperature atmospheric pressure flow reactor with an internal diameter of 10 cm.

The reactor can be considered effectively adiabatic.

Two different tests have been performed using two different mixtures (mixtures A and B) and initial conditions.

In table 6.1.1 initial conditions for each mixture are listed:

Mixture	Ti [K]	CO [%]	O_2 [%]	H_20 [%]	CH_3Cl [ppm]
A	1050	0.96	1.02	0.59	195
B	1145	0.53	0.55	0.95	195

Table 6.1.1: Experimental initial conditions for CH_3CL oxidation

Figure 6.1.9 display experimental data and simulated mole fraction profile as a function of flow reactor residence time.

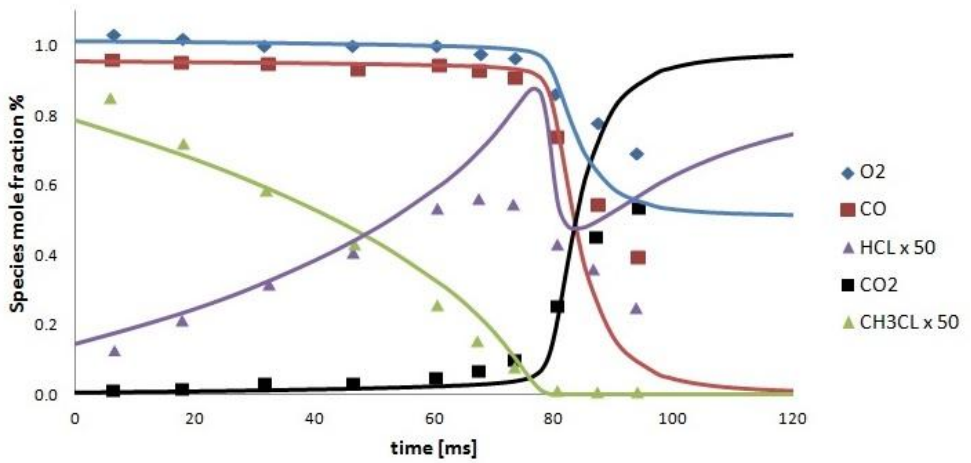

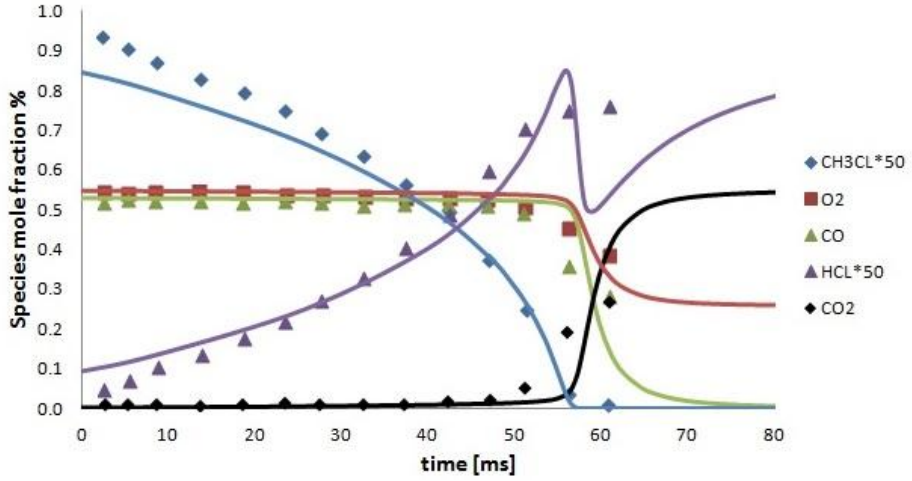

Figures 6.1.9: Comparison between experimental [58] data and model predictions for main species vs reaction time at T_0=1050 K (a) and T_0=1145 K (b). Simulated profile shifted to the 50% fuel combustion.

Looking at Figure 6.1.9a and Figure 6.1.9b, two two stages are clearly identified. Firstly, the methyl chloride is consumed in a $CO/H_2O/O_2$ reaction bath that remains virtually unchanged at isothermal conditions. Second, following nearly complete CH_3Cl disappearance, the CO is rapidly oxidized in a moist environment perturbed only by HCl.

This work is focused mainly on the first stage, while the second deal with HCl/CO mechanism, which has been previously studied by other authors [9].

The comparison between experimental data and simulations proves the reliable performances. The two-stage nature of the reaction system is very well reproduced.

For the T=1050 K case, the HCl peak is overestimated by 30%, while for temperature 1145 K the overestimation is contained within the experimental uncertainty. Again, with respect chloridric acid there is a steeper decrease in concentration, followed by a further steep increase is predicted by the kinetic model.

The smoothing of HCl experimental profile, clear also for the others species in the second stage, is likely due to locally increased axial diffusion effects resulting from large concentration gradients in the vicinity of the transition between the two stages, to the spatial unsteadiness of the reaction in this transition zone, and from probe sample volume averaging [58].

Some sensitivity analyses were performed to investigate CH_3Cl role in CO oxidation chemistry and its ihnibiting nature.

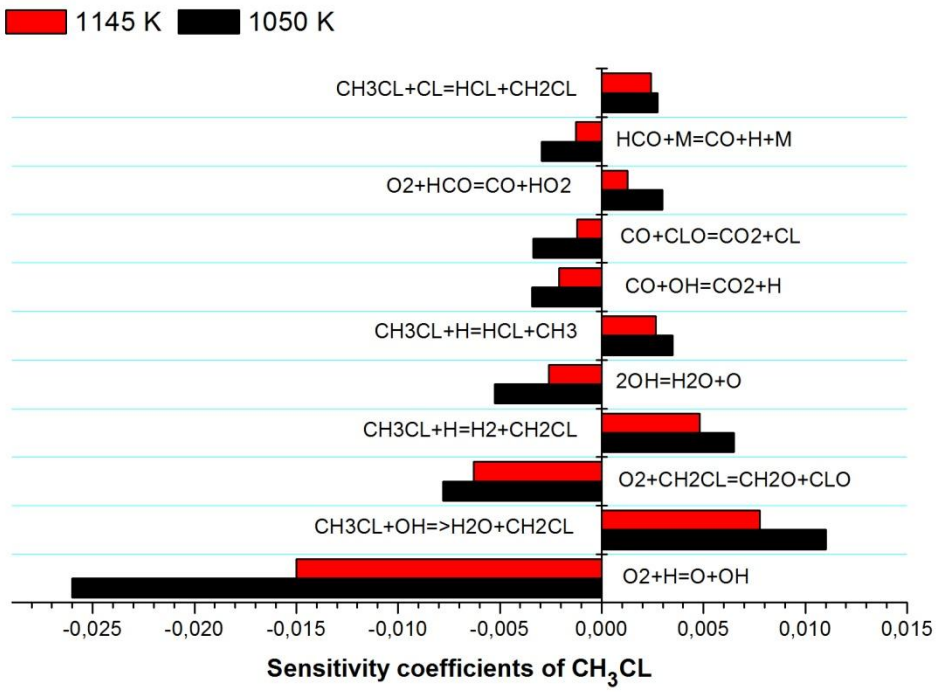

Figure 6.1.10: Local sensitivity coefficients of CH_3CL to rate constants for $CO/H_2O/O_2/CH_3CL$ mixture at 1050 and 1145 K

Local sensitivity analyses are performed for the first reaction stage (t = 0-55 ms). The analysis shows that, for both temperatures, reactions R249, R64, R247, mainly involved in radical consumption, dominate.

$$OH + CH_3CL = H_2O + CH_2CL \qquad \text{(R249)}$$

$$CH_3CL + H = CH_3 + HCL \qquad \text{(R64)}$$

$$H + CH_3CL = H_2 + CH_2CL \qquad \text{(R247)}$$

Reactions R64 and R247 compete for radical H depletion with the most important chain branching

$$H + O_2 = OH + O \qquad (6.5)$$

and reaction

$$H_2O + O = OH + OH \tag{6.6}$$

Reaction R249 competes for OH radical consumption with reaction

$$CO + OH = CO_2 + H \tag{6.7}$$

The relative importance and the competition between R64, R247 and the branching reaction (6.5) is confirmed by the decrease of ihnibition effect of CH_3Cl, due to its termination, followed by the increase of temperature.
Looking at Figure 6.1.11 it's visible the growth of R6.5 rate costant and the reset of R64 and R247 when CH_3Cl is close to total consumption.

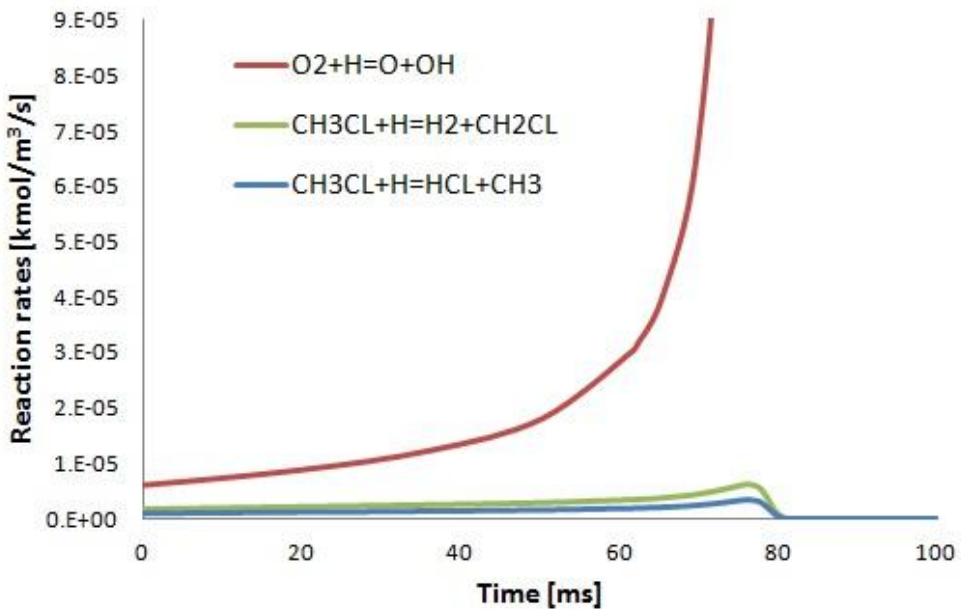

Figure 6.1.11: Rate costant of different reaction vs reaction time

Lower sensitivity is shown by reaction R184

$$CH_3CL + CL = HCL + CH_2CL \tag{R184}$$

Methyl-chloride has a great negative sensitivity (consumption) for the reaction R74 which can promote a kinetic cycle for methyl chloride consumption

$$CH_3CL + CL = CH_2CL + HCL \quad \text{(R146)}$$

$$CH_2CL + O_2 = CH_2O + CLO \quad \text{(R74)}$$

$$CLO + CO = CO_2 + CL \quad \text{(R48)}$$

To better evaluate the kinetic model also minor intermediate compound are compared in the following Figure 6.1.12

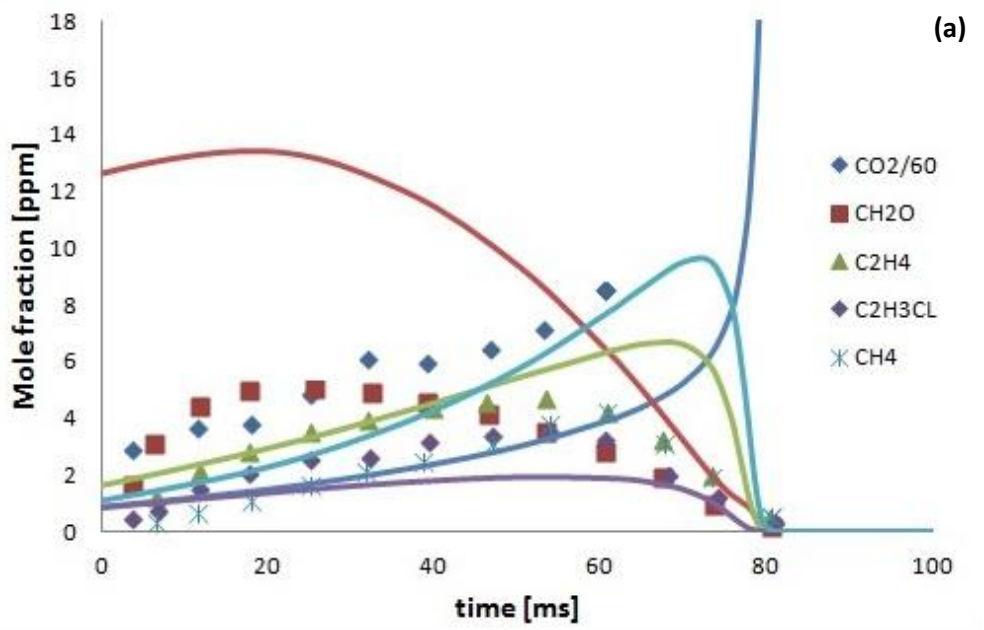

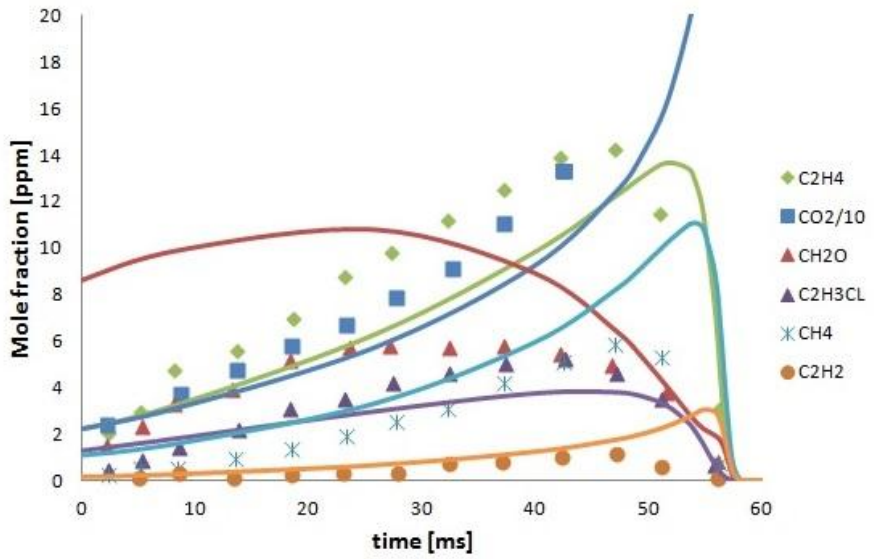

Figures 6.1.12: Comparison between experimental [58] data and model predictions for intermediate species vs reaction time at T_0=1050 K (a) and T_0=1145 K (b).

Simulated profiles, specially at low temperature, are not quantitatively very accurate, however the qualitative trends can be considered generally satisfactory. Furthermore, as mentioned before, the greater steepness of simulated profile with respect to the experimental data may be due to axial diffusion effect.

The species to be overestimated by the mechanism at both temperatures are methane and particularly formaldehyde.

While methane ovestimation is limited to its peak value, formaldehydeis over-estimated on the whole time coordinate.

Sensitivity analysis on CH_2O shows that the main reaction producing formaldehyde is R74. CH_2O compete with reaction R146 for react with Cl radical producing HCO in reaction R43. After this species reacts through reaction

$$HCO + O_2 = CO + HO_2 \tag{6.8}$$

producing CO, which is generally understimates by the model.

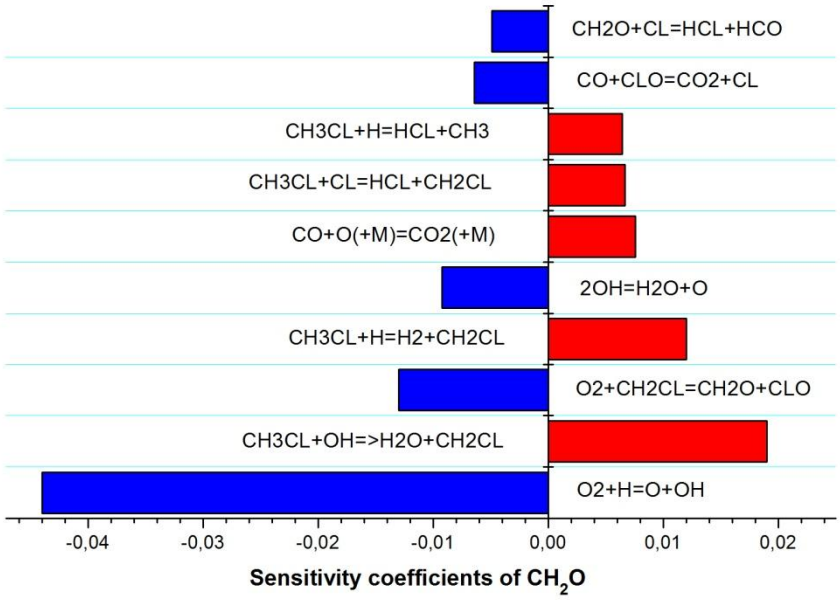

Figure 6.1.13: Sensitivity coefficients of CH_2O to rate constants for $CO/H_2O/O_2/CH_3Cl$ mixture at 1050 K

6.2 SHOCK TUBE IGNITION DELAYS

Although halogen compounds are generally known to inhibit combustion process, this behaviour can be reversed in some cases. In fact chloride has a "double" nature, which changes depending on reacting conditions. Ignition delay times were measured for different reacting systems involving pure CH_3Cl or CH_3Cl/CH_4 mixtures. The analyzed experimental studies have been performed using shock tube reactors in order to investigate their auto-iginition tendency. Simulation were performed using the OpenSMOKE assuming the constant volume, adiabatic conditions. The ignition delay time is defined as the time at which the CH (or OH) radical presents its maximum concentration.
The experimental data used for our analysis are taken from Wang et al. [74] and from Kuan et al. [75] works, dealing with pure CH_3Cl and CH_4/CH_3Cl mixture respectively.

6.2.1 IGNITION DELAY TIME OF CH_3Cl FUEL

In this section predictions of ignition delay times are compared with experimental mesaurements of Wang et al. [74].

Experimental tests have been performed in shock tube reactor, in a range of temperature from 1300 K to 1600 K and 2 atm reflectedpressure.
In Table 6.2.1 all the tested conditions are listed. Two different tests have been performed, the former uses pure CH_3Cl ,the latter uses also hydrogen in the mixture, both manteining the same unitary equivalence ratio.
An additional simulation with pure methane was also performed to better investigate CH3Cl behavior.

Mixture	CH_3Cl [%]	CH_4 [%]	H_2 [%]	O_2 [%]	Ar [%]
A	10	/	/	15	75
B	10	/	1	15.5	73.5
C	/	10	/	20	70

Table 6.2.1: Initial concentrations for the different experimental and simulation tests.

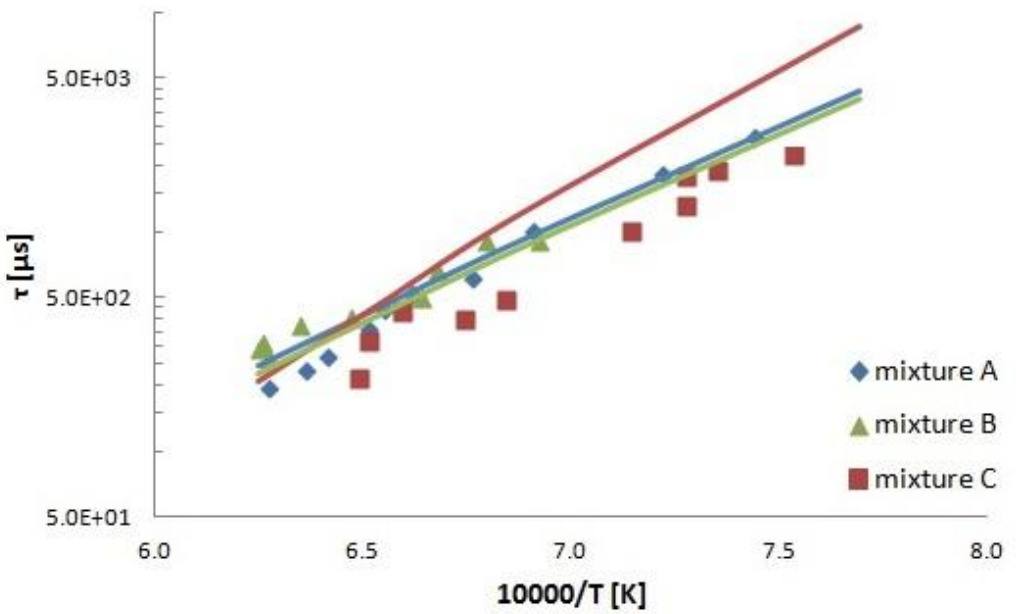

Figure 6.2.0: Experimental [74] and simulated ignition delay time for different reacting mixture.

While the mechanism predict longer ignition delay times for pure methane (Mixture C) compared to Mixture A and B, the opposite trend is observed in the experimental data. Choerently to the experimental measurements, no large

differences are observed between mixture A and B. Moreover in case A and B the model simulations fairly agree with the experimental ignition delay times.

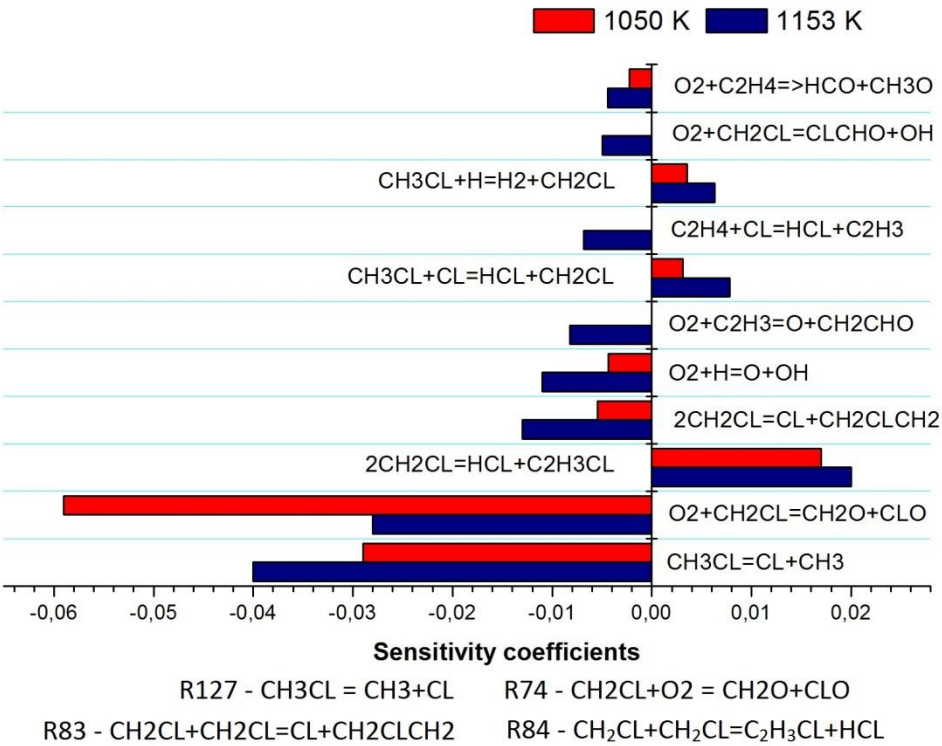

Figure 6.2.1: Sensitivity coefficients of CH radical to rate constants for mixture A at 1530 K and 1300 K

Thus the causes for the slight disagreement between experiments and simulations for mixture containig CH_3Cl could lie in the predictions for methane ignition. Therefore, resolving the minor disagreement between model and experiment for CH_3Cl, ignition requires the discrepancy in CH_4 ignition to be investigated at first. This is beyond the scope of the present work. Sensitivity analysis has been performed to investigate the ignition mechamism for the CH_3Cl containing system of interest, namely case A.

Reactions R127 and R74 show high sensitivity coefficients. The former is the starting step for the chain radical mechanism, while the latter is the shortest route for oxygen to attack methyl radical. At higher temperature pyrolisis reactions assume greater importance as represented by R83 and R84 sensitivity coefficients sensitivities.

In Figure 6.2.2 are presented molar fraction profiles for some molecular and radical species. At 1530 K the ignition occurs at 500 micro-seconds, exactly when CH_3Cl depletion is completed. At the same time the molar fraction profiles of the radical species grow giving indication about system ignition.

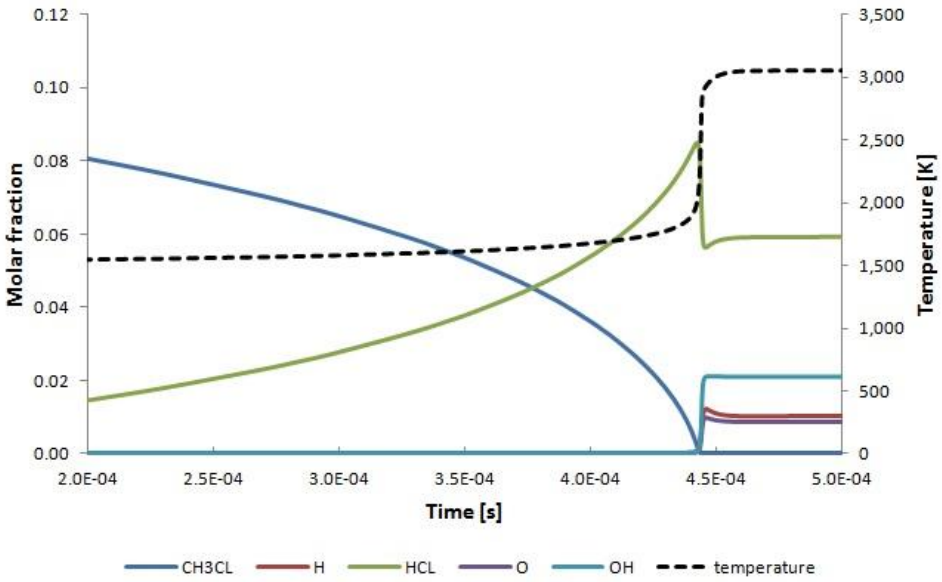

Figure 6.2.2: Molar fraction profiles for CH_3Cl ignition in shock.tube reactor

6.2.2 EFFECT OF CH_3Cl ADDITION ON METHANE IGNITION BEHIND REFLECT SHOCK WAVE

Kuan et al. [75] studied the effect of CH_3Cl addition to methane to evaluate its effect on ignition delay time.

Ignition delay time (τ) was defined as the time interval between the arrival of the reflected shock and the onset of the ignition, defined as a steep rise in pressure, either CH or OH profile. Unlike the previous Section 6.2.1, the mixtures analyzed here contains both methane and methyl-chloride, allowing a deeper undestanding of the occurring ihnibition process.

Table 6.2.2 reports the composition of different mixtures.

Mixture	CH_3Cl [%]	CH_4 [%]	O_2 [%]	Ar [%]	Φ
1	/	3.5	7	89.50	1
2	0.18	3.5	7	89.32	1.06
3	0.35	3.5	7	89.15	1.07

Table 6.2.2: Initial concentrations for the different experimental and simulation tests.

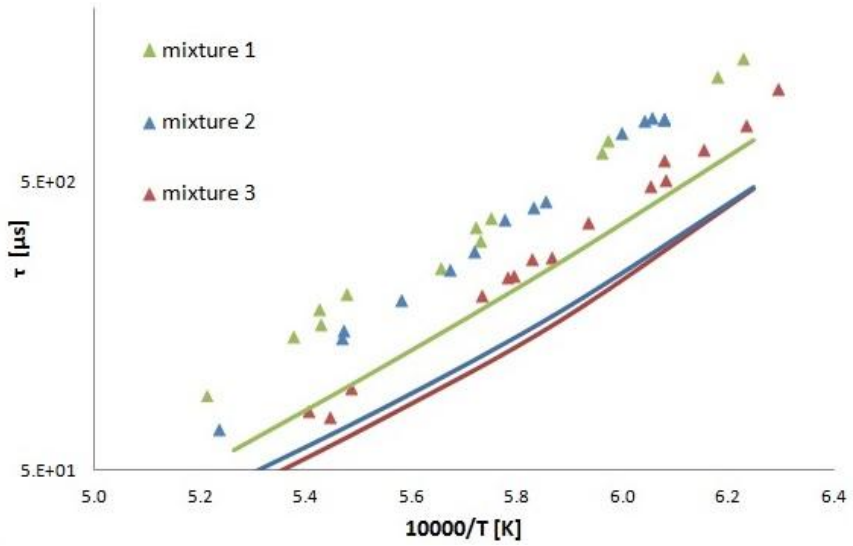

Figure 6.2.3: Experimental [75] and simulated ignition delay time for different $CH_3Cl/CH_4/O_2$ mixtures.

Figure 6.2.3 shows the ignition delay times for three different mixtures in the temperature range from 1600 K to 1900 K. Simply looking at experimental data, we can note that small CH_3Cl impurities do not affect greatly the system reactivity. In fact experimental IDTs for mixture 2 are very close to mixture 1 data. Increasing CH_3Cl quantities, as in mixture 3, IDTs considerably decrease making the system much more reactive. Therefore at low CH_3Cl loadings, as in mixture 2, the promoting effect does not seem to be clear, but as the amount of CH_3Cl increases it becomes clear that methyl-chloride has a promoting effect on methane ignition. Also the numerical results are reported in Figure 6.2.4. The results obtained by kinetic model deviate from the experiments. All the calculated IDT are considerably lower than the corresponding measured data. Anotherclear difference is that the kinetic model predicts small concentration dependence of CH_3Cl in methane ignition compared with the observed one. Anyway the kinetic model can simulate CH_3Cl promoting effect, providing for mixture 2 and 3 IDT value lower than mixture 1. As in Section 6.2.1, also here the mismatch between experimental and simulated data for mixture 1 suggests that discrepancies in the cases of mixtures 2 and 3 might be due to deficiencies in the C1-C3 submechanism. In order to verify our statement a comparison has been performed. For this purpose a different C1-C3 submechanism has been

implemented in our kinetic model, substituting the previous " C1C3HT1412" [8]. The new submechanism implemented for C1-C3 module is called "AramcoMech_1.3" and it was recently developed at the National University of Ireland, Galway [76].
Figure 6.2.5 shows this comparison confirming that the deviations between experimetal data and model previsions are most probably due to deficiencies in the " C1C3HT1412" mechanism.

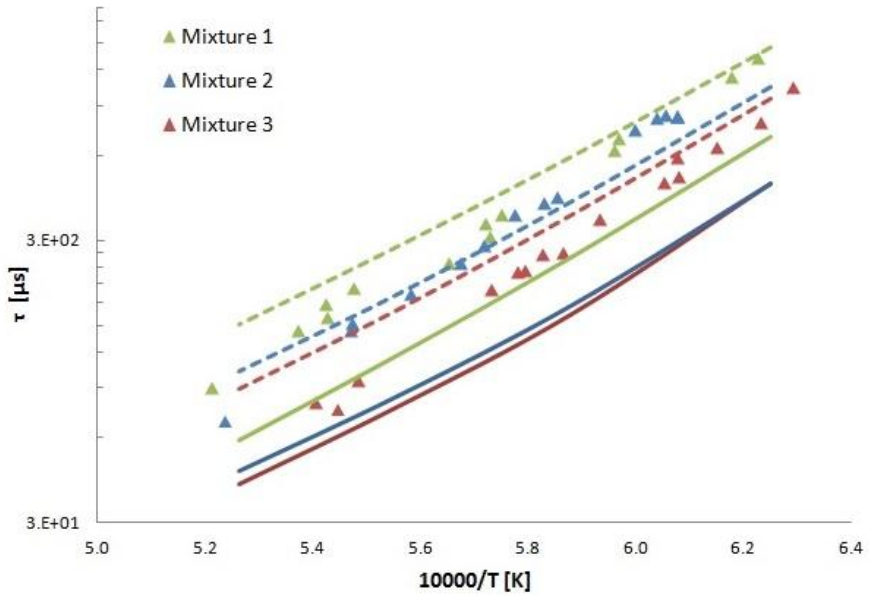

Figure 6.2.4: Experimental [75] and simulated ignition delay time for different $CH_3Cl/CH_4/O_2$ mixtures Comparison between different C1-C3 modules. "AramcoMech_1.3" (dashed), "C1C3HT1412" (solid)

The Aramco kinetic model implemented togheter with CH_3Cl submodule developed in this work, is able to better predict the ignition delay time of the different mixture analyzed. Simulated IDTs for mixture 1 generally overpredict the misurated value of about 10%, while the previous simulations by "C1C3HT1412" underpredicted the values of more than 50%.
Considering the reliability of the kinetic model developed for CH_3Cl sub-module, a further sensitivity analysis was carried out to investigate CH_3Cl effect in methane combustion.
As we can see in the sensitivity analysis plot of Figure 6.2.5 the ignition for CH_4 is controlled by the following reactions:

$$CH_4 + H = CH_3 + H_2 \tag{6.9}$$

$$CH_3 + O_2 = O + CH_3O \tag{6.10}$$

$$CH_3 + O = CH_2O + H \tag{6.11}$$

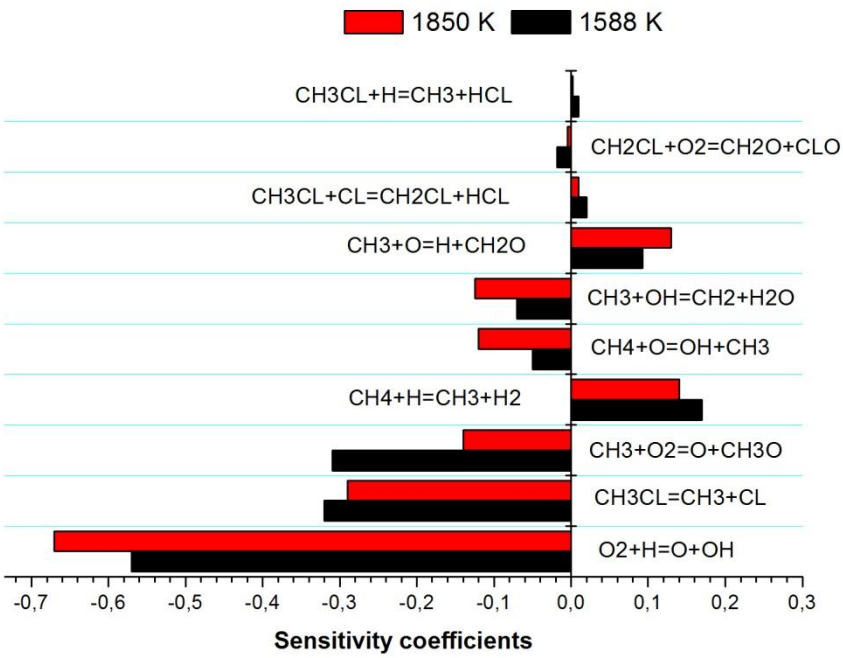

Figure 6.2.5: Sensitivity coefficients of IDT to rate constants for mixture 3 at 1588 K and 1850 K

involving species which can follow the sequence $CH_4 \rightarrow CH_3 \rightarrow CH_3O \rightarrow CH_2O \rightarrow CHO \rightarrow CO$ [75].

Great importance is assumed also by the branching reaction of $H+O_2=OH+O$, which consumes H radical pool. Clearly the CH_3CL addition modify the initiation step for mixture ignition. The initiation reaction is not $CH_4=CH_3+H$ but $CH_3Cl=CH_3+Cl$. The methane decomposition reaction CH4=CH3+H seems to not contribute to ignition. CH_3 radical is generated from methyl-chloride decomposition or from reaction

$$CL + CH_4 = HCL + CH_3 \tag{R62}$$

Methyl radical reacts with oxygen generating CH_2O or CH_3O that decomposes quickly to CH_2O and H. Hydrogen can then reacts with CH_4 or CH_3Cl, but this latter interaction is less important. This scheme shows that the additive, namely CH_3Cl, changes the rate of ignition reaction but not the main ignition mechanism. The promotion effect by addition of CH_3Cl on CH_4 ignition is due to the relatively fast decomposition rate of the additive $CH_3CL=CH_3+Cl$.

6.3 CH_3CL/CH_4 PREMIXED LAMINAR FLAMES

In this section the impact of chlorine on the combustion chemistry of hydrocarbons have been explored by considering different kind of reacting systems. In the previous chapters has been studied ideal reactors in which fluid mixing and thus its uncertainty is almost completely suppressed. In the previous sections, composition and temperature fields are only kinetically limited while in laminar flames, that we are going to consider, heat and mass transport can become rate limiting. Therefore flames always require considerations of transport phenomena along with reaction kinetics. In particular in laminar premixed flames mixing occurs because of heat and species diffusion at the flame front. Despite the greater calculation issues, these flames are are extremely useful for studying the kinetics of combustion and the speciation, at high temperature and in presence of diffusion of heat and mass.

6.3.1 CHEMICAL STRUCTURE OF CH_3CL/CH_4 PREMIXED FLAT FLAMES

Experimental results resulting from a laminar flame are compared with results obtained by numerical modeling. In particular misured data are taken from Karra er al. work [77]. The experiment has been carried out stabilizing an atmospheric-pressure premixed flat flames over a 5 cm diameter circular, porous, flat-flame burner. The detected species profiles own an ±0.25 mm estimated uncertainty in the absolute positions, while the relative positions among different profiles can be considered much more accurate.

Also temperature profile was experimetally measured and then corrected for radiation effects using standard technique (Kaskan, 1959). A ± 10 percent uncertainty in the absolute values of the temperatures, and an uncertainty of about ±0.20 mm in the absolute position of the temperature profiles have been estimated.

In figure 6.3.0 are plotted corrected temperature profiles for the analyzed reacting mixtures.

In Karra et al. work the impact of chlorine was studied comparing CH_3Cl/CH_4 flame with a pure CH_4 flame, namely methane was used as a reference system.

In this work the methane flame was only used to verify some inconsistencies detected during CH_3Cl/CH_4 flame simulation.

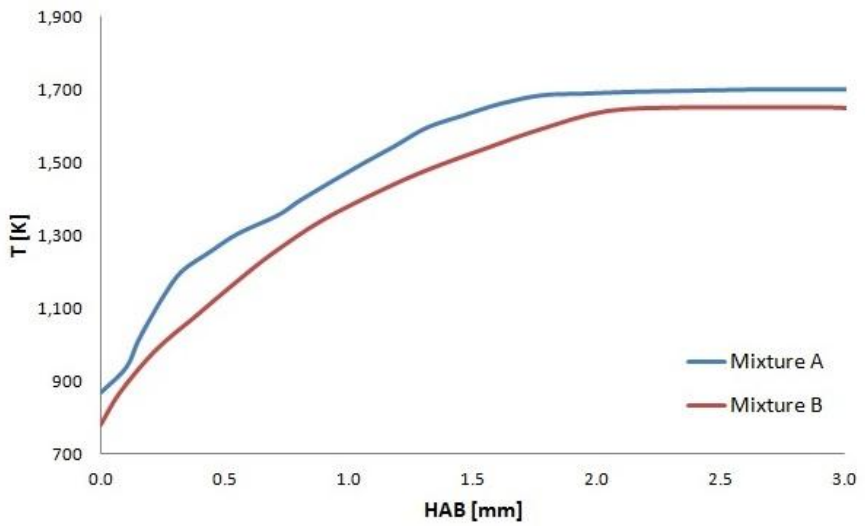

Figure 6.3.0: Corrected experimental temperature profiles [77] for laminar flat flames.

The mixture compositions are listen in table 6.3.1

Mixture	CH_3Cl [%]	CH_4 [%]	O_2 [%]	Ar [%]	Φ
A	13.4	26.6	36.7	23.3	1.79
B	/	36	35.1	28.9	2.05

Table 6.3.1: Initial concentrations for the different experimental and simulation tests.

As showed in figures 6.3.1 the profiles determined by kinetic model present both inconsistencies and good agreement with experimental data. Firstly it must be noted that experimental data within about 1 mm from the burner surface should be considered unreliable because probe-burner interactions are likely to disturb the flame structure. However this last statement doesn't justify the disagreement at greater distances. Looking at figure (a) we can note the greater reactivity of kinetic model compared with the real flame. Even if the experimental points were moved as much as the experimental uncertainty, there would be no overlap between previsions and misured data. Thus CH_3Cl, CH_4 and O_2 are consumed faster, generating amounts only slightly greater for CO and CO_2.

Also in figure (b) and (c) are visible the kinetic model imperfections. There are relevant overestimation in acetylene, ethylene and hydrogen profiles. About hydrogen profile, the experimental mole fraction profile for H_2 was determined from hydrogen atom balance. Consequently, it possess considerable uncertainties because of the cumulative nature of the uncertainties associated with the measurement of many species used in the atom balances.

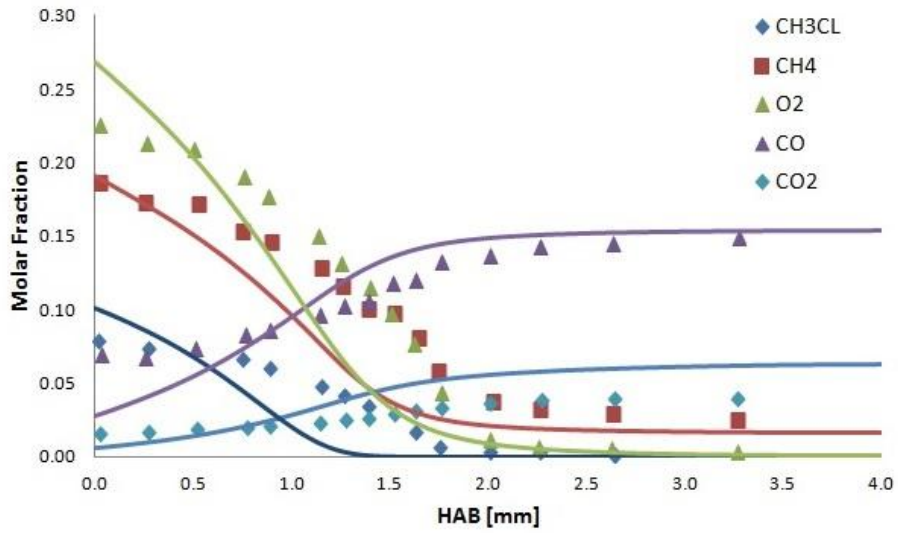

(a)

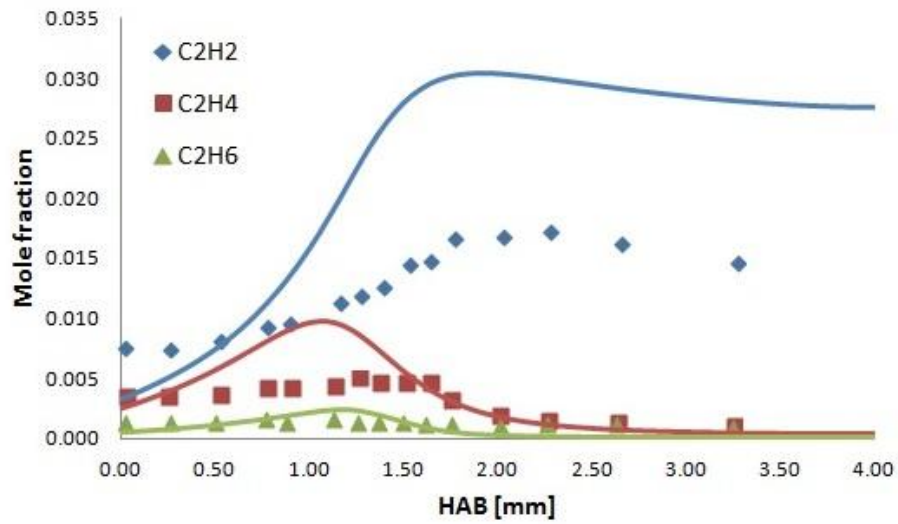

(b)

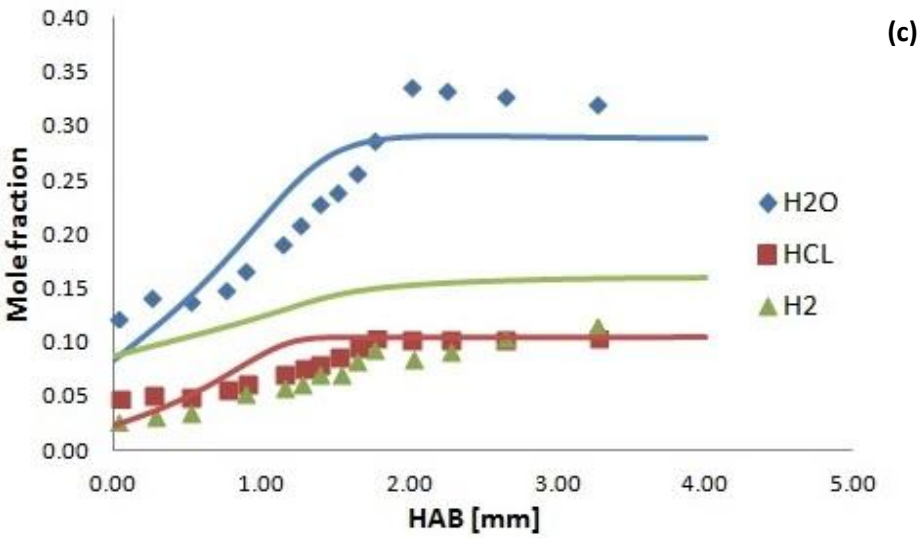

Figure 6.3.1: Comparison of experimental [77] and predicted profiles for CH_3Cl/CH_4 flame

Similarly to section 6.2 also here a mixed system including CH_3Cl and CH_4 as reacting fuels has been used. Therefore the inconsistencies observed in the previous figures could be caused by CH_4 submechanism imperfections. To verify this assestment kinetic model has been tested towards the pure CH_4 flame.

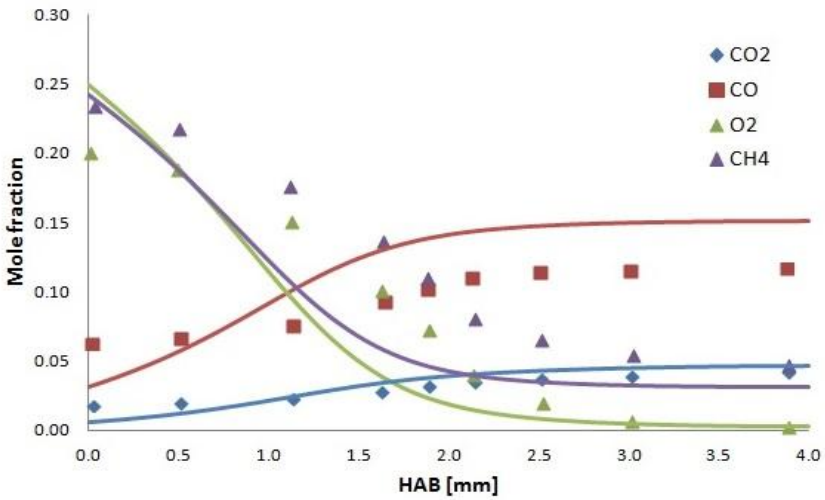

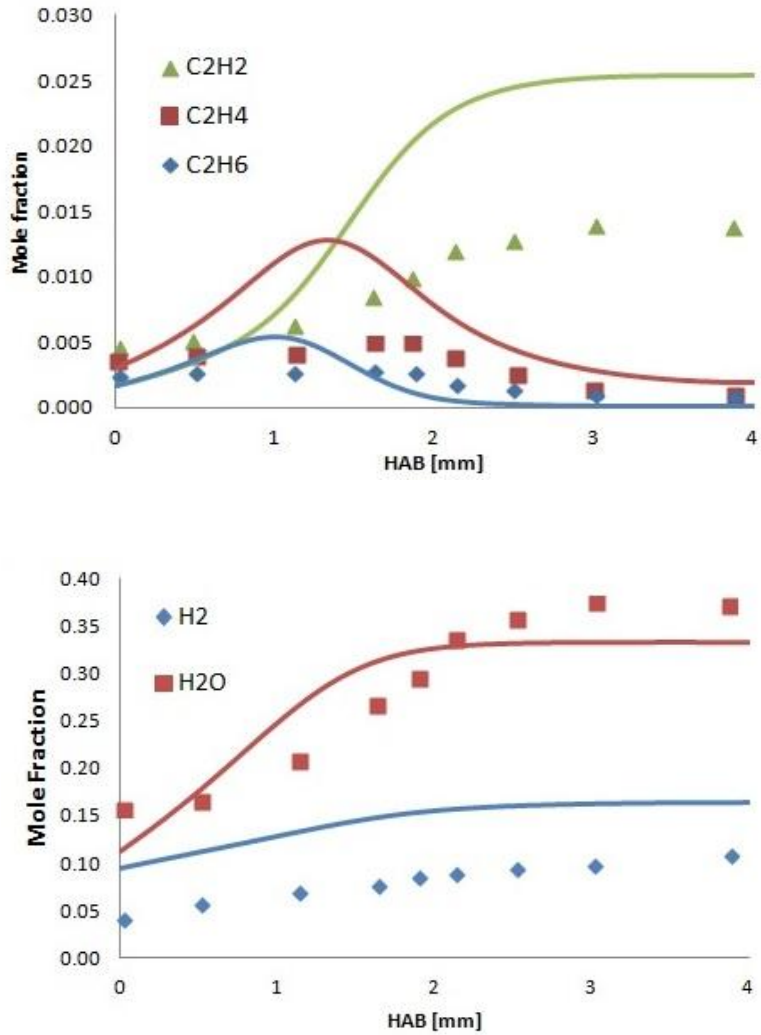

Figures 6.3.2: Comparison of experimental [77] and predicted profiles for CH_4 flame

The flame B, which consists in a $CH_4/O_2/Ar$ burning mixture, proves methane submechanism partial unreability. Thus an other possible source of errors, togheter with experimental inaccuracy, is the aformentioned one. Also in figure 6.3.2 kinetic model shows a greater reactivity which consumes fuel faster and overpredicts intemediate products like C2 hydrocarbons. As in section 6.2, methane sub-mechanism importance is valuated implementing the Aramco sub-mechanism [76] for methane instead of C1C3HT1412 submechanism by POLIMI (see chapter 6.2.2). This change brings many improvements in kinetic model prevision.

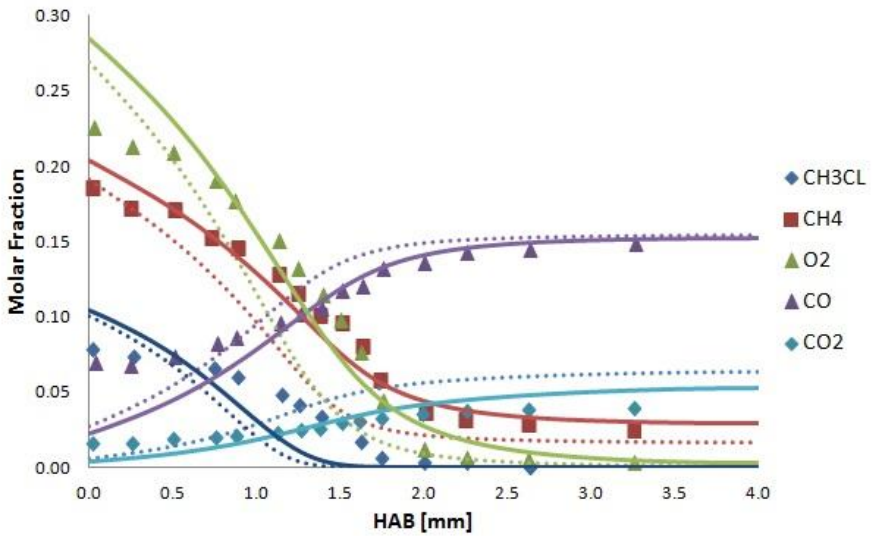

Figures 6.3.3: Comparison of experimental [77] and predicted profiles for CH_3Cl/CH_4 flame. Comparison between different C1-C3 modules. "AramcoMech_1.3" (solid), "C1C3HT1412" (dashed).

Figure 6.3.3 shows the comparison between POLIMI "C1C3HT1412" and Aramco "AramcoMech_1.3" submechanism. The new submechanism implemented shows a better prediction ability, specially for CH_4, O_2 consumption, and H_2 production. The improvement is less accentuate for CH_3Cl prediction, but definitely they are clearly visible.
Also for C2 species improvement can be observed, in particular for acetylene, whose peak value is consistently decreased if compared to the value obtain with POLIMI submechanism and then it's also more faithful to experimental misurations.

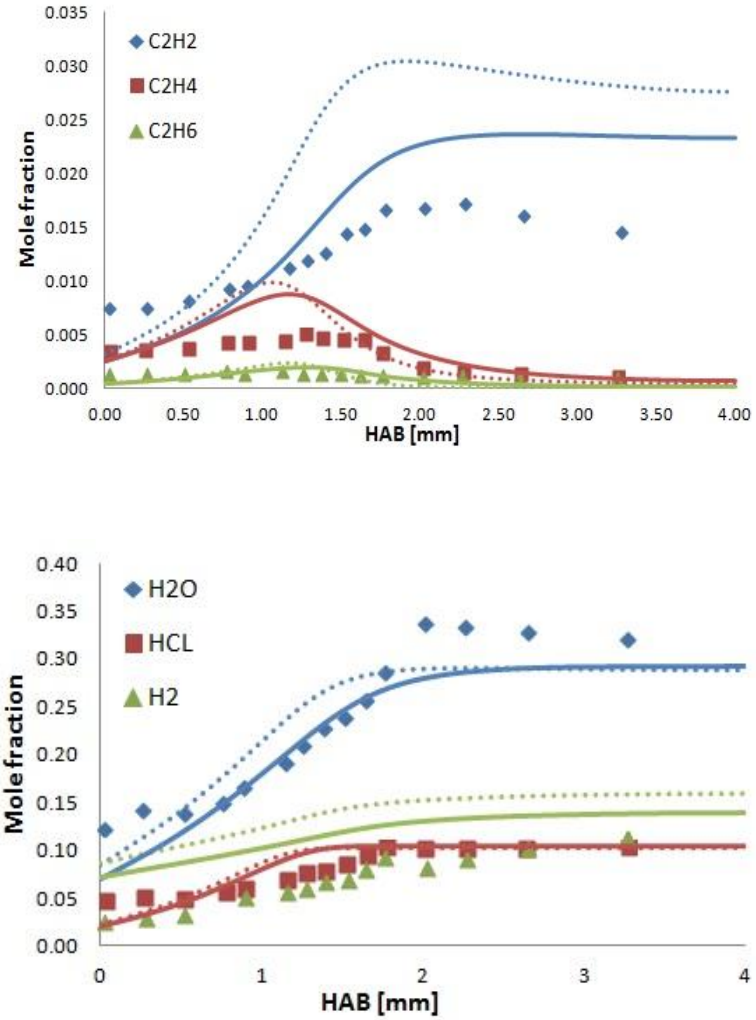

Figures 6.3.4: Comparison of experimental [77] and predicted profiles for CH_3Cl/CH_4 flame. Comparison between different C1-C3 modules. "AramcoMech_1.3" (solid), "C1C3HT1412" (dashed).

Sensitivity analysis and rate of production analysis have been performed and the important reaction analyzed.

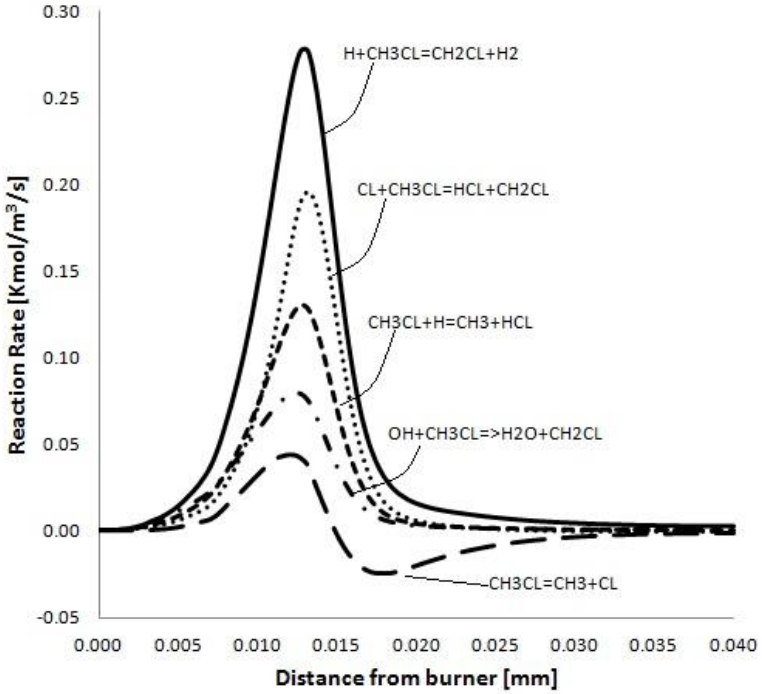

Figures 6.3.5: Rate profiles for reactions having the highest net rates that involve CH_3Cl.

As visible from the profiles in figure 6.3.5, CH_3Cl bulk is destroyed mainly by H, Cl and OH radicals through reaction R247, R146 and R249. In particular the first is the reaction competiting directly with the branching reaction $H+O_2=OH+O$. Rate profiles of reaction R127, shows that initially CH_3Cl is consumed by the reaction, but progressively the rate decreases and rate direction changes at 0.015 mm from the burner, i.e. the point at which methyl chloride is totally consumed. Sensitivity analysis performed reveals R127 as the most sensitives reaction for CH_3Cl consumption. For this reaction sensitivities coefficient is the greatest in the very early parts of the flame and the peak value occurs in advance with respect to the others. This because free radical concentrations is low the early part of the flame.

For methane predictions are in good agreement with experimental data if "Aramco" submodule is used. The main reaction producing and consuming CH_4 are presented in figure 6.3.6. As shown the reactions involve the presence of radical species which attack fuel later than CH_3Cl.

The methyl radical generated by CH_3Cl dissociation recombinates with hydrogen radical to form methane through reaction

$$CH_3 + H + M = CH_4 + M$$

Moreover methane consumption is retarded because reaction CH_4+H=CH_3+H_2 initially proceeds in reverse direction, starting consume methane only when CH_3Cl is almost consumed.

Acetylene simulation presents some discrepancies. Kinetic model slightly under predicts C_2H_2 mole fractions early in the flame zone, and slightly over predicts them in the post-flame zone. Near the burner the discrepancies can be caused by the probe-burner interactions which disturb the flame zone.

Reaction rate analysis suggests that C_2H_2 is formed mainly by reaction

$$C_2H_3 + M = C_2H_2 + H + M$$

However in the presence of CH_3Cl acetylene can formed through another path, which is through reaction R197.

The destruction of acetylene occurs primarily by O and OH radical attack at high temperature and since the concentrations of these radicals are affected by the temperature level in the system, acetylene destruction rate would be sensitive to the temperature profile used in the calculations. That is, part of the discrepancy is attributable to the uncertainties associated with the measured temperature data in the post flame zone.

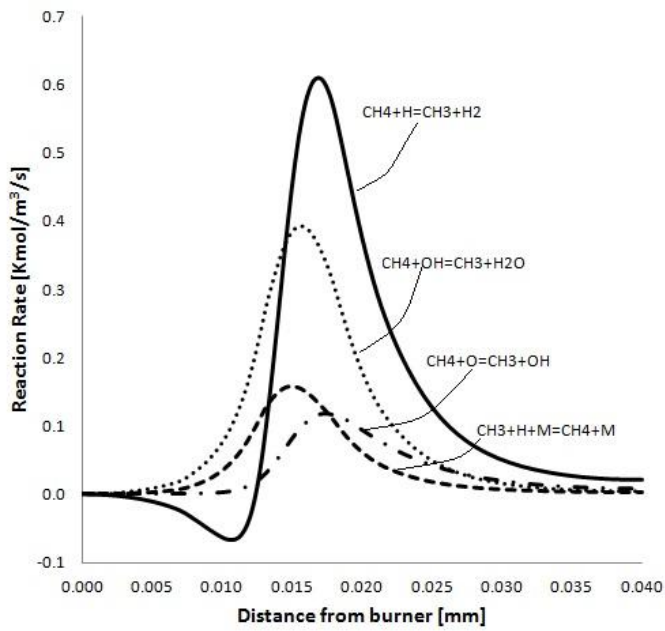

Figures 6.3.6: Rate profiles for reactions having the highest net rates that involve CH_4.

6.4 LAMINAR FLAME VELOCITIES

As in section 6.3 also here flame systems are simulated, compared with experimental results and analyzed in order to investigate CH_3Cl effects. The laminar burning velocity is an important physico-chemical property of a combustible mixture, the square of which is proportional to the overall rate of combustion [78]. Consequently the knowledge of this parameter is of interest both from practical and theoretical points of view. Large flame velocities normally indicate that combustion reactions are fast and that the reactants are rapidly consumed. Conversely, small burning velocities imply slow rates of combustion and in the limit potential emission problems due to flame quenching.

Even if the detailed chemistry of combustion is really complex, the overall CHC combustion can be examined heuristically. The molecular formula of generic chlorinated hydrocarbon can be written as $C_xH_yCl_z$, while the overall combustion stechiometry for y > z is

$$C_XH_YCL_Z + [x + (y - z)/4]O_2 \rightarrow xCO_2 + zHCL + [(y - z)/2]H_2O$$

this relation is not valid when y < z because also CL_2 formation should be considered. Since methane is used as auxiliary fuel, CH_3CL combustion stechiometry is defined as

$$CH_3CL + \frac{1}{R}CH_4 + \left[\frac{2}{R} + \frac{3}{2}\right]\left[O_2 + \frac{1-\Omega}{\Omega}\right]N_2 \rightarrow \left(1 + \frac{1}{R}\right)CO_2 + HCL + \left[\frac{2}{R} + 1\right]H_2O + \left[\frac{2}{R} + \frac{3}{2}\right]\frac{1-\Omega}{\Omega}N_2$$

where R is the molar ratio CH_3Cl/CH_4 and Ω is the oxygen mole fraction in the oxidizer, i.e., if air or oxygen as oxidizer is used, Ω= 0.21 or 1.0, respectively. The mixture equivalence ratio, defined as the ratio of the actual fuel/oxygen ratio to the stechiometric fuel/oxygen ratio, can be written as the following

$$\Phi = \frac{\left[\frac{2}{R} + \frac{3}{2}\right]}{actual\ O_2\ used}$$

That is, for Φ = 1.0, the actual O_2 used corresponds to the exact stoichiometric requirement, while Φ < 1.0 and Φ > 1.0 corresponds to oxygen-rich and fuel-rich mixtures, respectively.

6.4.1 LAMINAR BURNING VELOCITIES OF CH3CL/CH4/AIR FLAMES

In Valeiras et al. work [78] are presented different experimental relevations of laminar flame velocity. In particular are detected laminar velocities of CH_3Cl/CH_4 flames, with the aim of elucidate the chlorine effects on combustion. Experimental misurations have been made using Bunsen cone method. The flames were stabilized on a vertically positioned 1 cm ID quartz burner, which was sufficiently long to insure the presence of fully developed laminar flow at its tip. According to this method, the burning velocities can be obtained by simply dividing the volumetric flow rates of the un burnt gas mixtures to the flame front areas which are determined separately. However the determination of real flame front area is not so simple because is complicated by the curvature of the flame zone. According to the experimental semplicity adopted, the direct image flame photography was used in this study. However this method overestimates the actual flame front area and conseguently underestimates the laminar burning velocity. This experimental technique has a margin of error 10-20% on the flame velocities [78].

The methyl-chloride sub-module is tested towards the experimental misurations by Valeiras er al. and the unburnt mixture is held at temperature of 353 K.

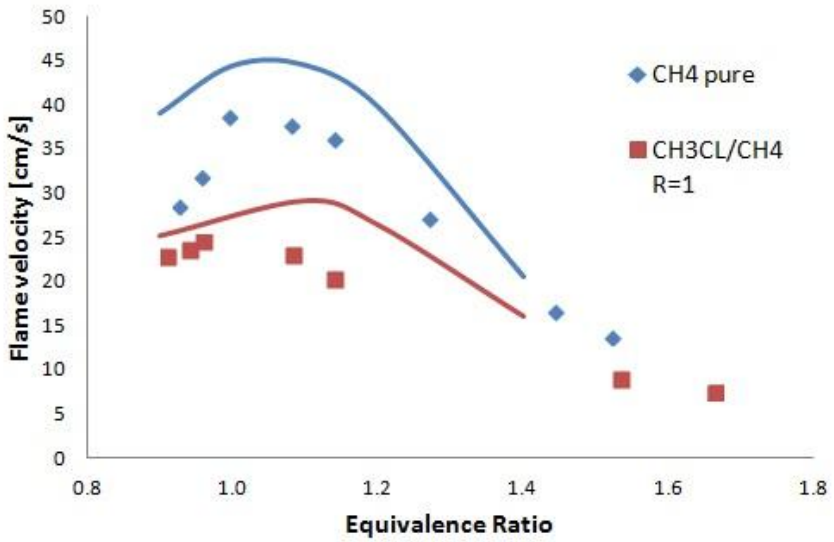

Figure 6.4.1: Experimental [78] and simulated laminar burning velocities of chlorinated and not chlorinated methane.

Firstly was indagated the chlorine effect compared with pure burning methane. In figure 6.4.1 are presented experimental and simulated values of laminar

velocities plotted as a function of the mixture equivalence ratio. Both experimental and simulated flame velocities detect the chlorine inhibition effect, represented by lower velocities for chlorinated flame. It's noticeable that chlorine slows down the system reactivity lowering greatly the burning velocity. Kinetic model previsions don't overlap experimental data, except for the values at high equivalence ratio. Laminar flame velocities are overestimated both for pure methane and chlorinated methane, however the overestimation it's contained within the experimental uncertainty and the general trends resemble those experimental. The peak values have been determined in the oxygen lean side for methyl-chloride, while pure methane peak value is more shifted towards stechiometric value.

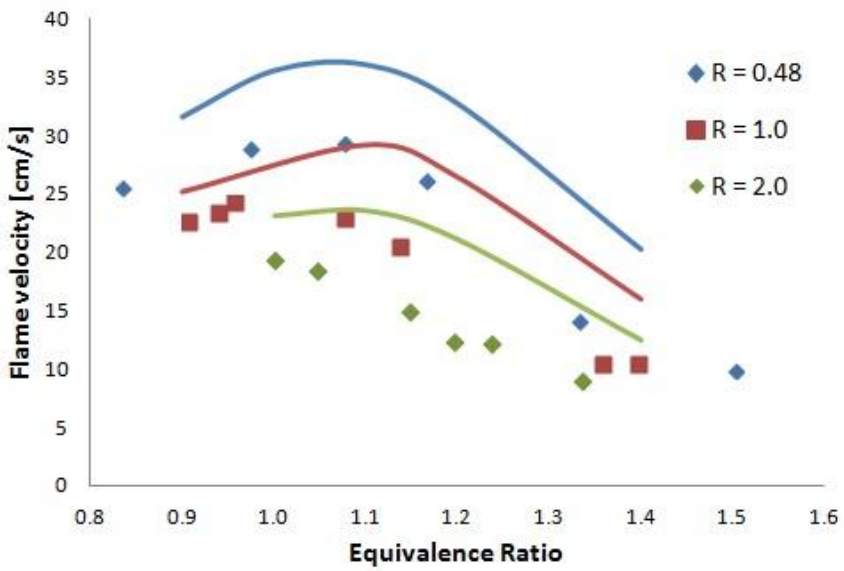

Figure 6.4.2: Experimental [78] and simulated laminar flame velocities of CH_3Cl-CH_4-air mixtures at different *R* values.

Different amount of chlorine are tested. Looking at figure 6.4.2 is visible the increasing inhibition effect due to the increase of chlorine in reacting mixture. Chemical inhibition is due to the free radical scavenging characteristics of chlorine and chlorinated compounds, which rapidly react with the H and OH radicals, and thus interfere with both the combustion chain propagation and branching reactions.

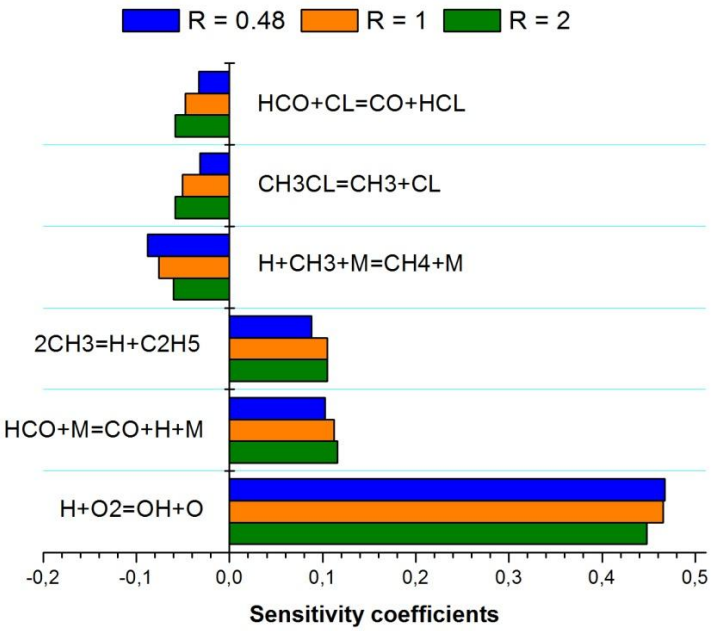

Figure 6.4.3: Sensitivity coefficients of LFS to rate constants for mixture at different R values.

Sensitivity analysis shows the different relevance assumed by reactions at different R values. Laminar flame speed is controlled mainly by branching reaction, and secondly by the reactions producing and consuming H radicals, which competes with branching reaction itself.
The starting reaction R127 is becoming increasingly important increasing the CH_3Cl amount in reacting mixture; in the same time branching reaction slightly lost its sensitivities.

6.4.2 STUDY OF $CH_4/CH_3Cl/O_2/N_2$ PREMIXED FLAMES UNDER OXYGEN ENRICHMENT

Shin et al. studied in their work [79] the influence of methyl-chloride added to a burning mixture. In particular they studied premixed flames under oxygen enrichment. Recent developments have led to enhance the traditional fuel–air combustion process by using oxidants with a higher proportion of oxygen than that in air. A number of industrial heating applications requiring high-temperature conditions are improved using this technique. The primary influences of oxygen enrichment on flame characteristics are higher flame temperatures and flame speeds, a reduction in length, an increase of flammability limit and better ignition characteristics. In addition to oxygen enrichment, Shin et al work deal with higher concentration of ihnibitor to

emphasize chlorine impact. The experimental test has been performed using laminar Bunsen flame at atmospheric pressure and room temperature (≈300 K) on a burner nozzle of 12 mm diameter. Here the laminar flame speed of the premixed flame is obtained by the Schlieren imaging technique.
Then experimental values have been simulated varying oxygen mole fraction Ω in the oxidizer (Ω changed from 0.21 to 0.35), varying the molar ratio of methyl chloride to methane *R* from 0 to 1.0, and finally varying the equivalence ratio ϕ of the unburned gas in the range of 0.7–1.3.

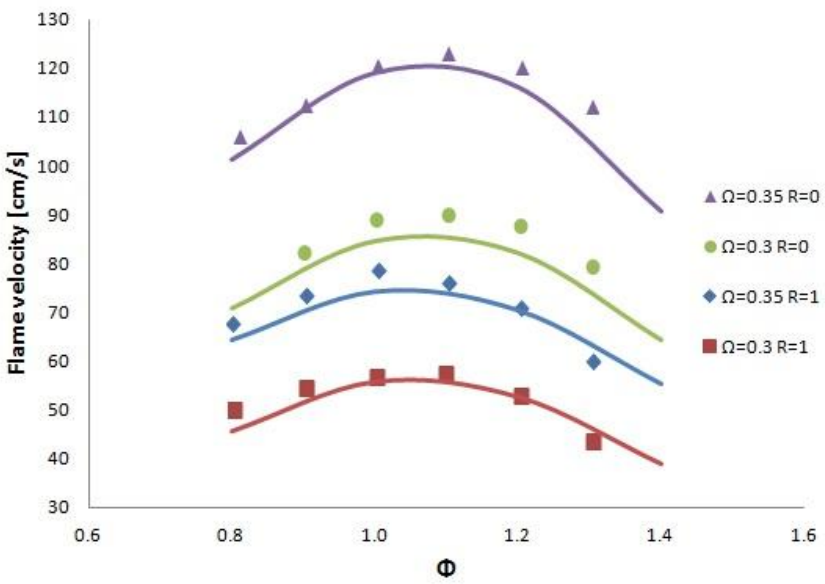

Figure 6.4.4: Experimental [79] and simulated laminar flame velocities for CH_4 and CH_4/CH_3Cl flames at different oxygen enrichments.

Firstly kinetic model was tested simulating LFS with constant oxygen enrichment and varying the equivalence ratio. In particular are compared pure methane flames (R=0) and mixed CH_3CL/CH_4 flames (R=1). The model is able to predict reasonable well both the types of flames. For chlorinated flames the estimation are slightly lower than experimental data, except for higher equivalence ratio, which are overestimated. The kinetic model is able to reproduce faithfully the main behaviour shown by experimental misurations, i.e. the flame velocity increasing due to the increase of oxygen fraction in the oxidizer, the inhibitory effect caused by chlorine presences, and the maximum flame speed occuring on the fuel rich side.

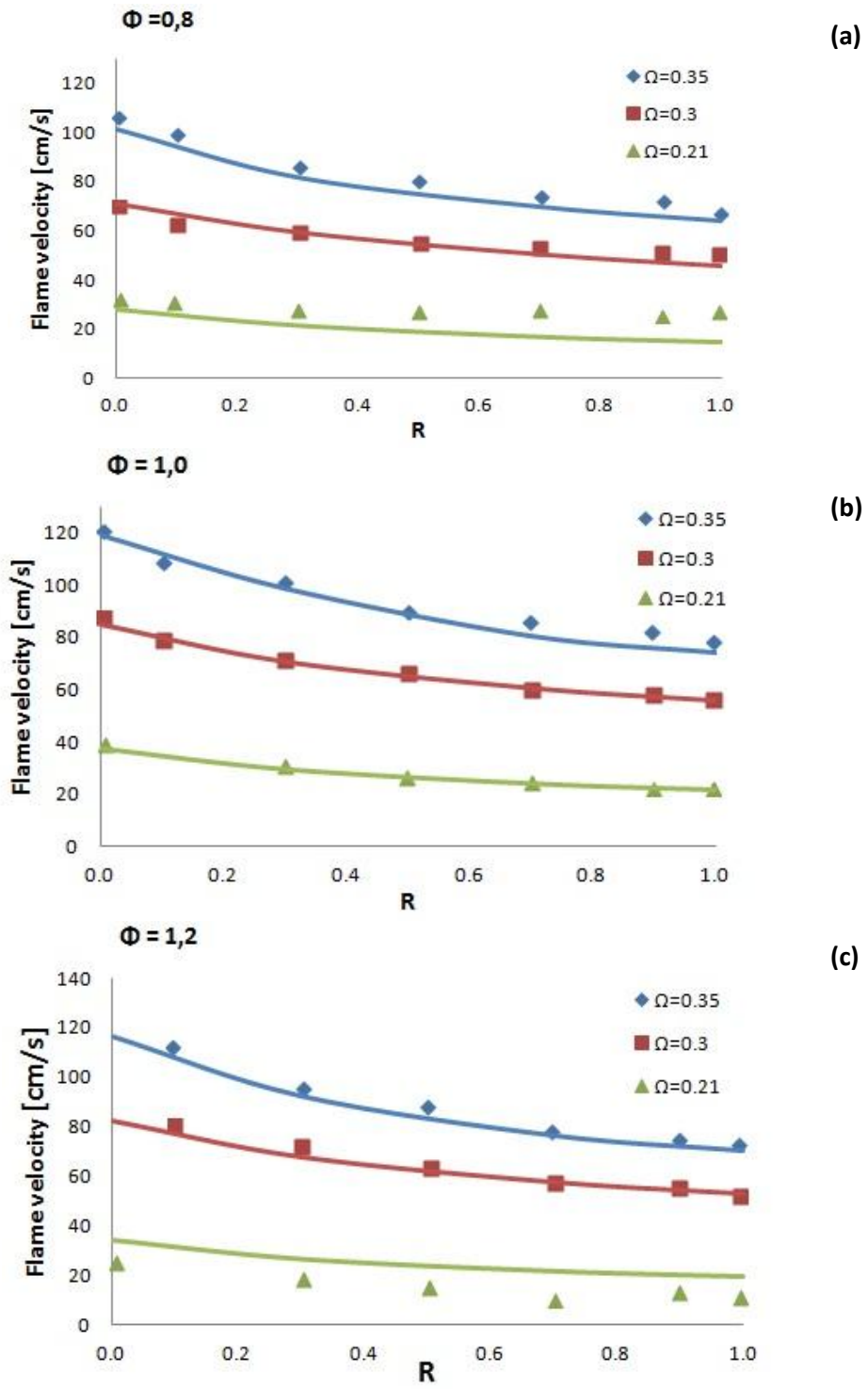

Figure 6.4.5: Comparison of the measured (points) [79] and calculated (curves) flame speeds different levels of oxygen enrichment and Φ= 0.8 (a), 1.0 (b), 1.2 (c)

As visible from figure 6.4.5 kinetic model can reproduce well laminar flame speed at different amount of CH_3Cl in the burning mixture. The greater difficulties appear at low oxygen enrichment: over and understimations are carried out for rich and lean mixture respectively. To show how CH_3Cl works to lower flame speed, the maximum concentrations of important radicals for flames, at ϕ = 0.8 and 1.2 and Ω = 0.21–0.35 with respect to the molar ratio R, is shown i figures 6.4.6.

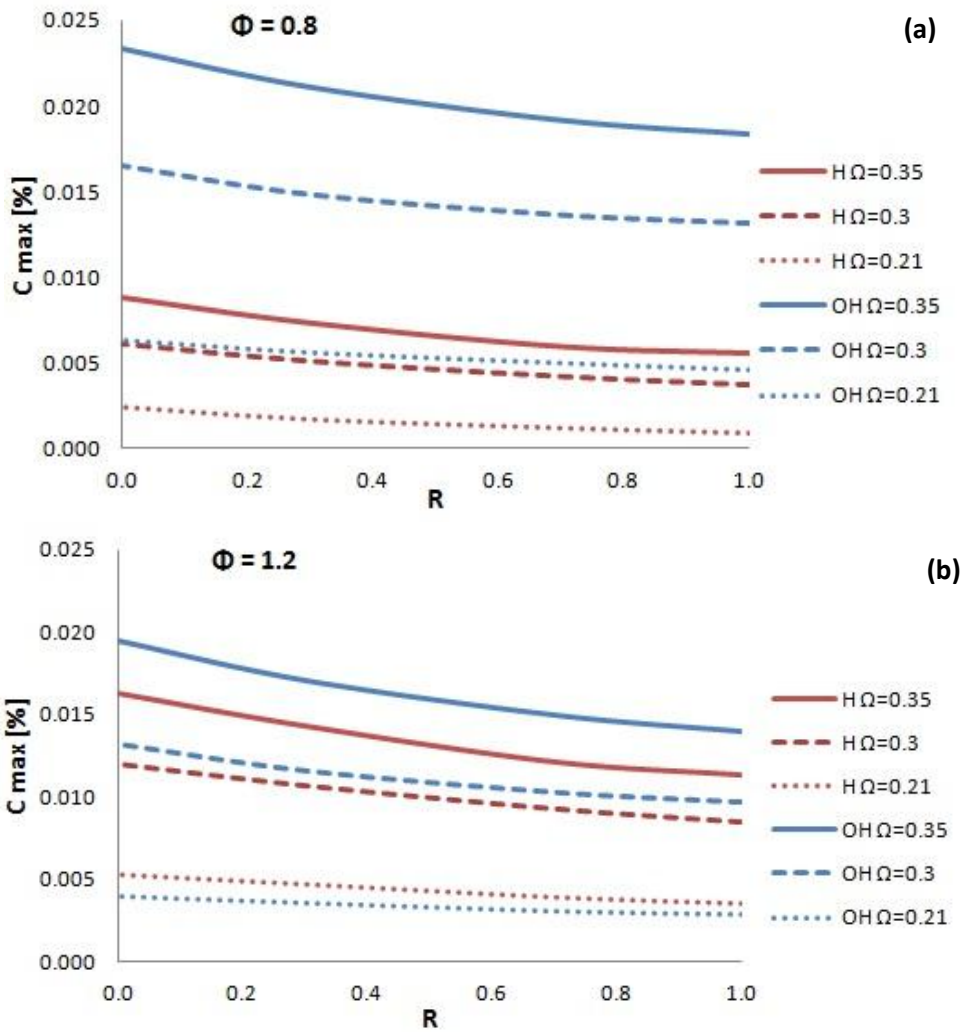

Figure 6.4.6: Concentration of radicals O, H, and OH for different levels of oxygen enrichment and Φ = 0.8 (a), 1.2 (b).

For combustion in air, but also for oxygen enriched atmosphere, an increase in chlorine loading results in a decrease of radicals concentration. Moreover the effects of chlorine are less accentuated for greater concentration of oxygen in the oxidizer, i.e. the reduction in radical concentrations is weakened as the oxygen mole fraction is increased. This effect is more pronounced in rich flames with abundant H radicals than in lean flames. Lower quantities of OH radicals for rich flame are caused by the competition for radicals H between branching reaction and H-containing reactions with chlorinated species.

6.4.3 STUDY ON PREMIXED FLAMES OF CH_3Cl/CH_4/Air

In this section experimental values, taken from Chelliah et al.work [80] for premixed flame of CH_3Cl/CH_4 in air, are compared with the simulations obtained with our kinetic model. Experimental burning velocities have been measured using counterflow technique, which involves the establishment of a premixed flame in the counterflow configuration, and the determination of the axial velocity profile along the centerline by laser-Doppler velocimetry.

The predictions of flame speed of CH_3Cl/CH_4/air and CH_3Cl/air mixtures, employing the chloromethane sub-mechanisms, were compared with experiments and are shown in Fig. 6.4.7.

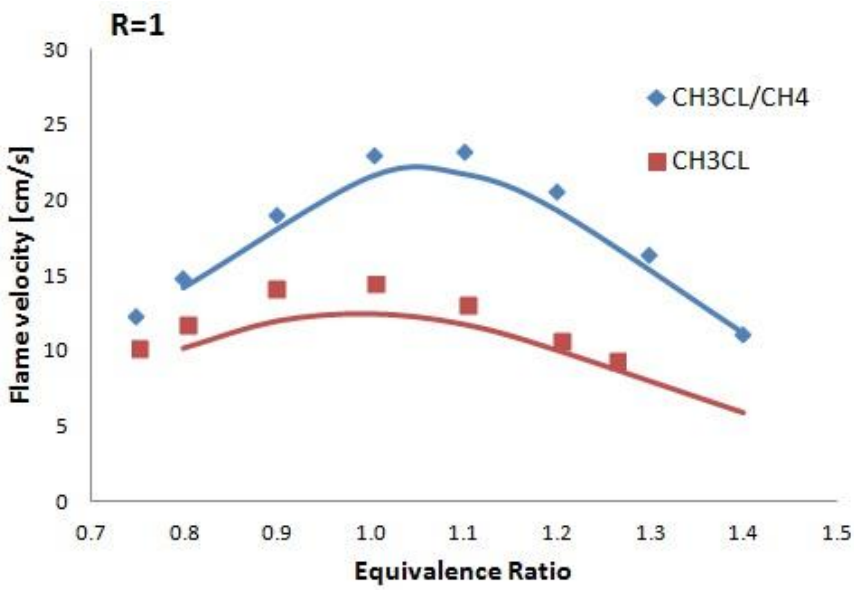

Figure 6.4.7: Experimental [80] and simulated laminar flame velocities as function of equivalnce ratio for CH_3Cl and CH_4/CH_3Cl flames.

As clear from the figure above, flame speed decreases considerably with the addition of methyl-chloride. As expected methyl-chloride flame assumes speed lower than CH_3Cl/CH_4. While the peak value for CH_3Cl/CH_4 flame occurs clearly in the fuel-rich side, for pure chloromethane it's occurs close to stoichiometric value. Moreover the general trend is quite flattened and therefore it's hard to understand if the greatest speed value falls in the rich or lean side. The simulations performed with the kinetic model generally underestimate the experimental values, but also resemble well the general trend defined by experimental points. Anyway for CH_3Cl/CH_4 flames, values determined through numerical modeling lying within the experimental uncertainty of 10% declared by the authors [80]. Differently the pure CH_3Cl flames at equivalence ratio ranging between 1.1 and 0.8 assume values undeniably slighlty lower than those measured.

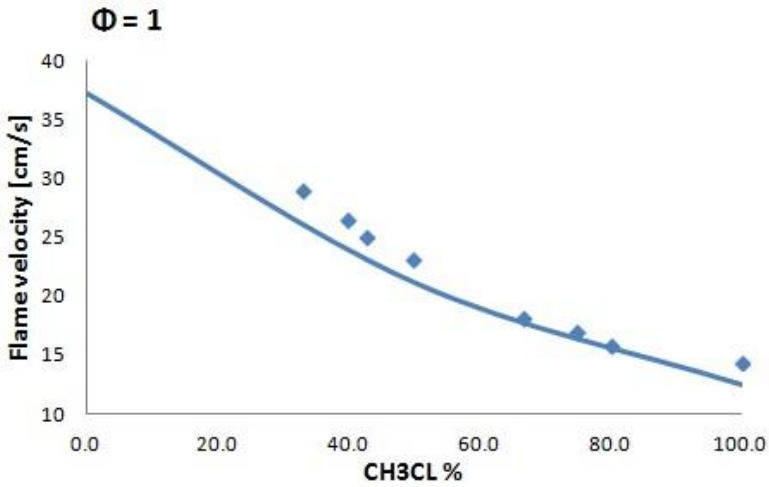

Figure 6.4.8: The variation of the burning velocity of stoichiometric mixtures of chloromethane, methane and air as a function of chloromethane mole-% in the fuel, from experiments (squares) [80] and simulation (line)

In figure 6.4.8 experimental data and simulations are compared revealing again the general underestimation contained within the experimental uncertainty. The graphic presents different flame speeds determined at stechiometric condition varying the molar ratio R. As expected increasing the chlorine concentration the flame speed decrease, apparently following two different trends. The former trend, ranging from pure CH_3Cl to 50% methyl-chloride contained in burning mixture, is relatively flatter than the latter which range from 50% to 0% of CH_3Cl. This second trend is fairly steep, indicating that at

low CH_3Cl concetrations the halogenated compounds shows the maximum ihnibiting effect. This effect changes progressively decreasing for higher Cl concetration.

7. CONCLUSIONS AND FUTURE OUTLOOKS

Since incineration is one of the main technique used for wastes disposal, it is necessary to better characterize the kinetic mechanism which lead to pollutants generation. In this work chlorinated species are investigated, in order to better understand formation mechanism and their influence on reacting systems. In particular the aim of the work was to define a reliable reaction mechanism with realiable kinetic parameters able to reproduce CH_3Cl pyrolysis and combustion in different reacting systems and conditions. Methyl-chloride is the simplest halogenated hydrocarbon and also the first step to understand how hazardous molecules like dioxines are generated. To achieve this purpose a kinetic model has been built coupling the new CH_3Cl sub-system with the C1-C3 module. Kinetic parameters were estimated based on analogy or from informations available in the literature. The mechanism has been validated over all the experimental data available in the literature. Kinetic analyses, togheter with previous work found in literature, have been used to characterize and understand how key steps in the kinetics involved.

Overall the kinetic model is able to reproduce satisfactorily the different systems analyzed in this work and the behaviuor of methyl-chloride, which dramatically changes according to the conditions considered. Still there are margins of improvement to reach a complete realiability of the mechanism. In particular the study of tubular flow reactor demostrated a greater reactivity at the lowest temperature analyzed. Starting from an excessive fuel consumption, other discrepancies are observed in the prediction of intermediates and products. The general trend of these species is always properly determined, but anyway some inaccurancies are present and they seem unavoidable. Great importance is assumed by the starting chain reaction $CH_3Cl=CH_3+Cl$, which is crucial to decide what effect the CH_3CL should have on reacting system, i.e. inhibitory or promotive.
Great concentration of chlorinate compounds always inhibit the combustion process, but in small quantities CH_3Cl can promote the ignition process, because the lower bond dissociation energy of C-Cl compared to C-H bond.
Other reactions have great importance in the kinetic model. Reactions like $CH_3Cl+H=CH_3+HCl$, the radical pool, are fundamental in the inhibition mechanism, because basically they compete with branching reactions typical of hydrocarbon oxidation. These results are evident in shock-tubes and laminar flames. Generally the simulations performed on these systems showed excellent agreeement with the experimental data, and the small

inconsistencies seem to be more related to C1-C3 submodules, whose study is beyond the scope of the present work.

The kinetic mechanism discussed in the present work has, overall, a good capability to predict experimental observations. However to further validate, improve and optimize the performances of the model and solve all the uncertainties, still a wider and newer experimental database is necessary, together with more accurate estimation of rate constants. In fact, being the HCl/Cl2/CH3Cl quite a small system, open questions could be easily faced through quantum chemistry methods, largely available and quite inexpensive for systems with low number of atoms. This would lead to a better determination of the kinetic rate constants, whose values are often scattered and aged. The above suggested future steps are of key importance to achieve a total understanding of the kinetics of such small chlorinated system, allowing a more reliable extension to higher molecular weight chlorinated species. It has to be highlighted that this mechanism constitutes the first in the literature validated over all of the experimental data available, therefore constitutes a robust starting point for future refinements.

APPENDIX A

THERMODYNAMIC NASA COEFFICIENTS

```
OCLO                    CL  1O   2          G    300.00   4000.00 1000.00      1
 .575169720E+01 .145708433E-02-.581201424E-06 .108923492E-09-.680077676E-14    2
 .986155572E+04-.279365208E+01 .312449152E+01 .743369650E-02-.207283342E-05    3
-.490714561E-08 .315149383E-11 .106200243E+05 .110060950E+02                   4
CL2                     CL  2              G    300.00   4000.00 1000.00      1
 .472497332E+01-.452025622E-03 .248339908E-06-.198734964E-10-.138247235E-14    2
-.150144014E+04-.218753211E+00 .274354106E+01 .778656796E-02-.144041508E-04    3
 .124869963E-07-.411292285E-11-.105955046E+04 .941507624E+01                   4
HCL                     H   1CL  1          G    300.00   4000.00 1000.00      1
 .275038607E+01 .146525702E-02-.485796370E-06 .790400572E-10-.488097333E-14    2
-.118941369E+05 .656298585E+01 .346434022E+01 .474166973E-03-.200403781E-05    3
 .332826880E-08-.145873238E-11-.121280024E+05 .266176266E+01                   4
HOCL                    H   1CL  1O   1     G    300.00   4000.00 1000.00      1
 .439872621E+01 .200818987E-02-.651636117E-06 .978163599E-10-.555502298E-14    2
-.107193417E+05 .261601151E+01 .349684680E+01 .269237691E-02 .436935723E-05    3
-.890075336E-08 .418971372E-11-.104226316E+05 .760199611E+01                   4
CH2CLO                  C   1H   2CL  1O   1G   300.000  5000.000   1000.00    1
 5.98576480E+00 3.03176018E-03-7.61874477E-07 9.66166300E-11-4.81906838E-15    2
 5.04137449E+03-1.63189956E+01 3.77819725E+00-2.18776322E-03 2.83524146E-05    3
-3.36441694E-08 1.20487706E-11 6.17841929E+03-2.17374906E+00                   4
CCL4                    C   1CL  4          G    300.00   4000.00 1000.00      1
 .116219486E+02 .143587698E-02-.568084026E-06 .976193732E-10-.609835495E-14    2
-.153554331E+05-.302030041E+02 .219698663E+01 .441047270E-01-.781537067E-04    3
 .655173998E-07-.210841442E-10-.135423579E+05 .144892060E+02                   4
CCL4                    C   1CL  4          G    300.00   4000.00 1000.00      1
 .116219486E+02 .143587698E-02-.568084026E-06 .976193732E-10-.609835495E-14    2
-.153554331E+05-.302030041E+02 .219698663E+01 .441047270E-01-.781537067E-04    3
 .655173998E-07-.210841442E-10-.135423579E+05 .144892060E+02                   4
CLCHO                   C   1H   1CL  1O   1G    300.00   4000.00 1000.00      1
 .551436106E+01 .413006211E-02-.151814401E-05 .249100882E-09-.150960767E-13    2
-.240836938E+05-.206855056E+01 .291952259E+01 .888172302E-02-.666881634E-06    3
-.601679587E-08 .324271587E-11-.232335282E+05 .119528458E+02                   4
CHCL3                   C   1H   1CL  3     G    300.00   4000.00 1000.00      1
 .887416412E+01 .380078645E-02-.139786730E-05 .229338126E-09-.138870953E-13    2
-.156076868E+05-.169517476E+02 .251402576E+01 .251578997E-01-.284529412E-04    3
 .151227888E-07-.284923874E-11-.140640395E+05 .148973098E+02                   4
CH2CL2                  C   1H   2CL  2     G    300.00   4000.00 1000.00      1
 .629318149E+01 .598773270E-02-.215635738E-05 .348717095E-09-.209014331E-13    2
-.139806830E+05-.590810756E+01 .309078884E+01 .835269259E-02 .125182071E-04    3
-.246845519E-07 .111752358E-10-.128332020E+05 .120563837E+02                   4
CH3CL                   C   1H   3CL  1     G    300.00   4000.00 1000.00      1
 .397883949E+01 .791729094E-02-.281713927E-05 .451715634E-09-.269086155E-13    2
-.116761879E+05 .258272676E+01 .396611858E+01-.505692958E-02 .402006413E-04    3
-.482781901E-07 .186721580E-10-.110729538E+05 .570446517E+01                   4
CCl2                    C   1CL  2          G    300.00   4000.00 1000.00      1
 0.80836736E+01-0.11686005E-02 0.47029320E-06-0.81695078E-10 0.51447645E-14    2
 0.25307376E+05-0.14232761E+02 0.96645165E+00 0.26370954E-01-0.34655778E-04    3
 0.14693679E-07-0.66489549E-13 0.26683995E+05 0.20047532E+02 0.27867073E+05    4
```

```
CH2CCL2                 C   2H   2Cl  2     G   200.000  6000.000 1000.00      1
 8.72532719E+00 6.52036240E-03-2.35515054E-06 3.81702547E-10-2.29160447E-14    2
-3.05938603E+03-1.79281778E+01 1.09096136E+00 3.38226307E-02-4.14124457E-05    3
 2.66327558E-08-6.88457658E-12-1.24748716E+03 1.99995964E+01 2.64597673E+02    4
C2HCL                   C   2H   1CL  1     G   300.00    4000.00 1000.00      1
 6.53097134E+00 3.41057344E-03-1.19750540E-06 1.90362242E-10-1.12736805E-14    2
 2.53105214E+04-9.41702620E+00 1.11105564E+00 3.10701253E-02-5.67940536E-05    3
 5.06488266E-08-1.71128260E-11 2.62385382E+04 1.56170473E+01 2.75410096E+04    4
CHCL                    C   1H   1CL  1     G   300.00   4000.00 1000.00       1
 6.56352786E+00 3.00134010E-04-9.88996592E-08 1.86048201E-11-1.31979002E-15    2
 3.61516077E+04-1.02479287E+01 4.57769406E+00-9.61303113E-03 4.74564190E-05    3
-5.89051409E-08 2.32661062E-11 3.73197024E+04 3.42962307E+00 3.85711245E+04    4
CH2CLCCL2               C   2H   2Cl  3     G   200.000  6000.000 1000.00      1
 1.28814098E+01 4.84112794E-03-1.70531628E-06 2.71889852E-10-1.61421474E-14    2
 4.16854880E+03-3.59731028E+01 9.01667949E-01 5.76069918E-02-9.43546438E-05    3
 7.56031207E-08-2.34841675E-11 6.50926522E+03 2.10954179E+01 8.64324945E+03    4
VCL4                    C   2CL  4          G    300.00   4000.00 1000.00      1
 .132027522E+02 .284270302E-02-.110833520E-05 .188694352E-09-.117139630E-13    2
-.705586076E+04-.360905501E+02 .311949409E+01 .449195301E-01-.736240531E-04    3
 .596895418E-07-.189904125E-10-.491858238E+04 .126542200E+02                   4
C2CL6                   C   2CL  6          G    300.00   4000.00 1000.00      1
 .188630387E+02 .324136618E-02-.136977241E-05 .236702848E-09-.146489708E-13    2
-.257902776E+05-.606433678E+02 .383016650E+01 .699619400E-01-.119578126E-03    3
 .972583947E-07-.305156890E-10-.228701227E+05 .108683334E+02                   4
C2HCL3                  C   2H   1CL  3     G    300.00   4000.00 1000.00      1
 .107946029E+02 .478341644E-02-.175748500E-05 .288222391E-09-.174502071E-13    2
-.524080882E+04-.245413236E+02 .252875646E+01 .346949768E-01-.451599761E-04    3
 .300517281E-07-.802417876E-11-.330277626E+04 .164273194E+02                   4
C2HCL5                  C   2H   1CL  5     G    300.00   4000.00 1000.00      1
 .161889108E+02 .602755857E-02-.252297714E-05 .442668370E-09-.278828019E-13    2
-.251861039E+05-.501366047E+02 .385594982E+01 .456073672E-01-.499565523E-04    3
 .245552722E-07-.395375908E-11-.220748312E+05 .121373851E+02                   4
CLCHCHCL                C   2H   2CL  2     G    300.00   4000.00 1000.00      1
 .869447423E+01 .654382105E-02-.236250428E-05 .382759308E-09-.229733966E-13    2
-.290045984E+04-.166953847E+02 .316930340E+01 .208998746E-01-.124510950E-04    3
-.140963241E-08 .302712632E-11-.135237424E+04 .119943240E+02                   4
CL2CHCHCL2              C   2H   2CL  4     G    300.00   4000.00 1000.00      1
 .174585900E+02 .248417790E-02-.512780220E-06 .226690800E-10 .237193200E-14    2
-.251069800E+05-.606521200E+02 .271174600E+01 .444127920E-01-.490596100E-04    3
 .263247200E-07-.546629190E-11-.205242000E+05 .162485700E+02                   4
CLCHCCL3                C   2H   2CL  4     G    300.00   4000.00 1000.00      1
 .174585900E+02 .248417790E-02-.512780220E-06 .226690800E-10 .237193200E-14    2
-.251069800E+05-.606521200E+02 .271174600E+01 .444127920E-01-.490596100E-04    3
 .263247200E-07-.546629190E-11-.205242000E+05 .162485700E+02                   4
C2H3CL                  C   2H   3CL  1     G    300.00   4000.00 1000.00      1
 .632341000E+01 .852343039E-02-.304197672E-05 .488915441E-09-.291775277E-13    2
-.464920470E+02-.774958634E+01 .227191109E+01 .125087140E-01 .121343633E-04    3
-.273077584E-07 .126573716E-10 .136544369E+04 .147576437E+02                   4
CLCH2CHCL               C   2H   3CL  2     G    300.00   4000.00 1000.00      1
 .129559300E+02 .300168800E-02-.416516090E-06-.390905500E-10 .904108990E-14    2
 .993207700E+03-.392538600E+02 .227618500E+01 .301140010E-01-.304766400E-04    3
 .165488000E-07-.361319810E-11 .483634000E+04 .179216600E+02                   4
CL2CHCH2                C   2H   3CL  2     G    300.00   4000.00 1000.00      1
 .130003500E+02 .294048410E-02-.374645590E-06-.504064290E-10 .100633200E-13    2
-.422881600E+03-.397986200E+02 .321347200E+01 .258737800E-01-.241999300E-04    3
 .127381700E-07-.278848100E-11 .332566200E+04 .133332000E+02                   4
```

```
CH3CCL3                 C   2H   3CL  3     G    300.00   4000.00 1000.00      1
 .120555087E+02 .844253446E-02-.304587523E-05 .493404612E-09-.296165491E-13    2
-.219789258E+05-.340314769E+02 .256424495E+01 .393928228E-01-.426660423E-04    3
 .242267750E-07-.560184447E-11-.195749809E+05 .138735787E+02                   4
C2H3Cl3                 C   2H   3CL  3     G    300.00   4000.00 1000.00      1
 .120555087E+02 .844253446E-02-.304587523E-05 .493404612E-09-.296165491E-13    2
-.219789258E+05-.340314769E+02 .256424495E+01 .393928228E-01-.426660423E-04    3
 .242267750E-07-.560184447E-11-.195749809E+05 .138735787E+02                   4
CH2CLCH2CL              C   2H   4CL  2     G    300.00   4000.00 1000.00      1
 .968476700E+01 .112630298E-01-.431576920E-05 .725209500E-09-.445818752E-13    2
-.199525878E+05-.239965067E+02 .468235340E+01 .393962518E-02 .507306234E-04    3
-.703930514E-07 .283531047E-10-.175372415E+05 .696581596E+01                   4
CH3CHCL2                C   2H   4CL  2     G    300.00   4000.00 1000.00      1
 .909567674E+01 .108697157E-01-.386741990E-05 .620397968E-09-.369782326E-13    2
-.191148895E+05-.197555082E+02 .318055846E+01 .194629497E-01 .784537538E-05    3
-.267053479E-07 .128978565E-10-.171561838E+05 .125299229E+02                   4
C2H5CL                  C   2H   5CL  1     G    300.00   4000.00 1000.00      1
 .677417343E+01 .130492053E-01-.467370081E-05 .752809912E-09-.449899075E-13    2
-.165816334E+05-.105157529E+02 .358369774E+01 .502103864E-02 .439001544E-04    3
-.622537878E-07 .256063949E-10-.149469870E+05 .985386437E+01                   4
C3H4CL2                 C   3H   4CL  2     G    300.00   4000.00 1000.00      1
-.253665500E+01 .380639840E-01-.152602410E-04 .198138730E-08 .000000000E+00    2
-.224861000E+04 .461079100E+02 .658050100E+01 .226768390E-01-.118374250E-04    3
 .482855840E-08 .000000000E+00-.552492500E+04-.414449800E+01                   4
CH2CHCH2CL              C   3H   5CL  1     G    300.00   4000.00 1000.00      1
 .852439580E+01 .139387683E-01-.494599494E-05 .787953151E-09-.466709395E-13    2
-.380684034E+04-.171514162E+02 .346378742E+01 .113302404E-01 .401782107E-04    3
-.644060622E-07 .276922751E-10-.173265523E+04 .126490551E+02                   4
C3H6CL2                 C   3H   6CL  2     G    300.00   4000.00 1000.00      1
-.233076900E+01 .409543510E-01-.163698930E-04 .212092610E-08 .000000000E+00    2
-.201013200E+05 .463065500E+02 .635055200E+01 .205782650E-01-.166169000E-05    3
-.892510450E-09 .000000000E+00-.227439700E+05 .364567400E+00                   4
CLCHCHCHCHCL            C   4H   4CL  2     G    300.00   4000.00 1000.00      1
-.503173800E+00 .375008990E-01-.147884150E-04 .189739220E-08 .000000000E+00    2
 .688081100E+04 .361425200E+02 .510497000E+01 .318862910E-01-.203836190E-04    3
 .749906270E-08 .000000000E+00 .454462100E+04 .394782300E+01                   4
C4CL                    C   4H   5CL  1     G    300.00   4000.00 1000.00      1
 .134895400E+02 .988687390E-02-.221942400E-05 .127024700E-09 .000000000E+00    2
 .385729400E+04-.440659500E+02 .195048000E+00 .453841090E-01-.333304310E-04    3
 .903528360E-08 .000000000E+00 .754643500E+04 .248579800E+02                   4
C4H6CL4                 C   4H   6CL  4     G    300.00   4000.00 1000.00      1
 .206511700E+02 .817008500E-02-.662310580E-06-.155415610E-09 .000000000E+00    2
-.367714100E+05-.682213500E+02 .839446400E+01 .416529510E-01-.308579510E-04    3
 .881405530E-08 .000000000E+00-.334333000E+05-.492991400E+01                   4
C4H7CL                  C   4H   7CL  1     G    300.00   4000.00 1000.00      1
-.503173800E+00 .375008990E-01-.147884150E-04 .189739220E-08 .000000000E+00    2
 .688081100E+04 .361425200E+02 .510497000E+01 .318862910E-01-.203836190E-04    3
 .749906270E-08 .000000000E+00 .454462100E+04 .394782300E+01                   4
CH3CCL2                 C   2H   3CL  2     G    300.00   4000.00 1000.00      1
 .130003500E+02 .294048410E-02-.374645590E-06-.504064290E-10 .100633200E-13    2
-.422881600E+03-.397986200E+02 .321347200E+01 .258737800E-01-.241999300E-04    3
 .127381700E-07-.278848100E-11 .332566200E+04 .133332000E+02                   4
CH2CLCH2                C   2H   4CL  1     G    300.00   4000.00 1000.00      1
 .599819049E+01 .111132750E-01-.398843798E-05 .643305132E-09-.384817170E-13    2
 .904451655E+04-.415831190E+01 .459020227E+01 .637689976E-03 .384996846E-04    3
-.491337133E-07 .191339874E-10 .101373505E+05 .659847208E+01                   4
```

```
CL                      CL  1               G    300.00   4000.00 1000.00      1
 .296123231E+01-.406760214E-03 .145948930E-06-.236008477E-10 .141691234E-14    2
 .136901066E+05 .302880221E+01 .223418328E+01 .173391135E-02-.115488156E-05    3
-.112443736E-08 .989461388E-12 .138580303E+05 .668075708E+01                   4
CLO                     CL  1O   1          G    300.00   4000.00 1000.00      1
 .445682803E+01-.594131131E-04 .131237646E-06-.311268672E-10 .180684649E-14    2
 .108403059E+05 .154178724E+01 .361933587E+01 .253362803E-02-.311179384E-05    3
 .194941709E-08-.491254605E-12 .110657642E+05 .581853677E+01                   4
CLOO                    CL  1O   2          G    300.00   4000.00 1000.00      1
 .594695297E+01 .106701562E-02-.416053875E-06 .709444017E-10-.441455027E-14    2
 .104214960E+05-.135477721E+01 .425061490E+01 .744877793E-02-.113047633E-04    3
 .965717296E-08-.338735791E-11 .108365543E+05 .707602978E+01                   4
CLCO                    C   1CL  1O   1     G    300.00   4000.00 1000.00      1
 .542654535E+01 .154940045E-02-.594189705E-06 .100270931E-09-.619621957E-14    2
-.424833161E+04 .204136268E+00 .324668040E+01 .122022603E-01-.228418578E-04    3
 .217889351E-07-.792018728E-11-.381837509E+04 .104820271E+02                   4
CCL3                    C   1CL  3          G    300.00   4000.00 1000.00      1
 .886167674E+01 .118055486E-02-.465765318E-06 .798915627E-10-.498464418E-14    2
 .560193095E+04-.157461775E+02 .266358332E+01 .271296370E-01-.442402957E-04    3
 .346851463E-07-.105866977E-10 .688202237E+04 .141172615E+02                   4
CHCL2                   C   1H   1CL  2     G    300.00   4000.00 1000.00      1
 .680210912E+01 .286000875E-02-.103664482E-05 .168416656E-09-.101027167E-13    2
 .916929806E+04-.570765415E+01 .341194137E+01 .140168850E-01-.142771614E-04    3
 .624721839E-08-.615096358E-12 .999583151E+04 .112991582E+02                   4
CH2CL                   C   1H   2CL  1     G    300.00   4000.00 1000.00      1
 .458143318E+01 .470002394E-02-.165867811E-05 .264426164E-09-.156861143E-13    2
 .126224801E+05 .140525938E+01 .352075492E+01 .499532931E-02 .440178197E-05    3
-.908417002E-08 .403782288E-11 .130417996E+05 .750945133E+01                   4
C2CL5                   C   2CL  5          G    300.00   4000.00 1000.00      1
 .162520195E+02 .187037729E-02-.749842407E-06 .129830325E-09-.814928062E-14    2
-.276548298E+04-.456861627E+02 .391975280E+01 .549682504E-01-.927440565E-04    3
 .745660842E-07-.232157955E-10-.284949040E+03 .133911785E+02                   4
CL2CCHCL2               C   2H   1CL  4     G    300.00   4000.00 1000.00      1
 .145236396E+02 .429972946E-02-.177166296E-05 .307646634E-09-.192515584E-13    2
-.257510890E+04-.404511621E+02 .315151526E+01 .441094266E-01-.575511181E-04    3
 .373697567E-07-.973947933E-11 .163836575E+03 .162607402E+02                   4
CL3CCHCL                C   2H   1CL  4     G    300.00   4000.00 1000.00      1
 .145236396E+02 .429972946E-02-.177166296E-05 .307646634E-09-.192515584E-13    2
-.257510890E+04-.404511621E+02 .315151526E+01 .441094266E-01-.575511181E-04    3
 .373697567E-07-.973947933E-11 .163836575E+03 .162607402E+02                   4
CHCLCH                  C   2H   2CL  1     G    300.00   4000.00 1000.00      1
 .657992662E+01 .550498054E-02-.193056595E-05 .306672838E-09-.181536735E-13    2
 .305524286E+05-.726735678E+01 .175764780E+01 .207031239E-01-.184481964E-04    3
 .631043021E-08 .119854774E-12 .317529714E+05 .170686824E+02                   4
C2H2CL3                 C   2H   2CL  3     G    300.00   4000.00 1000.00      1
 .128814098E+02 .484112794E-02-.170531628E-05 .271889852E-09-.161421474E-13    2
 .416854880E+04-.359731028E+02 .901667949E+00 .576069918E-01-.943546438E-04    3
 .756031207E-07-.234841675E-10 .650926522E+04 .210954179E+02                   4
CH3CHCL                 C   2H   4CL  1     G    300.00   4000.00 1000.00      1
 .633557579E+01 .105535090E-01-.372692346E-05 .594577539E-09-.352943207E-13    2
 .700241054E+04-.542089862E+01 .452093357E+01 .718692942E-02 .181348982E-04    3
-.269955922E-07 .108742755E-10 .792869711E+04 .601920526E+01                   4
CLCH2CH2CHCL            C   3H   5CL  2     G    300.00   4000.00 1000.00      1
-.810464500E+01 .471134190E-01-.195003690E-04 .258847370E-08 .000000000E+00    2
 .609649500E+04 .783070400E+02 .592812900E+01 .191305620E-01-.563298640E-05    3
 .267117350E-08 .000000000E+00 .141201300E+04 .239367200E+01                   4
```

APPENDIX B

Species	Shape	eps/kb	sigma	mu	alfa	zRot298
CL	0	130.800	3.613	0.000	0.000	1.000
CL2	1	316.000	4.217	0.000	0.000	1.000
HCL	1	344.700	3.339	0.000	0.000	1.000
CCL4	2	327.000	5.881	0.000	0.000	1.000
CHCL3	2	327.000	5.430	0.000	0.000	1.000
CH2CL2	2	406.000	4.759	0.000	0.000	1.000
CH3CL	2	855.000	3.375	0.000	0.000	1.000
CH2CL	2	858.000	3.400	0.000	0.000	0.000
C2HCL3	2	280.000	3.971	0.000	0.000	0.000
CCL	1	98.100	3.650	0.000	1.950	1.800
CLCHO	2	498.000	3.590	0.000	0.000	0.000
HOCL	2	107.400	3.458	0.000	0.000	0.000
CLCO	2	860.000	4.000	0.000	0.000	0.000
CLO	2	110.000	3.590	0.000	0.000	0.000
CL2O	2	356.000	2.649	0.000	0.000	0.000
CLOO	2	107.400	3.458	0.000	0.000	0.000
CH3CL	2	855.000	3.375	0.000	0.000	0.000
OCLO	2	107.400	3.458	0.000	0.000	0.000
O3	2	180.000	4.100	0.000	0.000	2.000
VCL4	2	299.719	4.565	0.000	0.000	1.000
C2CL6	2	297.351	4.490	0.000	0.000	1.000
C2HCL5	2	291.631	4.561	0.000	0.000	1.000
CLCHCCL3	2	291.452	4.610	0.000	0.000	1.000
CL2CHCHCL2	2	285.939	4.633	0.000	0.000	1.000
C2H3CL3	2	298.934	4.638	0.000	0.000	1.000
CH3CHCL2	2	293.153	4.710	0.000	0.000	1.000
CH2CLCH2CL	2	285.595	4.731	0.000	0.000	1.000
C2H5CL	2	292.955	4.758	0.000	0.000	1.000
C3H4CL2	2	311.824	4.995	0.000	0.000	1.000
C3H6CL2	2	304.009	5.058	0.000	0.000	1.000
CLCHCHCHCHCL	2	305.073	5.434	0.000	0.000	1.000
C4CL	2	328.778	5.220	0.000	0.000	1.000
C4H6CL4	2	305.730	5.335	0.000	0.000	1.000
C4H7CL	2	317.089	5.346	0.000	0.000	1.000
CLCHCHCL	2	301.256	4.647	0.000	0.000	1.000

C2H3CL	2	296.512	4.649	0.000	0.000	1.000
CH3CCL3	2	298.934	4.638	0.000	0.000	1.000
CH2CHCH2CL	2	307.674	4.997	0.000	0.000	1.000
CCL3	2	271.082	4.267	0.000	0.000	1.000
CHCL2	2	271.021	4.316	0.000	0.000	1.000
C2CL5	2	289.342	4.495	0.000	0.000	1.000
CL2CCHCL2	2	283.627	4.567	0.000	0.000	1.000
CHCLCH	2	294.230	4.583	0.000	0.000	1.000
C2H2CL3	2	296.669	4.572	0.000	0.000	1.000
CLCH2CHCL	2	283.298	4.666	0.000	0.000	1.000
CL2CHCH2	2	290.864	4.644	0.000	0.000	1.000
CH3CCL2	2	290.864	4.644	0.000	0.000	1.000
CH2CLCH2	2	290.673	4.693	0.000	0.000	1.000
CH3CHCL	2	290.673	4.693	0.000	0.000	1.000
CLCH2CH2CHCL	2	293.726	5.017	0.000	0.000	1.000
CLCH2CLCHCH2	2	301.582	4.993	0.000	0.000	1.000
CL3CCHCL	2	289.171	4.544	0.000	0.000	1.000
CH2CCL2	2	295.748	4.609	0.000	0.000	1.000
CCL2	2	268.829	4.250	0.000	0.000	1.000
CHCL	2	275.984	4.278	0.000	0.000	1.000
CH2CLCCL2	2	283.464	4.617	0.000	0.000	1.000
C2HCL	1	304.619	4.386	0.000	0.000	1.000
CH2CLO	2	286.866	4.526	0.000	0.000	1.000

BIBLIOGRAPHY

[1] Granada A., Karra S. B., Senkan S. M. (1987). Conversion of CH_4 into C_2H_2 and C_2H_4 by the Chlorine Catalyzed Oxidative-Pyrolysis (CCOP) Process. 1. Oxidative Pyrolysis of CH_3CL. *Industrial Engineering and Chemical Research,* 26, 1901-1905.

[2] Glarborg P. (2007). Hidden interactions - Trace species governing combustion and emissions. *Proceedings of the combustion institute,* 77-98.

[3] Chuang S.C., Bozzelli. J. (1986). Conversion of chloroform to hydrochloric acid by reaction with hydrogen and water vapor. *Environmental Science and Technology* , 20, 568–574.

[4] Senkan S.M. (2000). Combustion of chlorinated hydrocarbon. *NATO science series*, 303-336.

[5] Cuoci A., Frassoldati A., Faravelli T., Eliseo R. (2015). An object-oriented framework for the numerical modeling of reactive systems with detailed kinetic mechanisms. *Computer Physics Communications*.

[6] Buzzi-Ferraris G., Manenti. F. (2012). BzzMath: Library Overview and Recent Advances in Numerical Methods. *Computer-Aided Chemical Engineering* , 30(2), 1312-1316.

[7] CRECK Modeling. *Gas phase combustion scheme.* Retrieved April 7, 2015, from *http://creckmodeling.chem.polimi.it/index.php/kinetic-schemes*

[8] E. Ranzi, Frassoldati A., Grana R., Cuoci A., Faravelli T., Kelley A.P., Law C.K., (2012). Hierarchical and comparative kinetic modeling of laminar flame speeds of hydrocarbon and oxygenated fuels. *Progress in Energy and Combustion Science* , 38 (4), 468-501.

[9] Pelucchi M., Frassoldati A., Faravelli T., Ruscic B., Glarborg P. (2015). High-temperature chemistry of HCL and CL_2. *Combustion and Flame*, 162, 2693-2704.

[10] Burcat A., Ruscic B. (2005). *Third millennium ideal gas and condensed phase thermochemical database for combustion with updates from active thermochemical tables.* Chemistry Division, Argonne National Laboratory.

[11] Kee R.J., Rupley F.M., Miller J.A., Coltrin M.E., Grcar J.F., Meeks E. et al. (2000). A software package for the evaluation of gas-phase, multicomponent transport properties. In *CHEMKIN Collection Release 3.6.*

[12] DeMore W.B., Sander S.P. Howard CJ., Ravishankara A.R., Golden D.M., Kolb C.E. (1992). *Chemical Kinetics and Photochemical Data for Use in Stratospheric Modeling, Evaluation Number 10,* JPL Publication, 92-20.

[13] NATO Institute Advanced study. (1998). *pollutant from combustion - formation and impact on atmospheric chemistry.* 305-307.

[14] Frassoldati A., Faravelli T.,Ranzi E. (2007). The ignition, combustion and flame structure of carbon monoxide/hydrogen mixtures. Note 1: Detailed kinetic modeling of syngas combustion also in presence of nitrogen compounds. *International Journal of Hydrogen Energy*, 32, 15, 3471-3485

[15] A. Cuoci, Frassoldati A., Faravelli T. (2007). The ignition, combustion and flame structure of carbon monoxide/hydrogen mixtures. Note 2: Fluid dynamics and kinetic aspects of syngas combustion. *International Journal of Hydrogen Energy* , Volume 32, Issue 15, 3486-3500.

[16] McBride B., Gordon S. (1992). Computer program for calculating and fitting. *Tech. Rep. NASA* , Ref. Pub. 1271.

[17] Hickson K. M., Keyser L. F. (2005). A Kinetic and Product Study of the CL + HO_2 Reaction. *the journal of physical chemistry* , 109, 6887-6900.

[18] Schading G.N., Roth P. (1994). Thermal decomposition of HCl measured by ARAS and IR diode laser spectroscopy . *Combustion and Flame*, 99, 3-4, 467-474.

[19] Fishburne E. S. (1966). Gaseous Reaction Rates at High Temperatures. II. The Dissociation of Hydrogen Chloride. *The Journal of Chemical Physics*, 45, 4053.

[20] Jacobs T. A., Cohen N., Giedt R. R. (1963). Dissociation of CL_2 in Shock Waves. *Journal of Chemical Physics*, 39, 749.

[21] Seery D.J., Bowman C. T. (1968). Dissociation of HCL Behind Shock Waves. *The Journal of Chemical Physics*, 48, 4314.

[22] Giedt R. R., Jacobs T. A. (1971). Further Shock Tube Studies of HCL Dissociation Rates. *The Journal of Chemical Physics*, 55, 4144.

[23] Breshears W. D., Bird P. F. (1972). Density Gradient Measurements of HCL Dissociation in Shock Waves. *The Journal of Chemical Physics*, 56, 5347.

[24] Ambidge P. F., Bradley J. N., Whytock D. A. (1976). Kinetic study of the reaction of hydrogen atoms with hydrogen chloride. *Journal of the Chemical Society, Faraday Transactions 1: Physical Chemistry in Condensed Phases*, 72, 2143-2149

[25] Miller J. C., Gordon R. J. (1981). Kinetics of the CL–H_2 system. I. Detailed balance in the CL+H_2 reaction. *The Journal of Chemical Physics*, 75, 5305.

[26] Kita D., Stedman D. H. (1982). Kinetic studies of reactions of hydrogen atoms with HCL, CL_2 and NOCL, and chlorine atoms with H_2 and NOCL. *Journal of the Chemical Society, Faraday Transactions 2: Molecular and Chemical Physics*, 78, 1249-1259.

[27] Adusei G. Y., Fontijn A. (1993). A high-temperature photochemistry study of the H+ HCL= H_2+CL reaction from 298 to 1192 K. *The Journal of Physical Chemistry*, 97, 1409-1412.

[28] Adusei G. Y., Fontijn A. (1994). Experimental studies of CL-atom reactions at high temperatures: CL+H_2→HCL+H from 291 to 1283 K. *Twenty-Fifth Symposium (International) on Combustion*, 25, 1, 801–808.

[29] Westenberg A. A., De Haas N. (1968). Atom–Molecule Kinetics using ESR Detection. IV. Results for CL + H_2 ⇄ HCL + H in Both Directions. *The Journal of Chemical Physics*, 48, 4405.

[30] Lee J. H., Michael J. V., Payne W. A., Stief L. J., Whytock D. A. (1977). Absolute rate of the reaction of CL (2P) with molecular hydrogen from 200–500 K . *Journal of the Chemical Society, Faraday Transactions 1: Physical Chemistry in Condensed Phases*, 73, 1530-1536.

[31] Su F., Calvert J. G., Lindley C. R., Uselman W. M., Shaw J. H. (1979). Fourier transform infrared kinetic study of hypochlorous acid and its absolute integrated infrared band intensities. *Journal of Phyical Chemistry*, 83, 912–920.

[32] Kumaran S., Lim K., Michael J. (1994). Thermal rate constants for the CL+H_2 and CL+D_2 reactions between 296 and 3000 K, *Journal of Chemical Physics*, 101, 9487-9408.

[33] Husain D., Plane J. M. C., Xiang C. C. (1984). *Journal of the Chemical Society, Faraday Transactions 2: Molecular and Chemical Physics*, 80, 713-728.

[34] Ravishankara A. R., Wine P. H., Wells J. R., Thompson R. L. (1985). Kinetic study of the reaction of OH with HCL from 240–1055 K. *International Journal of Chemical Kinetics*, 17, 12, 1281–1297.

[35] Bryukov M.G., Dellinger B. (2006). Kinetics of the Gas-Phase Reaction of OH with HCL. *Journal of Phyical Chemistry*, 110, 936–943.

[36] Atkinson R., Baulch D. L., Cox R. A., Crowley J. N., Hampson R. F., Hynes R. G., Jenkin M. E. (2007). Evaluated kinetic and photochemical data for atmospheric chemistry: Volume III – gas phase reactions of inorganic halogens . *Atmospheric Chemistry Physics*, 7, 981-1191.

[37] Gavriliv A., Kochubei V., Moin F. (1957). Kinetics of oxidation of hydrogen-chloride by oxygen, *Kinetic and Catalysis*, 16, 666.

[38] Louis F., Gonzalez C. A., Sawerysyn J.P. (2003). Ab Initio Study of the Oxidation Reaction of CO by CLO Radicals. *Journal of Phyical Chemistry*, 107, 9931–9936.

[39] Clyne M. A. A., Watson R. T. (1974). Kinetic studies of diatomic free radicals using mass spectrometry. Part 2.—Rapid bimolecular reactions involving the CLO X 2 Πradical. *Journal of Chemical Society*, 70, 2250-2259.

[40] Lloyd A.C. (1971). A critical review of the kinetics of the dissociation-recombination reactions of fluorine and chlorine. *Journal Chemical Kinetic*, 3, 1, 39–68.

[41] Baulch D.L., Duxbury J., Grant S.J., Montague D.C., (1981). Evaluated Kinetic Data for High Temperature Reactions. Volume 4. Homogeneous Gas Phase Reactions of Halogen and Cyanide-Containing Species, *National Standard Reference Data System,*723.

[42] Blauer J.A., McMath H.G., Jaye F.C. (1969). Thermal dissociation of chlorine trifluoride behind incident shock waves. *Journal of Physiscal Chemistry*, 73 (8), 2683–2688.

[43] Ruscic B., Burcat A. (2005). Third Millennium Ideal Gas and Condensed Phase Thermochemical Database for Combustion with Updates from Active Thermochemical Tables . *Joint Report: ANL-05/20, Argonne National Laboratory, Argonne, IL, USA, and TAE 960, Technion – Israel Institute of Technology, Haifa, Israel*.

[44] William H. Green, Joshua W. Allen, Beat A. Buesser, Robert W. Ashcraft, Gregory J. Beran, Caleb A. Class, Connie Gao, C. Franklin Goldsmith, Michael R. Harper, Amrit Jalan, Murat Keceli, Gregory R. Magoon, David M. Matheu, Shamel S. Merchant, Jeffrey D. M. (2013). RMG - Reaction Mechanism Generator v4.0.1., from *http://rmg.mit.edu/*

[45] Karra S. B., Senkan S. M. (1988). A Detailed Chemical Kinetic Mechanism for the Oxidative Pyrolysis of CH_3CL. *Industrial Engineering and Chemical Research*, 27, 1163-1168.

[46] Kondo O., Saito K., Murakami I. (1980). Thermal molecular decomposition of CH_3CL behind shock waves. *Bulletin of Chemical Society Japan*, 53, 2133-2140.

[47] Lim K.P., Michael J.V. (1993). The thermal decomposition of CH_3CL using the CL-atom absorption method and the bimolecular rate constant for O + CH_3 (1609-2002 K) with a pyrolysis photolysis-shock tube technique. *Journal of Chemical Physics*, 98, 3919-3928.

[48] Abadzhev S.S., Dzikh I.P., Shevchuk V.U. (1990). Kinetic features of joint pyrolysis of methyl chloride and methane. *Kinetic and Catalysis*, 30, 893-897.

[49] Shilov A., Sabirova R.D. (1959). Mechanism of the primary act of the thermal decomposition of methane derivatives. *Zhurnal Fizicheskoi Khimii*, 6, 1365.

[50] Ho W., Yu Q.R., Bozzelli J.W. (1992). Kinetic Study on Pyrolysis and Oxidation of CH_3CL in $Ar/H_2/O_2$ Mixtures. *Combustion Science and Technology*, 85, 23-63.

[51] Bryukov M.G., Slagle I.R., Knyazev V.D. (2001). Kinetics of Reactions of H Atoms with Methane and Chlorinated Methanes. *Journal Physical Chemistry*, 105, 107-3122.

[52] Louis F., Gonzalez C.A., Sawerysyn J.P. (2004). Direct combined ab initio/transition state theory study of the kinetics of the abstraction reactions of halogenated methanes with hydrogen atoms. *Journal of Physical Chemistry*, 108, 10586-10593.

[53] Westenberg A.A., De Haas N. (1975). Rates of H + CH_3X reactions. *Journal of Chemical Physics*, 62, 3321-3325.

[54] Aders W., Pangritz D., Wagner H. (1975). Untersuchungen zur reaktion von wasserstoffatomen mit methylfluoride, methylchlorid und methylbromid. *Berichte der Bunsengesellschaft für physikalische Chemie*, vol 79.

[55] Kerr J.A., Moss S.J. (1981). *Handbook 0f Bimolecular and Thermolecular Gas Reaction Vol. 1 & 2.* CRC Press.

[56] Sarzynski D., Gola A.A., Drys A., Jodkowski J.T. (2009). Kinetic study of the reaction of chlorine atoms with chloromethane in the gas phase. *Chemical Physics Letters* , 476, 138-142.

[57] Clyne M.A.A., Walker R.F. (1973). Absolute rate constants for elementary reactions in the chlorination of CH_4, CD_4, CH_3CL, CH_2CL_2, $CHCL_3$, $CDCL_3$ and $CBrCL_3$. *Journal of the Chemical Society, Faraday Transactions 1*, 69, 1547-1567.

[58] Roesler J.F., Yetter R.A., Dryer F.L. (1994). Perturbation of Moist CO Oxidation by Trace Quantities of CH_3CL. *Combustion Science and Technology*, 101, 199-229.

[59] Senkan S.M. (1993). *Survey of Rate Constants in the C/H/CL/O System combustion Chemistry,* W.C. Gardine Jr. Editor.

[60] Garcia J., Corchado J.C. (1996). Analytical potential energy surface for the CH_4+CL→CH3+HCL reaction: application of the variational transition state theory and analysis of the kinetic isotope effects. *Journal of Chemical Physics*,105, 3517-3523.

[61] Takahashi K., Yamamot O., Inomata T. (2002). Direct measurements of the rate coefficients for the reactions of some hydrocarbons with chlorine atoms at high temperatures. *Proceeding of Combustion Institute*, 29, 2447-2453.

[62] Senkan S.M., Sankaram B., Karra, Selim M. (1988). Analysis of the Chemically Activated CH_2CL/CH_2CL and CH_3/CH_2CL Recombination Reactions at Elevated Temperatures Using the Bimolecular Quantum Rice-Ramsperger-Kassel (QRRK) Method. *Industrial Engineering and Chemical Research*, 27, 447-451.

[63] Wang J., Ding Y.H., Zhang S.W., Sun C.C. (2007). Theoretical study on the methyl radical with chlorinated methyl radicals CH_3-nCLn (n=1, 2, 3) and CCL2, *Journal of Computational Chemistry*, vol 28, 865-876.

[64] Zabel F. (1977). Thermal Gas-Phase Decomposition of Chloroethylenes. II. Vinyl Chloride. *International Journal of Chemical Kinetics*, 9, 651-662.

[65] Dean A.M. (1985). Predictions of Pressure and Temperature Effects upon Radical Addition and Recombination Reactions. *Journal of Combustion Science and Technology*, 34, 177.

[66] Chiang H. M. (1995). Ph.D. thesis. *New Jersey Institute*.

[67] Pilgrim J.S., Taatjes C.A. (1997). Infrared absorption probing of the CL + C_2H_4 reaction: direct measurement of Arrhenius parameters for hydrogen abstraction. *Journal of Physical Chemistry A* , 101, 4172-4177.

[68] Dobis O., Benson S.W. (1991). Temperature coefficients of the rates of CL atom reactions with C_2H_6, C_2H_5, and C_2H_4. The rates of disproportionation and recombination of ethyl radical. *Journal of American Chemical Society*, 113, 6377-6386

[69] Kaiser E.W., Wallington T.J. (1996). Kinetics of the reactions of chlorine atoms with C_2H_4 (k1) and C_2H_2 (K2): a determination of ΔH_f(298°) for C_2H_3. *Journal of Physical Chemistry*, 100, 4111-4119.

[70] Shestov A., Konstantin V., Knyazev V. (2005). Kinetics of the CH_2CL + CH_3 and $CHCL_2$ + CH_3 Radical-Radical Reactions. *Journal of Physical Chemistry A*, 109, 6249-6254.

[71] Won Y.S. (2007). Thermal Stability and Reaction Mechanism of Chloromethanes. *Journal of Industrial Engineering and Chemistry*, 13, 400-405.

[72] Granada A., Karra S. B., Senkan S. M. (1987). Conversion of CH_4 into C_2H_2 and C_2H_4 by the Chlorine-Catalyzed Oxidative-Pyrolysis (CCOP) process: Oxidative pyrolysis of CH_3CL. *Industrial engineering and chemistry research*, 26, 1901.

[73] Wu Y., Won Y.S. (2000). Pyrolysis of Chloromethanes. *Combustion and flames*, 122, 312–326.

[74] Wang H., Hahn T., Sung C.J., Law C.K. (1996). Detailed Oxidation Kinetics and Flame Inhibition Effects of Chloromethane. *Combustion and Flame*, 105, 291-307.

[75] Shin K., Park K., Kim K. (2001). The Addition Effect of CH_3CL on Methane Ignition behind Reflected Shock Waves. *Bulletin of Korean Chemical Society*, 22, 330-332.

[76] From http://www.saudiaramco.com/en/home.html

[77] Senkan S.M., Karra S.B. (1987). Chemical Structures of Sooting $CH_3CL/CH_4/O_2$/Ar and CH_4/O_2/Ar Flames. *Combustion Science and Technology,* 54, 333-347.

[78] Valeiras H., Gupta A.K., Senkan S.M. (1984). Laminar Burning Velocities of Chlorinated Hydrocarbon-Methane-Air Flames. *Combustion Science and Technology*, 36, 123-133.

[79] Shin S.S., Vega E.V., Lee K.Y. (2006). Experimental and Numerical Study of $CH_4/CH_3CL/O_2/N_2$. *Combustion, Explosion, and Shock Waves*, 42, 6, 715–722.

[80] Chelliah H.K., Yu G., Hahn T.O., Law C. K. (1192) An Experimental and numerical study on the global and detailed kinetics of premixed and non premixed flames of chloromethane, methane, oxygen and nitrogen. *Twenty-Fourth Symposium (International) on Combustion*, 1083-1090.

Ringraziamenti

Alla fine di un lungo lavoro è sempre doveroso citare e ringraziare chi, in modi differenti, ha contribuito alla sua buona riuscita. Per questo nelle poche righe che seguono spero di essere esaustivo e di non tralasciare nessuno.

Per prima cosa ringrazio il professor Faravelli per avermi dato la possibilità di svolgere questo lavoro di tesi sotto la sua supervisione, e per la pazienza dimostrata nonostante la mia lungaggine.
Ringrazio sentitamente l'ingegnere Matteo Pelucchi, per la costante disponibilità e assistenza fornita, per la sua grande competenza, senza cui non sarei mai riuscito a completare questo lavoro in un tempo ragionevole.

Ringrazio i miei compagni di corso Alessandro, Edoardo, Francesco e Giorgio per la loro compagnia e amicizia, senza le quali le giornate in università sarebbero state di sicuro meno arricchenti. Sono grato anche per essermi stati da stimolo con i brillanti risultati da loro conseguiti.

Infine ringrazio la mia famiglia senza il cui sostegno e il supporto morale non sarei mai riuscito a completare il percorso di studi, e dedico queste pagine a mio nonno, sicuro che sarebbe stato felice di vedermi raggiungere questo traguardo.